

1

**Division of Applied Sciences
Harvard University — Cambridge, Massachusetts**

AD-A239 295



ANNUAL PROGRESS REPORT NO. 105



DTIC
ELECTR
AUG 07 1991
S C D

JOINT SERVICES ELECTRONICS PROGRAM

N00014-89-J-1023

Covering Period

August 1, 1990 — July 31, 1991

July 1991

91-07004



91 8 06 007

REPORT DOCUMENTATION PAGE

Form Approved
CMB No 0704-0138

1a. REPORT SECURITY CLASSIFICATION Unclassified		1b. RESTRICTIVE MARKINGS	
2a. SECURITY CLASSIFICATION AUTHORITY N/A		3. DISTRIBUTION/AVAILABILITY OF REPORT Unclassified/Unlimited	
2b. DECLASSIFICATION/DOWNGRADING SCHEDULE N/A			
4. PERFORMING ORGANIZATION REPORT NUMBER(S) Annual Progress Report No. 105		5. MONITORING ORGANIZATION REPORT NUMBER(S) Office of Naval Research	
6a. NAME OF PERFORMING ORGANIZATION Harvard University	6b. OFFICE SYMBOL (if applicable)	7a. NAME OF MONITORING ORGANIZATION Office of Naval Research	
6c. ADDRESS (City, State, and ZIP Code) Division of Applied Sciences Harvard University Cambridge, MA 02138		7b. ADDRESS (City, State, and ZIP Code) 800 N. Quincy Street Arlington, VA 22217	
8a. NAME OF FUNDING/SPONSORING ORGANIZATION Office of Naval Research	8b. OFFICE SYMBOL (if applicable)	9. PROCUREMENT INSTRUMENT IDENTIFICATION NUMBER N00014-89-J-1023	
8c. ADDRESS (City, State, and ZIP Code) 800 N. Quincy Street Arling, VA 22217		10. SOURCE OF FUNDING NUMBERS	
		PROGRAM ELEMENT NO.	PROJECT NO.
		TASK NO.	WORK UNIT ACCESSION NO.
11. TITLE (Include Security Classification) Annual Progress Report No. 105			
12. PERSONAL AUTHOR(S) Prof. Michael Tinkham			
13a. TYPE OF REPORT Technical	13b. TIME COVERED FROM 8/1/90 TO 7/31/91	14. DATE OF REPORT (Year, Month, Day) July 1991	15. PAGE COUNT 131
16. SUPPLEMENTARY NOTATION			
17. COSATI CODES		18. SUBJECT TERMS (Continue on reverse if necessary and identify by block number)	
FIELD	GROUP	SUB-GROUP	
19. ABSTRACT (Continue on reverse if necessary and identify by block number)			
<p>→ An annual report of the JSEP (Joint Services Electronics Program) in solid state electronics, quantum electronics, information electronics, control and optimization, and electromagnetic phenomena is presented. Results of the research to date are summarized and significant accomplishments are discussed.</p>			
20. DISTRIBUTION/AVAILABILITY OF ABSTRACT <input type="checkbox"/> UNCLASSIFIED/UNLIMITED <input type="checkbox"/> SAME AS RPT. <input type="checkbox"/> DTIC USERS		21. ABSTRACT SECURITY CLASSIFICATION Unclassified	
22a. NAME OF RESPONSIBLE INDIVIDUAL Prof. Michael Tinkham, Director		22b. TELEPHONE (Include Area Code) (617) 495-3735	22c. OFFICE SYMBOL

Joint Services Electronics Program

N00014-89-J-1023

ANNUAL PROGRESS REPORT NO. 105



Covering Period

August 1, 1990 — July 31, 1991

Approved for	
with Special	<input checked="" type="checkbox"/>
DTIC Tab	<input type="checkbox"/>
Unclassified	<input type="checkbox"/>
Justification	
by	
Distribution	
Availability Code	
Availability	
Dist	Special
A-1	

The research reported in this document, unless otherwise indicated, was made possible through support extended to the Division of Applied Sciences, Harvard University by the U. S. Army Research Office, the U. S. Air Force Office of Scientific Research and the U. S. Office of Naval Research under the Joint Services Electronics Program by Grant N00014-89-J-1023. Related research sponsored by the Office of Naval Research, the National Science Foundation, the National Aeronautic and Space Administration, and by the University is also reported briefly with appropriate acknowledgment.

Division of Applied Sciences
Harvard University
Cambridge, Massachusetts

ANNUAL PROGRESS REPORT NO. 105

Joint Services Grant

N00014-89-J-1023

The Steering Committee

Related Contracts and Grants

N00014-86-K-0033

N00014-86-K-0760

N00014-89-J-1565

N00014-89-J-1592

N00014-90-J-1093

N00014-90-J-1234

N00014-90-J-1582

H. Ehrenreich

H. Ehrenreich

M. Tinkham

R. M. Westervelt

Y. C. Ho

J. A. Golovchenko

H. Ehrenreich

NSF-CDR-88-00108

NSF-CDR-88-03012

NSF-DMR-88-12855

NSF-DMR-88-17309

NSF-DMR-88-58075

NSF-DMR-89-12927

NSF-DMR-89-1486

NSF-DMR-89-20490

J. J. Clark

J. Y. C. Ho, J. J. Clark

P. S. Pershan

R. M. Westervelt

E. Mazur

M. Tinkham

W. Paul

H. Ehrenreich, A. Golovchenko

E. Mazur, W. Paul, P. S. Pershan,

M. Tinkham, R. M. Westervelt

Y. C. Ho

J. J. Clark

NSF-ECS-85-15449

NSF-IRI-90-03306

DAAL03-88-K-0114

DAAL03-88-G-0078

DAAL02-89-K-0097

DAAL03-89-G-0076

E. Mazur

E. Mazur

T. T. Wu

R. M. Westervelt

DE-FG02-84-ER40158

DE-FG02-88-ER45379

DE-FG02-89-ER45399

T. T. Wu

P. S. Pershan

J. A. Golovchenko

F19628-88-K-0024

T. T. Wu

AFOSR-89-0506

AFOSR-90-0248

R. M. Westervelt

J. A. Golovchenko

JOINT SERVICES ELECTRONICS PROGRAM

August 1, 1990 — July 31, 1991

ADMINISTRATIVE STAFF

Grant

N00014-89-J-1023

The Steering Committee

Prof. N. Bloembergen
Assoc. Prof. J. J. Clark
Prof. H. Ehrenreich
Prof. J. A. Golovchenko
Prof. Y. C. Ho
Prof. E. Mazur
Prof. W. Paul
Prof. P. S. Pershan
Prof. M. Tinkham
Prof. R. M. Westervelt
Prof. T. T. Wu

RESEARCH STAFF

Dr. N. Bloembergen
Dr. J. H. Burnett
Dr. J. J. Clark
Dr. H. Ehrenreich
Dr. Y. C. Ho
Dr. P. M. Hui
Dr. R. W. P. King
Dr. C. Z. Lü
Dr. C. M. Marcus
Dr. E. Mazur
Dr. J. M. Myers
Dr. W. Paul

Dr. P. S. Pershan
Dr. T. Rabedeau
Dr. M. Rzechowski
Dr. S. S. Sandler
Dr. H.-M. Shen
Dr. R. Sreenivas
Dr. Z. B. Tang
Dr. M. Tinkham
Dr. M. Tuominen
Dr. R. M. Westervelt
Dr. T. T. Wu
Dr. M. Ziegler

INTRODUCTION

This report covers progress made during the past year in the work of eleven Research Units funded under the Joint Services Electronics Program at Harvard University. It is broken down into four major divisions of electronic research: *Solid state electronics*, *Quantum electronics*, *Information electronics*, and *Electromagnetic phenomena*. Following the report of the work of each Unit, there is a complete annual report of the associated Publications/Patents/Presentations/Honors. This report also includes a section on *Significant Accomplishments* which contains selected highlights from four of these Units. These are "Study of the Band Gap in HgTe/CdTe Superlattices through the Pressure Dependence of the Photoluminescence" by Research Unit 2, "Structure of the Si/SiO₂ Interface" by Research Unit 3, "Fluxon Motion in Superconducting Junction Arrays" by Research Unit 4, and "A Comprehensive Study of Electromagnetic Methods for the Detection of Submerged Submarines" by Research Unit 11.

CONTENTS

CONTRACTS AND GRANTS	iii
STAFF	v
INTRODUCTION	vii
CONTENTS	ix

I. SOLID STATE ELECTRONICS

1. Electronic Theory of Semiconductor Microstructures and Superlattices. <i>H. Ehrenreich</i>	1
<i>Annual Report of Publications/Patents/Presentations/Honors</i>	7
2. Pressure Dependence of Photoluminescence and Photoluminescence/ Excitation in Quantum Wells and Superlattices. <i>J. H. Burnett, H. M. Cheong and W. Paul</i>	8
<i>Annual Report of Publications/Patents/Presentations/Honors</i>	13
3. X-Ray Surface Characterization. <i>I. Tidswell, T. Rabedeau and P. S. Pershan</i>	14
<i>Annual Report of Publications/Patents/Presentations/Honors</i>	23
4. Superconducting Josephson Junction Arrays. <i>M. S. Rzchowski, L. L. Sohn, and M. Tinkham</i>	24
5. Single-Electron Tunneling Devices. <i>A. Hanna, M. Tuominen, and M. Tinkham</i>	28
<i>Annual Report of Publications/Patents/Presentations/Honors</i>	31
6. Planar Networks for Vision Processing. <i>F. R. Waugh and R. M. Westervelt</i>	33
7. Spurious Fixed-point Attractors in Analog Neural Networks. <i>F. R. Waugh, C. M. Marcus, and R. M. Westervelt</i>	35
8. Dynamics of Magnetic Bubble Arrays. <i>R. Seshadri and R. M. Westervelt</i>	35
<i>Annual Report of Publications/Patents/Presentations/Honors</i>	38

9. Structural and Electronic Studies of Semiconductor Interfaces and Surfaces.	
<i>J. A. Golovchenko</i>	40
<i>Annual Report of Publications/Patents/Presentations/Honors</i>	46

II. QUANTUM ELECTRONICS

1. Ultrashort Laser Interactions with Semiconductor Surfaces.	
<i>N. Bloembergen, E. Mazur, P. Saeta, Y. Siegal, and J. K. Wang</i>	47
2. Laser Light Scattering from Surfaces and Monolayers.	
<i>E. Mazur and K. Y. Lee</i>	49
<i>Annual Report of Publications/Patents/Presentations/Honors</i>	51
3. Multiphoton Vibrational Excitation of Molecules.	
<i>E. Mazur, C. Z. Lü, S. Deliwala, and J. Goldman</i>	53
<i>Annual Report of Publications/Patents/Presentations/Honors</i>	55

III. INFORMATION ELECTRONICS: CIRCUITS AND SYSTEMS

1. CMOS Current Mode Realizations of Neural Network Structures.	
<i>J. J. Clark</i>	57
<i>Annual Report of Publications/Patents/Presentations/Honors</i>	69
2. Discrete Event Dynamic Systems Study.	
<i>Y. C. Ho</i>	70
<i>Annual Report of Publications/Patents/Presentations/Honors</i>	72

IV. ELECTROMAGNETIC PHENOMENA

1. On the Radiation Efficiency of a Vertical Electric Dipole in Air Above A Dielectric Half-Space.	
<i>R. W. P. King, B. H. Sandler, and M. Owens</i>	76
2. The Circuit Properties and Complete Fields of Wave Antennas and Arrays.	
<i>R. W. P. King</i>	77
3. Generalized Theory for a Three-Layered Region: Application to Microstrip and Patch Antennas on Microstrip.	
<i>R. W. P. King, B. H. Sandler, M. Owens, and T. T. Wu</i>	80

4. Generalized Theory for a Three-Layered Region: Application to Remote Sensing from the Artic Ice. R. W. P. King	82
5. The Propagation of a Gaussian Pulse in Sea Water; Application to the Detection of Submarines. R. W. P. King	83
6. The Propagation of a Low-Frequency Burst in Sea Water. R. W. P. King	85
7. The Detection of Dielectric Spheres Submerged in Water. R. W. P. King and S. S. Sandler	87
8. Lateral Electromagnetic Waves (Manuscript for Book). R. W. P. King, T. T. Wu, M. Owens, and B. H. Sandler	88
9. Theoretical Study of Electromagnetic Pulses with a Slow Rate of Decay. T. T. Wu, J. M. Myers, H. M. Shen, R. W. P. King, and V. Houdzoumis	90
10. Experimental Study of Electromagnetic Pulses with a Slow Rate of Decay. H.-M. Shen, R. W. P. King, and T. T. Wu	91
11. Indiosyncrasy in Optimal Quantum Measurements. J. M. Myers	93
12. Theoretical Studies of Large Circular Arrays of Dipoles. T. T. Wu, R. W. P. King, and G. Fikioris, D. K. Freeman, B. H. Sandler, and H.-M. Shen	95
13. Improved Analysis of the Resonant Circular Array. G. Fikioris, D. K. Freeman, R. W. P. King, H.-M. Shen, and T. T. Wu	98
14. Closed Loops of Parallel Coplanar Dipoles — Arrays of Arbitrary Shape. T. T. Wu, R. W. P. King, G. Fikioris, and H.-M. Shen	100
15. Properties of Closed Loops of Pseudodipoles. T. T. Wu and D. K. Freeman	101
16. Experimental Studies of the Resonance of a Circular Array. H.-M. Shen and G. Fikioris	104
17. Plasma Waveguide: A Concept to Transfer EM Energy in Space. H.-M. Shen	107
<i>Annual Report of Publications/Patents/Presentations/Honors</i>	<i>109</i>

V. SIGNIFICANT ACCOMPLISHMENTS REPORT

1. Study of the Band Gap in HgTe/CdTe Superlattices through the Pressure Dependence of the Photoluminescence. <i>H. M. Cheong, J. H. Burnett, and W. Paul</i>	111
2. Structure of the Si/SiO ₂ Interface. <i>T. Rabedeau, I. Tidswell, and P. S. Pershan</i>	113
3. Fluxon Motion in Superconducting Junction Arrays. <i>M. Tinkham</i>	117
4. A Comprehensive Study of Electromagnetic Methods for the Detection of Submerged Submarines. <i>R. W. P. King and T. T. Wu</i>	120

I. SOLID STATE ELECTRONICS

Personnel

Prof. H. Ehrenreich	Dr. M. Tuominen
Prof. J. A. Golovchenko	Dr. M. Ziegler
Prof. W. Paul	Mr. N. Anand
Prof. P. S. Pershan	Mr. H. Cheong
Prof. M. Tinkham	Ms. N. Hecker
Prof. R. M. Westervelt	Mr. S. Kosowsky
Dr. J. H. Burnett	Ms. S. K. Leonard
Dr. E. Ganz	Ms. R. Seshadri
Dr. P.-M. Hui	Mr. I. Tidswell
Dr. C. M. Marcus	Mr. F. R. Waugh
Dr. T. Rabedeau	Mr. P. M. Young
Dr. M. S. Rzchowski	

I.1 Electronic Theory of Semiconductor Microstructures and Superlattices. H. Ehrenreich, Grant N00014-89-J-1023; Research Unit 1.

During the past year the research efforts of H. Ehrenreich's group have concentrated on two topics. The first concerns the electronic and optical properties of superlattices. This work is strongly focussed on the calculation of exciton effects and what can be learned from them. We have been able to show that it is possible to use the results to infer information about band offsets and the existence of possible internal electric fields induced during the superlattice growth process. The second topic represents a new ingredient for this research program. It concerns the electrical, optical and noise properties of semiconductor nanostructures, in particular, double barrier quantum wells. We are currently investigating properties such as the peak/valley ratio of the current voltage characteristic, the tunneling time, and the effects of alloy and phonon effects on coherent tunneling. The signal/noise ratio is bound to be a problem in such delicate structures. Since such effects may well limit their utility in actual devices we have begun an investigation of noise processes in individual structures.

A. Optical Properties of III-V and II-VI Superlattices

Research concerning electronic structure and optical properties of superlattices was initially motivated by practical interest in infrared detectors like HgTe/CdTe. The III-V superlattices (SLs) are being considered because of their intrinsic importance and because much of the most reliable data exists for these materials.

A simple and versatile nonvariational approach for calculating SL exciton binding energies has been developed by the group utilizing the crystal coordinate representation and a basis consisting of SL Wannier functions [1]. This formalism underlines the utility of exploiting three-dimensional periodicity in calculating SL properties. It is applicable to type I, II, and III SLs with arbitrary layer widths and thus ranges from the thin barrier limit to the quantum well case. In order to perform the calculations nonvariationally it is assumed that the charge distributions associated with electron and hole Wannier functions are well described by uniformly charged rods with lengths corresponding to the extent of the respective Wannier function along the growth axis and a cross section determined by the constituent lattice constant. Judging from the extent of the agreement with both variational calculations and experiment for GaAs/GaAlAs and InGaAs/InAlAs SLs, this approximation is found to be very good if the Wannier function along the growth direction is confined to a single well and the neighboring barriers.

The previously used computer codes [2] have been completely rewritten to permit calculations of the electronic structure and optical properties for any zincblende SL using only ten minutes of computer time on a newly installed SUN system. In addition to excitonic effects, the optical absorption results take into account continuum state Coulomb effects described by the Sommerfeld factor. As before, the input parameters consist only of constituent bulk constants, band offsets, and, for the present generalization, excitonic line widths. Band structures and optical matrix elements are obtained from $k \cdot p$ theory in the envelope function approximation. The excitonic line

width at low temperatures is well explained by assuming island-like interfaces having a roughness of a single layer width.

The agreement between theory and experiment is remarkable. Of the twelve III-V systems for which absolute absorption coefficient measurements exist, we have been able to explain eleven quantitatively. Exciton line positions agree within 2-3 meV and the magnitude of the absorption coefficient is within 10%. Since the twelfth sample, for which agreement was not obtained, is an early one, it may be that its quality is inferior to the others that have been considered.

This theoretical analysis suggests that optical absorption measurements may be useful as an aid in SL characterization. Two examples follow:

Band Offsets: Results for the III-Vs show that it is possible to set limits on band offsets by computing the absorption coefficient for different values of the offset and comparing with experiment. This procedure produces excellent agreement for the III-Vs and may therefore also be applicable to II-VI SLs and III-V, II-VI heterostructures.

Superlattice Growth Imperfections: Small, hitherto unexplained structure in the absorption coefficient can be accounted for by postulating that electric fields of the order of 10^4 V/cm may be incorporated in a SL, presumably during the growth process. This structure is present to varying degrees in all samples considered except one due to Chemla and Miller's group at AT&T Bell Labs.

We emphasize that the exploration of such effects is possible only because of the modest computer requirements for implementing this type of systematic analysis. While comparison with the large scale and time intensive computer codes utilized by some other groups certainly helps to provide confidence in the present results, these programs do not have the required flexibility to investigate the kind of subtle effects mentioned here within reasonable time constraints. A survey of potentially interesting SL material combinations that have not been investigated experimentally

to any appreciable degree is therefore possible since the theory is apparently predictive. This fact is of particular importance in candidate materials like (Zn,Cd)Se/ZnSe and related systems such as CdTe/MnTe of interest in blue-green lasers for which reliable experimental data are only becoming available now.

Two papers describing these results are nearing completion. One of these will be submitted for publication before (7/91).

References:

1. N. F. Johnson, "Excitons in Superlattices," *J. Phys. Condens. Matter* **2**, 2099 (1990).
2. N. F. Johnson, H. Ehrenreich, P. M. Hui and P. M. Young, "Electronic and Optical Properties of III-V and II-VI Semiconductor Superlattices," *Phys. Rev.* **B41**, 3655 (1990).

B. Superlattice Strain and Other External Field Effects

The above results pertain to unstrained SLs. Strained SLs can be beneficial to exciton stability by increasing band offsets. Accordingly we have begun a generalization of the existing computer codes to include strain effects within perturbation theory using known deformation potentials. We have also included the effects of external electric fields and the concomitant Stark shifts and splittings. These modifications are relatively straightforward and do not lengthen computer time, and hence affect the flexibility of this approach, appreciably.

C. Superlattice Band Offsets

Some time ago, we resolved the valence-band offset controversy in HgTe/CdTe superlattices by showing that the large valence band offset observed by photoemission ($\sim 350\text{--}400$ eV) is consistent with magneto-optical data which was previously thought to reflect a much smaller value (~ 40 meV) [1]. This is due to the fact that, as had been appreciated, the SL becomes semimetallic as the offset is increased, but for even larger values *reverts* to semiconducting behavior. A recent paper [2] reopened the

controversy with data for other samples. Despite assertions to the contrary in that paper, we have shown that the consistency with larger offsets remains valid [3].

References:

1. N. F. Johnson, P. M. Hui and H. Ehrenreich, "Valence Band Offset Controversy in HgTe/CdTe Superlattices: A Possible Resolution," *Phys. Rev. Lett.* **61**, 1993 (1988).
2. J. B. Choi, L. Ghenim, R. Mani, H. D. Drew, K. H. Yoo and J. T. Cheung, *Phys. Rev.* **B41**, 10872 (1990).
3. P. M. Young and H. Ehrenreich, "Additional Evidence Concerning the Valence-Band Offset in HgTe/CdTe", *Phys. Rev.* **B43**, 12057 (1991).

D. Diluted Magnetic Semiconductors

Consideration of these materials has been completed. The last of a sequence of papers dealt with the electronic structure of superlattices incorporating diluted magnetic semiconductors by including the effects of d bands explicitly [1]. These results may be useful in considerations of blue-green laser candidate materials.

Reference:

1. P. M. Young, H. Ehrenreich, P. M. Hui and K. C. Hass, "Electronic Structure of Superlattices Incorporating Diluted Magnetic Semiconductors", *Phys. Rev.* **B43**, 2305 (1991).

E. Electronic Transport in Semiconducting Nanostructures

Research concerning electronic transport in double barrier quantum well (DBQW) nanostructures has begun only during the past year. Because of tunneling effects, the theoretical approach involves a Green's function-based quantum transport theory. In the negative resistance region, for example, external biases are sufficiently large that the formalism must include nonlinear response effects. The approach used here is closely related to that developed for theoretical analyses of laser action.

The goals of this work are investigations of (1) coherent vs. sequential tunneling in DBQWs; (2) the effects of alloy and phonon scattering in the well as they influence tunneling processes; (3) the current-voltage characteristics, in particular, the peak to

valley ratio; (4) the time required for tunneling, which can be defined either as a transit time as determined by optical differential absorption spectroscopy [1] or, in our view, in terms of a time reflecting the phase lag in the frequency response to small AC fields applied in addition to the biasing field; and (5) electrical noise characteristics of individual structures.

The model used visualizes the well structure to consist of "chains" of molecules reflecting the quantization of well states along the growth direction. These chains consist of III-V molecules constituting the well alloy and arranged in random order. The energies of the chains have a Gaussian distribution. The resulting two-dimensional arrangement of chains is treated within the coherent potential approximation. At present, investigations of phonon scattering still neglect important dynamical effects. The model for the electron phonon interaction is similar in some respects to that used in Sumi and Toyozawa's analysis of the Urbach tail problem.

Some results have been obtained for all of the topics listed above. These results will help guide the future direction of the present research. For example, we have shown that the shot noise spectrum for a DBQW is explicitly frequency dependent because of the correlation between incoming and outgoing electrons.

Because these investigations represent a new departure for the group and involve theoretical techniques with which we have had to become familiar, there have been no publications as yet. However, calculations for the DC response are sufficiently far along that two papers are currently in preparation.

In addition to the items on the list above, further work will involve the effects of Coulomb interactions in the well on device speed and investigations of the possible properties of three terminal devices.

Reference:

1. I. Bar-Joseph, T. K. Woodward, D. S. Chemla *et al.*, *Superlattices and Microstructures* **8**, 409 (1990).

**ANNUAL REPORT OF
PUBLICATIONS/PATENTS/PRESENTATIONS/HONORS**

b. Papers Published in Refereed Journals

N. F. Johnson, "Excitons in Superlattices," *J. Phys. Condens. Matter* **2**, 2099-2104 (1990).

P. M. Young, H. Ehrenreich, P. M. Hui, and K. C. Hass, "Electronic Structure of Superlattices Incorporating Diluted Magnetic Semiconductors," *Phys. Rev.* **B43**, 2305 (1991).

P. M. Young and H. Ehrenreich, "Additional Evidence Concerning the Valence-Band Offset in HgTe/CdTe," *Phys. Rev.* **B43**, 12057 (1991). (Partially supported by N00014-89-J-1023 and N00014-86-K-0033.)

c. Books (and sections thereof) Submitted for Publication

H. Ehrenreich, "Solid State Physics," an article in *Academic Press Dictionary of Science*, in press.

d. Books (and sections thereof) Published

H. Ehrenreich and D. Turnbull, editors, *Solid State Physics*, Vols. **44/45** (Academic Press, 1991).

h. Contributed Presentations at Topical or Scientific/Technical Society Conferences

E. Runge and H. Ehrenreich, "Influence of Alloy- and Phonon-scattering on Tunneling Transport," 1991 March Meeting of the American Physical Society, March 18-22, 1991.

P. M. Young, P. M. Hui, and H. Ehrenreich, "Excitons and Inter-band Transitions in III-V Superlattices," 1991 March Meeting of the American Physical Society, March 18-22, 1991.

j. Graduate Students and Postdoctorals Supported under the JSEP for the Year Ending July 31, 1991

Drs. Pak-Ming Hui and Michael Ziegler, and Mr. Paul M. Young.

I.2 Pressure Dependence of Photoluminescence and Photoluminescence Excitation in Quantum Wells and Superlattices. J. H. Burnett, H. M. Cheong, and W. Paul, Grant N00014-89-J-1023; Research Unit 2.

A. GaAs/Al_xGa_{1-x}As Quantum Wells

This work has been successfully completed, embodied in the thesis of J. H. Burnett, and written up for journal publication.

B. Pressure Media

The pressure-transmitting medium conventionally used in the early research using diamond anvil cells at room temperature was a 4:1 methanol-ethanol mixture, which remained hydrostatic up to 104 kbar. Subsequently, it was shown that He, Ne and H₂ extended the range of nearly hydrostatic pressure to ~ 500 kbar. For low temperature work, Ar was generally recommended, and it was assumed that the methanol-ethanol mixture was unsuitable.

Our pressure measurements at low temperature using Ar led us to question its suitability. We have now carried out a study of the broadening of the R1 luminescence line of ruby, and of the photoluminescence peak in GaAs/Al_{0.3}Ga_{0.7}As quantum wells, at 4.6 K to pressures of approximately 30 kbar. The methanol/ethanol mixture and also Xe, Ar and He were used as pressure transmitting media. The criterion for suitability as a medium was that the PL lines not broaden *when the pressure was changed at low temperature*. Only the He passes this rigorous test. Our published paper has generated a vigorous correspondence, and our conclusions are widely accepted. It should be noted that, if pressure is applied, the temperature lowered, and the pressure is not then changed, the FWHM of the PL is found to be slightly increased at high pressures for the Ar and the methanol-ethanol mixture, and unchanged for He. Thus, He is the best pressure medium for low temperature, high pressure experimentation. However, if facilities for use of He are not available, then — contrary to the previous

belief that methanol-ethanol was unusable at low temperatures — it is as good as Ar, and, in fact, is preferable because of its easier manipulation.

C. Photoluminescence of CdTe

As a preliminary to our projected work on HgTe/CdTe superlattices, we considered it necessary to determine an accurate pressure dependence of the band gap of undoped CdTe at low temperature. Previous measurements had determined the pressure dependence of the gap in undoped material at room temperature and in doped material at low temperature.

A sample of undoped material, ground, polished and etched to a rectangular shape of $150 \mu\text{m} \times 100 \mu\text{m}$ and $\sim 35 \mu\text{m}$ thick, was measured at 80 K in a diamond anvil cell which contained a ruby chip to determine pressure. A 4:1 methanol-ethanol mixture was used to transmit pressure; for each measurement, the pressure was changed at room temperature and the value determined at 80 K.

A single peak near the known band-gap energy is attributed to band-to-band recombination, although corrections for a small Stokes shift and excitonic binding effects might be made; these are not expected, on theoretical grounds, to alter the band-gap pressure coefficient. The variation of the band gap with pressure to above 38 kbar is best fit to a quadratic function:

$$E_g(P) = 1.578 + 8.57 \times 10^{-3} P - 4.78 \times 10^{-5} P^2 ,$$

where P is measured in kbar and E_g in eV. For pressures below 20 kbar, the gap increases almost linearly with a linear pressure coefficient of 7.9 ± 0.2 meV/kbar. These results are satisfactorily consistent with earlier studies.

We have also confirmed that a phase transition occurs near 39 kbar which destroys the photoluminescence.

D. Photoluminescence of HgTe/CdTe Superlattices

In order to study the PL of HgTe/CdTe superlattices, a new infrared pressure system was set up. The infrared range of the dispersion spectrometer used was from 6 to 14 μm . A type IIA diamond, transparent in this wavelength range, was bought for the pressure cell. For better sensitivity, we have substituted an IR Associates HgCdTe infrared detector for our earlier Ge:Cu detector. The samples studied were obtained from Professor J. Schetzina at North Carolina State University, but the finishing of the samples to a size suitable for installation in our pressure vessel was carried out by us. Measurements of the PL at 80 K but at ambient pressure gave a large peak near 10 μm , which is consistent with the measurements of other groups on similar samples. The largest peak is usually ascribed to the lowest superlattice transition, and its energy considered in satisfactory agreement with theoretical estimates. As we shall describe, it appears that this identification may have to be revised.

Figure I.1 shows how the PL spectrum changes as the pressure is raised to ~ 14 kbar: (1) the peak dominant at ambient pressure shifts slowly to higher energy (the actual rate is ~ 1 meV/kbar) and decreases in intensity, (2) a new peak appears at lower energy, and it too shifts slowly to higher energy, at approximately the same rate. However, its intensity increases with pressure, and it becomes the dominant peak at the top pressure, (3) a peak which is present at high energy in the ambient pressure spectrum shifts to higher energy with pressure at what appears to be a higher rate; however, there are too few points near the top pressure for this to be certain.

These results are significant in view of calculations carried out by Mr. Paul Young of Professor Ehrenreich's group using the envelope function approximation and assuming a pressure coefficient of the HgTe (buried) band gap at P of 10 meV/kbar. Mr. Young's calculations yield a predicted pressure coefficient for the lowest superlattice transition of ~ 5 meV/kbar and suggest that the shift in energy be nonlinear with pressure. This is inconsistent with our observations, leading us to conclude, either

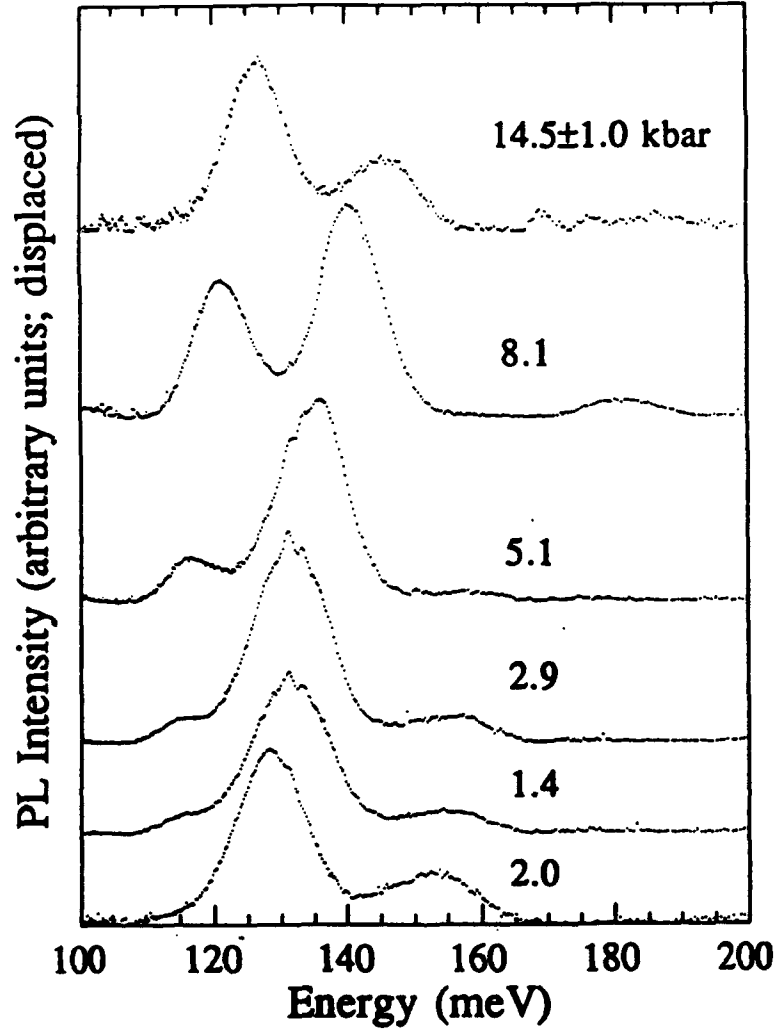


Figure 1.1. Photoluminescence Spectra of a HgTe/CdTe Superlattice as a Function of Pressure at Low Temperature.

(1) if the usual assignment of the strong PL peak to the fundamental SL transition is correct, then the envelope function approximation may be an inappropriate vehicle to determine it and its pressure coefficient, or (2) if the envelope function approximation is appropriate, then our assignment of the strong PL peak at atmospheric pressure to the fundamental SL transition is incorrect. The practice in the literature of assigning the strongest PL peak to the fundamental SL transition is a dangerous one. Finally, (3) the use of the envelope approximation to calculate the band gap and its

pressure coefficient may be inappropriate, because a defected atomic arrangement at the HgTe/CdTe interface is determining one or both of the band edge states.

It is to be noted that the spectra at different pressures show the existence of two quite narrow PL peaks of apparently different origin. The appearance of a strong PL peak at lower energy (than the one dominant at ambient pressure) at high pressure is not understood, yet the data of Figure I.1 show that there is no question concerning its independent existence. It is also to be noted that the shift with pressure of this peak is about the same as that of the peak dominant at atmospheric pressure, so that the remarks in (1) and (2) above apply also to this second peak.

More experiments are needed, with more pressure points and other samples. The precise (nonlinear?) pressure dependence of this highest energy peak needs to be more accurately determined. With more pressure points, fixing the shift with pressure of all three PL peaks with small error, the experiment will become a definitive test of the present theory for the SL band structure. The temperature dependence of the peaks should also be determined and compared with theory. In this respect, it is recalled that there already exists a discrepancy between the temperature dependence of the PL peaks and that of the absorption edge.

**ANNUAL REPORT OF
PUBLICATIONS/PATENTS/PRESENTATIONS/HONORS**

a. Papers Submitted to Refereed Journals (and not yet published)

J. H. Burnett, H. M. Cheong and W. Paul, "Study of Γ -X Wave Function Mixing in GaAs/ $\text{Al}_x\text{Ga}_{1-x}$ As Quantum Wells through the Pressure Dependence of Photoluminescence Excitation Spectroscopy of Coupled Double Quantum Wells," prepared for submission to *Physical Review B*.

H. M. Cheong, J. H. Burnett and W. Paul, "Pressure Dependence of the Photoluminescence of HgTe/CdTe Superlattices as a Test of their Band Structures," prepared for submission to *Journal of Applied Physics*.

b. Papers Published in Refereed Journals

J. H. Burnett, H. M. Cheong and W. Paul, "The Inert Gases Ar, Xe and He as Cryogenic Pressure Media," *Rev. Sci. Instrum.* **61**, 3904 (1990).

H. M. Cheong, J. H. Burnett and W. Paul, "Photoluminescence of CdTe under Hydrostatic Pressure," *Solid State Commun.* **77**, 565 (1991).

i. Honors/Awards/Prizes

William Paul was appointed Mallinckrodt Professor of Applied Physics, from 1 July 1991.

j. Graduate Students and Postdoctorals Supported under the JSEP for the Year Ending July 31, 1991

Dr. J. H. Burnett and Mr. H. M. Cheong.

I.3 X-ray Surface Characterization. I. Tidswell, T. Rabedeau, and P. S. Pershan, Grants N00014-89-J-1023 NSF DMR-88-12855, NSF DMR-89-20490, DOE DE-FG02-88-ER45379; Research Unit 3.

As electronic devices become smaller and smaller and the composite structures become increasingly complex, both the design and function of electronic devices are more and more dependent on the properties of surfaces [1]. To this end major research efforts are currently directed towards developing new, and improved, techniques for characterization of solid surfaces [2]. These include electron diffraction and electron microscopy as well as newer techniques such as tunneling electron microscopy and ion beam diffraction. On the other hand the only technique that currently appears capable of nondestructive characterization of the structure of buried interfaces appears to be X-ray scattering. There is now a growing literature dealing with the manner in which a combination of X-ray specular reflection, grazing incidence diffraction, and truncation rod studies have been used for these purposes [3].

The surface specificity of all of these X-ray scattering techniques is based on the fact that the optical properties of X-rays can be approximately described by a dielectric constant, $\epsilon \approx 1 - \rho_{\infty} r_e \lambda^2 / \pi$, where ρ_{∞} is the average electron density in the bulk of the material, λ is the X-ray wavelength and r_e is the classical radius of the electron [4]. If X-rays are incident at an angle θ with respect to the surface (i.e., defined such grazing incidence corresponds to $\theta = 0$) and if θ' is the corresponding angle of the refracted wave in the material, Snell's law has the form $\cos(\theta) = (\sqrt{\epsilon}) \cos(\theta')$. Since $\epsilon < 1$, the condition $\cos(\theta_c) = \sqrt{\epsilon}$ defines a critical angle such that for $\theta \leq \theta_c$ the only allowed values of the refracted angle θ' are imaginary. In analogy with the optical phenomena of total internal reflection, this corresponds to total external reflection. Typical values of θ_c for 8 to 10 keV X-rays are of the order of 0.2° , corresponding to $1 - \epsilon \cong 10^{-5}$.

For θ greater than three or four times the critical angle, that is for $\theta \geq 0.8^\circ$ the ratio between the reflected intensity $R(\theta)$ and the theoretical Fresnel Reflection

Law of classical optics $R_F(\theta)$ for a sharp flat surface with no structure is given by the relation:

$$\frac{R(\theta)}{R_F(\theta)} = \left| \rho_\infty^{-1} \int dz \left\langle \frac{\partial \rho}{\partial z} \right\rangle \exp[-iQ_z z] \right|^2$$

where $Q_z = (4\pi/\lambda) \sin(\theta)$; $R_F(\theta) \approx (\theta_c/2\theta)^4$ when $\theta \gg \theta_c$. For a rough, or diffuse surface $\rho_\infty^{-1} \langle \partial \rho / \partial z \rangle \approx (\sqrt{2\pi\sigma^2})^{-1/2} \exp(-z^2/2\sigma^2)$ and the decay of $R(\theta)/R_F(\theta)$ with increasing θ is reminiscent of a Debye-Waller effect; e.g., $R(\theta)/R_F(\theta) \approx \exp(-Q_z^2 \sigma^2)$. In cases where there is some sort of layering at the surface, as for liquid crystals or most solid surfaces, there are oscillations in the z -dependence of $\rho_\infty^{-1} \langle \partial \rho / \partial z \rangle$ and the Fourier transform of these gives rise to maxima and minima in the angular, or Q_z , dependence of the specular reflectivity $R(\theta)$. The real space structure of the electron density, along the surface normal, can be derived from the measured Q_z dependence of the reflectivity $R(\theta)$. Thus specular reflectivity is a relatively straightforward and direct method for probing the x - y average of the structure along the surface normal (i.e., the z -direction) for both crystalline and amorphous surfaces. In particular, in the case of a thin layer of electron density ρ_1 and thickness d , on top of a bulk material of electron density ρ_∞ , the specular reflectivity will be an oscillatory function of θ , or Q_z , with period $\Delta Q_z \cong 2\pi/d$ and amplitude that depends on $(\rho_1 - \rho_\infty)$ [5]. Thus this is one direct way to measure the thickness of thin layers of either amorphous or crystalline surface layers. Depending on the intensity of the X-rays this technique is practical for films anywhere from $\sim 1\text{\AA}$ to 1000\AA thick.

If the spectrometer is slightly tuned off of the specular condition, for example by moving the detector such that detected X-rays make an angle $\theta'' \neq \theta$ it is possible to study either diffuse scattering from disordered surface irregularities, or diffraction from long wavelength features such as regularly ordered surface steps. In this geometry, with the detected radiation in the plane of incidence, the characteristic length scales vary typically from $\sim 100\text{\AA}$ to $10\text{ }\mu\text{m}$ [6,7].

Grazing incidence diffraction (GID) is based on the idea that when the incident

angle $\theta < \theta_c$ the incident beam is $\sim 100\%$ reflected, and the X-rays only penetrate below the surface as $\sim \exp(-\kappa z)$; where $\kappa \cong (2\pi/\lambda) \sqrt{\theta_c^2 - \theta^2}$ is typically of the order of 0.02 \AA^{-1} . If the detector is moved out of the plane of incidence by an angle Ψ , and above the plane of the surface by an angle θ'' , scattering is observed at a wavevector transfer with components $Q_z \cong (2\pi/\lambda) \sin \theta''$ and $Q_{\perp} \cong \sqrt{1 + \cos^2 \theta'' - 2 \cos \theta \sin \Psi}$. Since the incident radiation does not penetrate distances much larger than $1/\kappa$, the Q_{\perp} dependence of the scattering can be analyzed to determine the atomic structure parallel to, and within a distance $1/\kappa$ from, the surface [8,9].

From the way in which it depends on the detector angle θ'' , the scattering can be analyzed to give information on the way in which the in-plane surface order varies with distance along the surface normal. This gives information on the structure along the normal within deposited surface layers and the spatial relationship between the adsorbed layers and the crystalline lattice.

Some experimental studies on surface structure along the surface normal at $Q_{\perp} = 0$ can be carried out by specular reflectivity measurements at the Harvard Materials Research Laboratory Rotating Anodes X-Ray Facility, however most of the studies must eventually be completed using the higher intensity, and other properties, of synchrotron radiation. To this end a significant fraction of our experimental program is carried out at the National Synchrotron Light Source, Brookhaven National Laboratory.

This project has been carried out in collaboration with Dr. Jose Bevk of AT&T Bell Laboratories. Samples are prepared by Dr. Jose Bevk of AT&T Bell Laboratories in a high vacuum MBE chamber with multiple surface sensitive probes. Following preparation and characterization using the standard surface methods the samples are transferred to the special purpose portable UHV X-ray cell and transported to NSLS under UHV conditions for X-ray measurement. If necessary the sample can eventually be returned to the AT&T MBE chamber without exposure to non-UHV atmosphere.

During the present report period we extended our previous studies of the structure of the Si/SiO₂ interface by making a set of measurements on the effect of exposing the MBE-prepared dry-oxidized sample to wet, or humid, room air. Following that we completed the theoretical analysis of these and previous results and have prepared two papers for publication [10,11].

The first of these papers deals with diffraction measurements of the in-plane-interfacial order at the SiO₂/Si(001) interface for dry oxides grown on highly ordered Si surfaces at room temperature. Grazing incidence diffraction (GID) peaks were observed for 21 fractional order momentum transfers of the form $[m/2, n/2, 0]$ with m, n odd integers; the momentum transfers are expressed in terms of bulk reciprocal lattice units ($1 \text{ rlu} = 1.157 \text{ \AA}^{-1}$). For 17 of these peaks it was possible to carry out transverse, or "rocking scans" in order to obtain reliable measures of their intensities. The absence of detectable signals above background at in-plane momentum transfers of the form $[m, 0, 0]$ and $[m/4, n/4, 0]$ indicates that the scattering is due to interfacial regions with 2×1 (and coexisting 1×2) order rather than either 2×2 or $4 \times i$ (where i is an integer) order. Rod scans along the surface normal were carried out for the $(\pm 1/2, 1/2, q)$, and $(1/2, 3/2, q)$. The absence of intensity modulations along any of these indicates that the 2×1 interfacial structure is no thicker than ~ 2 to 3 \AA . Quantitative analysis of the absolute intensities for the three rod scans at fractional-in-plane wavevector transfer indicate that the ordered interfacial regions cover only ~ 8 to 10% of the surface. The fact that the coverage decreases significantly if the surface is exposed to moist air or if it is subjected to a mild thermal anneal suggests that the interfacial order is only metastable. These data are not consistent with proposals relating the interfacial order to variants of either bulk cristobalite [12] or tridymite [13].

Table I.1 lists a comparison between the GID intensities measured on the dry oxidized wafer, corrected for viewed area and Lorentz factors, and the predictions of

two models for the interfacial order. Rocking scans were obtained for 17 different in-plane fractional order peaks; however, since some of these are related by symmetry operations there are only eight physically independent intensities. These models were developed by considering various distortions of the symmetric dimer model for the bare Si(001) surface [14]. Model I corresponds roughly to a 21° rotation of the dimer axis about the surface normal with a slight contraction of the dimer bond length. The interlayer spacing between the dimer and the underlying plane of Si atoms was fixed at the symmetric dimer model value of 1.15\AA . A slightly better fit to the data was obtained with model II which incorporated oxygen. A sketch of the 1×2 interfacial unit cell is shown in Figure I.2.

Table I.1:
Comparison between measured and
model intensities for fractional order surface peaks

(h,k)	Measured	Model I	Model II
(-1/2,1/2)	1000 ± 127	977	971
(-3/2,3/2)	1220 ± 155	819	1379
(-1/2,5/2)	63 ± 8	62	68
(1/2,3/2)	351 ± 32	347	313
(3/2,5/2)	140 ± 15	164	127
(1/2,7/2)	156 ± 28	126	168
(5/2,7/2)	32 ± 8	38	42
(3/2,9/2)	75 ± 24	58	63

The second paper was concerned with specular reflectivity, or the $(0,0,q)$ rod scan, and $(\pm 1,1,q)$ bulk truncation rod scans. On the basis of the specular reflectivity we conclude that the total thickness of the "native" dry oxide is approximately 5\AA with a 1\AA thick interface between the oxide and the vacuum. This layer consists of some combination of regions of amorphous and ordered SiO_2 . The data are best represented by a model in which the residual laminar order in the electron density of

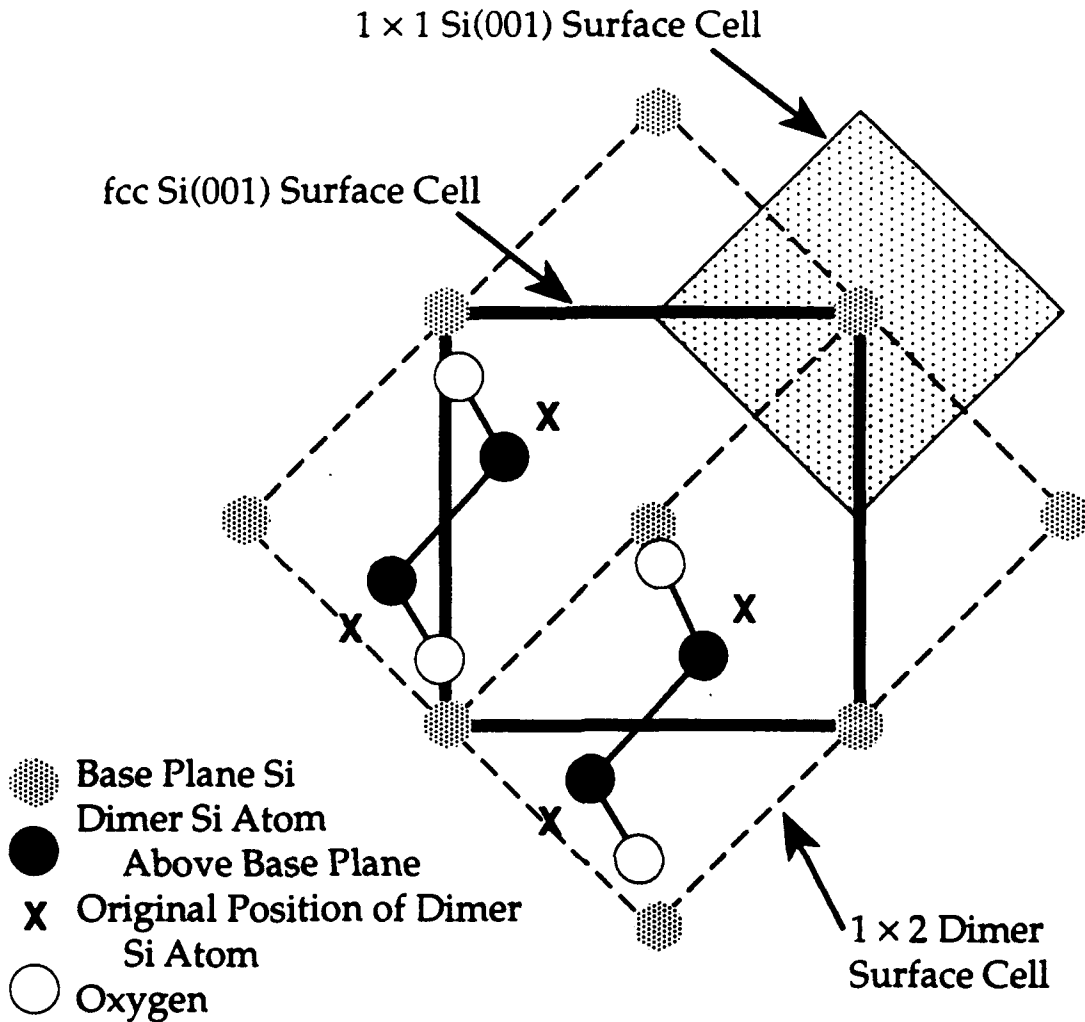


Figure I.2. Sketch of dimer model for ordered component of Si/SiO₂ interface.

the oxide decays exponentially with distance from the Si(001) interface with a decay length $\sim 2.7\text{\AA}$. Figure I.3 illustrates the results of transverse scans through the bulk truncation rods at the $(\pm 1, 1, 0)$ positions. The multiple peaks result from highly ordered arrays of terraces separated by monatomic steps. Presumably these arrays are stabilized by the 0.05° miscut between the sample surface and the Si lattice. The solid lines represent a theoretical model for the step distribution. The observed differences between the two scans indicates that the steps are not along one of the principal axis of the substrate.

Finally, we are currently measuring the first Ge(001) sample that was formed

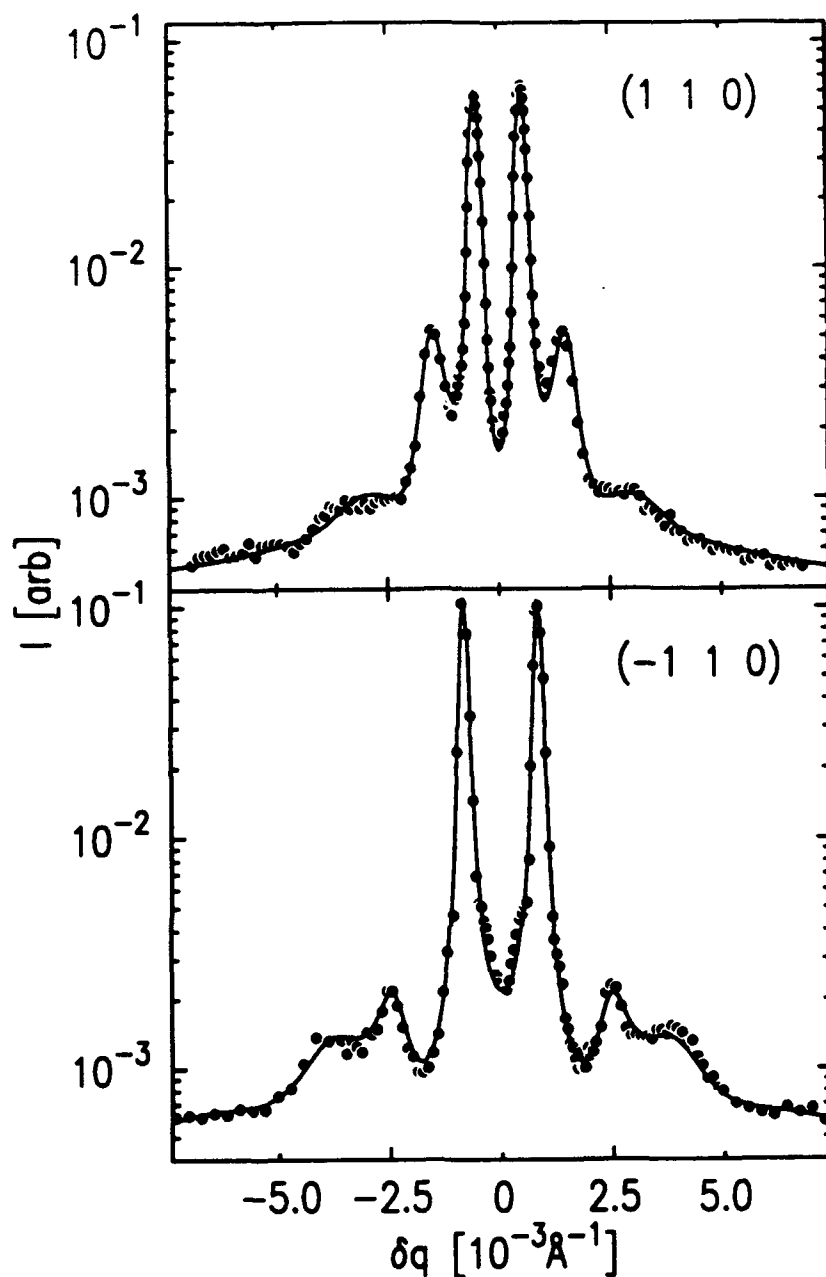


Figure 1.3. Transverse scans through the $(\pm 1, 1, 0)$ truncation rods of the $\text{SiO}_2/\text{Si}(001)$ interface. The oscillatory structure is caused by a regular array of terraces that are separated by monatomic steps. The differences between the two scans illustrate that the terraces are not along one of the symmetry axis of the substrate. The solid line represents the prediction of a model.

with a thin epitaxial layer of Si. The sample was exposed to dry O_2 which we believe should only have oxidized the Si. As a result we expect that the sample will consist of an epitaxial SiO_2 layer on the $\text{Ge}(001)$ surface. One motivation for studying this system is that the lattice parameter for epitaxial silicon on $\text{Ge}(001)$ is approximately 4% larger than that of $\text{Si}(001)$. We would like to determine whether an increase of

the lattice parameter will affect either the coverage of the ordered fraction of the SiO₂ layer on Si(001), which was only about 10% on the unstrained Si(001), or the thermal stability of the ordered fraction. The preliminary results from measurements currently taking place indicate that the sample surfaces are considerably rougher than the Si surfaces that we have previously studied. We believe this might be the consequence of a relatively larger mismatch between the Ge(001) lattice planes and the surface. One of the first objectives will be to obtain better oriented crystal. The present sample has only 2 atomic layers of Si and the oxidation was at a relatively high pO₂ and it will be necessary to systematically investigate the effects of varying pressure and temperature on the nature of the oxide. Further studies will deal with oxidation of epitaxial deposition on Si_xGe_{1-x} substrates. Almost any other possible electronically interesting interface can be studied by these same techniques and future choices for systems to study will be partially based on the technological issues that most interest our collaborators at AT&T.

References:

1. J. Bevk, J. P. Mannaerts, L. C. Feldman, and B. A. Davidson, *Appl. Phys. Lett.* **49**, 286 (1988).
2. See, for example, several articles in the Proceedings of a Symposium *Interfaces and Thin Films* at the National Academy of Sciences, Washington, D.C., March 23 and 24, 1987; *Proc. Natl. Acad. Sci. USA* **84**, 4665 (1987).
3. See, for example, several articles in *Structure of Surfaces and Interfaces as Studied Using Synchrotron Radiation*, *Faraday Discussions of the Chemical Society* **89**, (1990).
4. P. S. Pershan, "Structure of Surfaces and Interfaces as Studied using Synchrotron Radiation: Liquid Surfaces," *Faraday Discussions of the Chemical Society* **89**, 231 (1990).
5. P. S. Pershan, A. Braslau, A. H. Weiss and J. Als-Nielsen, "Smectic Layering at the Free Surface of Liquid Crystals in the Nematic Phase: X-ray Reflectivity," *Phys. Rev.* **A35**, 4800 (1987).
6. D. K. Schwartz, M. L. Schlossman, E. H. Kawamoto, G. J. Kellogg, P. S. Pershan, and B. M. Ocko, "Thermal Diffuse Scattering Studies of the Water-vapor Interface," *Phys. Rev.* **A41**, 5687 (1990).

7. M. K. Sanyal, S. K. Sinha, K. G. Huang, and B. M. Ocko, "X-ray Scattering Study of Capillary Wave Fluctuations at a Liquid Surface," *Phys. Rev. Lett.* **66**, 628 (1991).
8. W. C. Marra, P. E. Eisenberger, and A. Y. Cho, *J. Appl. Phys.* **50**, 6927 (1979).
9. See Reference 3 above.
10. T. A. Rabedeau, I. M. Tidswell, P. S. Pershan, J. Bevk and B. S. Freer, "X-ray Scattering Studies of the SiO₂/Si(001) Interfacial Structure," *Appl. Phys. Lett.* (to appear) (1991).
11. T. A. Rabedeau, I. M. Tidswell, P. S. Pershan, J. Bevk and B. S. Freer, "X-ray Reflectivity Studies of SiO₂/Si(001)," *Appl. Phys. Lett.* (submitted for publication).
12. F. Herman and R. V. Kasowski, *J. Vac. Sci. Technol.* **19**, 395 (1981).
13. A. Ourmazd, D. W. Taylor, J. A. Rentschler, and J. Bevk, "Si to SiO₂ Transformation: Interfacial Structure and Mechanism," *Phys. Rev. Lett.* **59**, 213 (1987).
14. J. A. Applebaum and D. R. Hamann, *Surf. Sci.* **74**, 21 (1978).

**ANNUAL REPORT OF
PUBLICATIONS/PATENTS/PRESENTATIONS/HONORS**

a. Papers Submitted to Refereed Journals (and not yet published)

M. V. Baker, G. M. Whitesides, I. M. Tidswell, T. A. Rabedeau, and P. S. Pershan, "Characterization of Self-assembled Monolayers of Sulfur-containing Alkylsiloxanes on Silicon by Low Angle X-ray Reflectivity," *Langmuir*, submitted (Partial support from DMR-86-14003)

T. A. Rabedeau, I. M. Tidswell, P. S. Pershan, J. Bevk, and B. S. Freer, "X-ray Scattering Studies of the SiO₂/Si(001) Interfacial Structure," *Appl. Phys. Lett.* (1991) to appear.

T. A. Rabedeau, I. M. Tidswell, P. S. Pershan, J. Bevk, and B. S. Freer, "X-ray Reflectivity Studies of SiO₂/Si(001)," *Appl. Phys. Lett.* (submitted for publication).

c. Invited Papers at Conferences

P. S. Pershan, "X-ray Scattering Studies of Liquid Surfaces," American Physical Society, Symposium on Chemical Physics, Cincinnati, 3/19/91.

P. S. Pershan, "X-ray Scattering Studies of Bulk Liquids and Thin Wetting Layers," National Synchrotron Light Source, 1991 Annual User's Meeting, Brookhaven National Laboratory, 5/21/91.

h. Contributed Presentations at Topical, or Scientific/Technical Society Conferences

T. A. Rabedeau, I. M. Tidswell, P. S. Pershan, J. Bevk and B. S. Freer, "X-ray Scattering Studies of the Si(001)/SiO₂ Interface Structure," Proceedings of the Conference *Advances in Surface and Thin Film Diffraction*, Symposium J, MRS Fall Meeting, Materials Research Society, Boston, 1990.

j. Graduate Students and Postdoctorals Supported under the JSEP for the Year Ending July 31, 1991

Mr. Seth Kosowsky, Mr. Ian Tidswell and Dr. Tom Rabedeau

I.4 Superconducting Josephson Junction Arrays. M. S. Rzchowski, L. L. Sohn, and M. Tinkham, Grants N00014-89-J-1023, N00014-89-J-1565, and DMR-89-12927; Research Unit 4.

The focus of our work in this area has shifted from the d.c. properties of pinning and critical currents of SNS arrays in the presence of strongly commensurate magnetic fields, to the response of these arrays to high-frequency radiation in the presence of such fields. (Strongly commensurate field values are those for which the imposed flux per unit cell of the array is a fraction $f = p/q$ of the flux quantum $\Phi_0 = hc/2e$, in which p and q are small integers.)

When we apply an a.c. current with frequency ν in the kHz to MHz range to our $N \times N$ ($N = 1000$) arrays, we find that the d.c. I-V curve displays "giant Shapiro steps" [1] at voltages equal to N times the step voltage $h\nu/2e$ for a single Josephson junction driven at the same frequency. Although the regularity of these data are evidence for the high perfection of our arrays, such effects are not new. What we have observed that is new and unexpected is that application of a strongly commensurate d.c. magnetic field $f = p/q$ (such as $f = 1/2$ or $1/3$) causes the appearance of *fractional* giant Shapiro steps at voltages that are multiples of $(N/q)h\nu/2e$. Qualitatively, it is plausible that these fractional giant Shapiro steps result from the systematic motion of the $q \times q$ vortex superlattice (which is the minimum energy configuration for $f = p/q$) across the array in synchronism with the a.c. driving current. The essence of the argument is that if it takes q r.f. cycles to translate the superlattice pattern through q cells, resulting in coincidence with the starting fluxon configuration, the d.c. voltage of the step will correspond to that of an ordinary giant step at a frequency lower by a factor of $1/q$ than the actual drive frequency. We have confirmed this interpretation by means of detailed simulations [2] which follow the time evolution of the phase differences across the various Josephson junctions in the array.

These experimental demonstrations of *coherent* dynamics across these large 2-dimensional arrays suggest possible applications of arrays as efficient generators and detectors of electromagnetic waves. In fact, by going to 10×10 arrays of similar geometry but made with SIS junctions instead of SNS junctions, Benz (now at NIST, Boulder, after finishing his Ph.D. in the JSEP program here) has recently experimentally demonstrated generation of $\sim 1 \mu\text{W}$ of power, voltage-tunable from 60 to 210 GHz as expected. This power level is near the theoretical limit for coherent emission from this array, which suggests that more power should be obtainable from larger arrays [3].

In the past year, our major new work has been to fabricate a series of 2-dimensional array samples with different geometries and current feed directions (see Fig. I.4), and study their r.f.-response. In these experiments, the arrays are all macroscopically rectangular ($1 \text{ mm} \times 10 \text{ mm}$) with current feed along the long direction, but the internal geometry is modified. In the first variation (Fig. I.4b), the square unit cells ($10 \mu \times 10 \mu$) of junctions were oriented so that the direction of the macroscopic current is along the unit cell *diagonal* ($\langle 11 \rangle$ -direction), whereas in all our previous work the $\langle 10 \rangle$ -direction of the underlying unit cells was oriented along the macroscopic current direction. When we measured the giant Shapiro steps of these new diagonal arrays in the presence of a perpendicular magnetic field giving a strongly commensurate flux density, such as $f = 1/2$ (i.e., $1/2$ flux quantum per unit cell), we were very surprised to find that their properties were entirely different than the previously studied $\langle 10 \rangle$ arrays: *no fractional steps at all were observed* with the diagonal current feed! The absence of the fractional steps was puzzling, since the qualitative explanation seemed rather general, leading us to expect the same behavior in the arrays with diagonal current feed. Moreover, theoretical work by Halsey [4] had predicted that this would be the case.

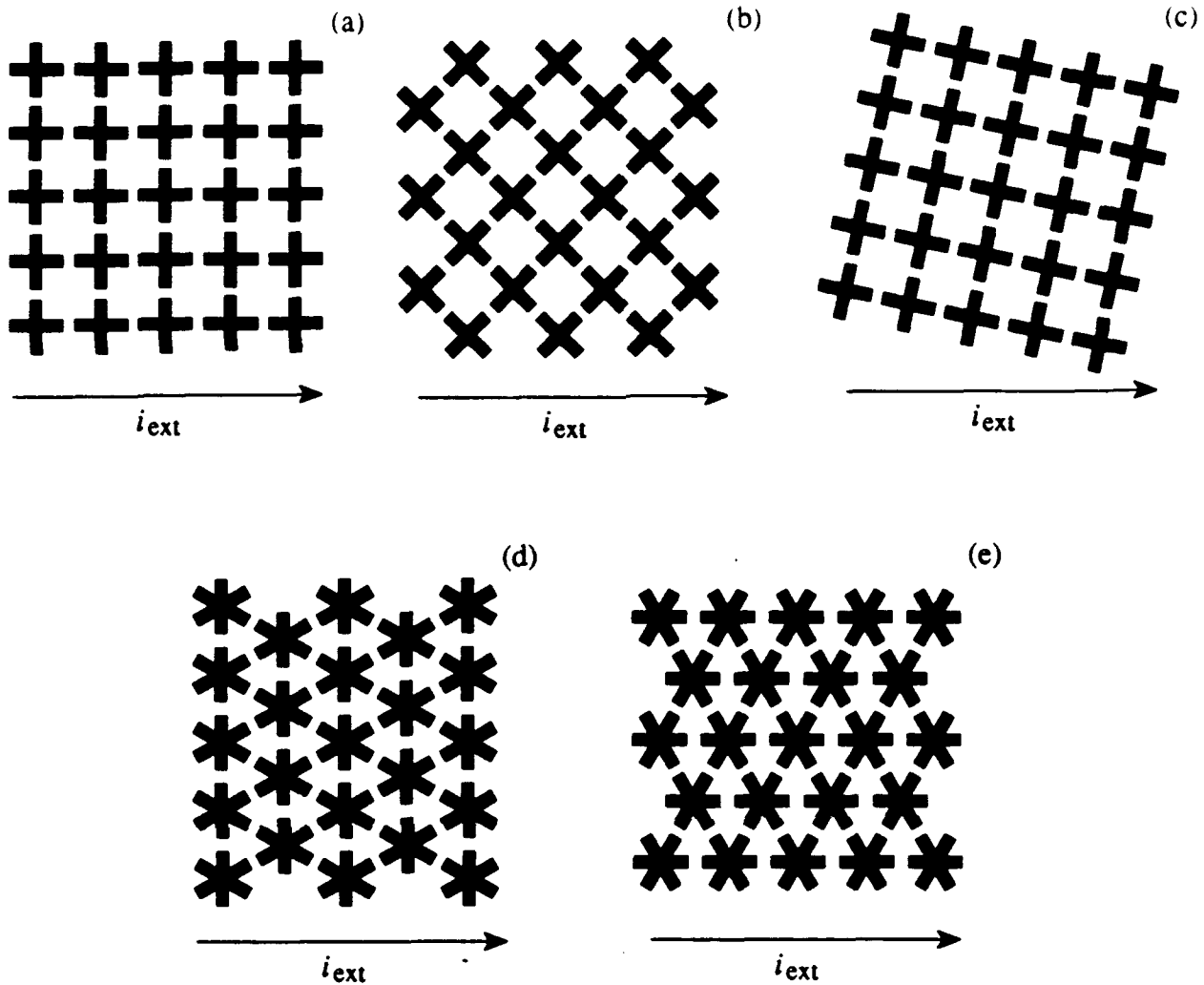


Figure 1.4. Segments of the various array configurations described in text. The black crosses and asterisks are the Nb islands, which are coupled by proximity effect superconductivity through the underlying Cu film, forming SNS Josephson junctions. The length of the junction gap is $2 \mu\text{m}$ in all cases; the lattice constant is $10 \mu\text{m}$ in the square arrays and $16 \mu\text{m}$ in the triangular arrays.

To find an explanation for this surprising behavior, we attacked the problem with both digital simulations on relatively small arrays and by analytic means, concentrating on the simple but important case of $f = 1/2$. Our simulations confirm the absence of fractional steps with the diagonal current feed pattern, eliminating any possibility that the experimentally observed effect was due to some defect in the arrays. They also confirmed the dominance of time-varying “ladder” current patterns, which alternated (during a single cycle of the r.f. current) between forming a vortex superlattice and other patterns with no obvious vorticity. From study of these patterns we found that at

$f = 1/2$ an analytic solution should be possible with a 2×2 superlattice cell repeating to form a periodic pattern of currents. Dynamic equations could be solved for this case at low drive frequencies, which reduced the problem to that of a *single* driven Josephson junction, which has long been known [4] to show no subharmonic responses. This reduction provides a mathematical explanation of the missing fractional steps. Such a reduction to a single junction problem does not occur for $\langle 10 \rangle$ arrays, explaining the difference in behavior. This work has been accepted for publication as a Rapid Communication in *Phys. Rev. B*.

To gain further understanding of this surprising dependence upon the current direction, we subsequently fabricated other array geometries. In the first (Fig. I.4c), we retained the square array structure, but rotated it only 15° instead of the full 45° . As might be expected, the results were intermediate to the previous cases: very weak fractional steps were observed. Next, we changed the array pattern from square to triangular, with each superconducting island having an "asterisk" shape, surrounded by 6 other islands. Again, we found a strong dependence on current direction. For current along the $\langle 10\bar{1} \rangle$ direction (Fig. I.4d), fractional steps were observed, while none were observed for current along the $\langle 2\bar{1}\bar{1} \rangle$ direction (Fig. I.4e), only 30° away.

Combining this new information with that from the two previous configurations, we conclude that fractional steps are most prominent in configurations containing junctions perpendicular to the macroscopic current flow; they are least visible when all junctions participate equally in carrying the current, so that symmetry is preserved even in the presence of the current. Another insight which has been obtained [6] by analysis of the regular square array response is that the fractional steps decrease sharply in amplitude for frequencies above the characteristic frequency $2eI_cR/h$, because then most of the current flows as a normal current, and there is very little current in the cross link junctions. This minimizes the importance of the moving vortices, and reduces the problem to a set of parallel 1-dimension chain arrays, which are known to

show only *integer* giant Shapiro steps. Our simple analytical results are in excellent agreement with supercomputer calculations made by others at the same time.

References:

1. S. P. Benz, M. S. Rzchowski, M. Tinkham, and C. J. Lobb, *Phys. Rev. Lett.* **64**, 693 (1990).
2. J. U. Free, S. P. Benz, M. Rzchowski, M. Tinkham, C. J. Lobb, and M. Octavio, *Phys. Rev.* **B41**, 7267 (1990).
3. S. P. Benz and C. J. Burroughs, *Appl. Phys. Lett.* **58**, 2162 (1991).
4. T. C. Halsey, *Phys. Rev.* **B41**, 11634 (1990).
5. M. J. Renne and D. Polder, *Revs. Phys. Appl.* **9**, 25 (1974).
6. M. S. Rzchowski, L. L. Sohn, and M. Tinkham, *Phys. Rev.* **B43**, 8682 (1991).

I.5 Single-Electron Tunneling Devices A. Hanna, M. Tuominen, and M. Tinkham, Grants N00014-89-J-1023, N00014-89-J-1565, and DMR-89-12927; Research Unit 4.

In a new effort, we are starting to explore the physics of single-electron tunnel devices. These require structures of such small capacitance (and hence size) that the Coulomb charging energy $e^2/2C$ of a single electronic charge dominates over thermal energies and quantum uncertainties. We are proceeding along two paths: fabricated submicron junctions and use of a scanning tunnelling microscope (STM) system. Our fabrication efforts (led by Tuominen) are being aided by a newly acquired SEM for use in *e*-beam pattern writing, and work is proceeding to identify optimum resists, exposures, and development procedures.

During the same period, Hanna has used his home-made STM at 4° K to obtain a large amount of extremely high quality I-V data, showing the "Coulomb blockade," the "Coulomb staircase," and "single-electron transistor action" in a double junction configuration. We have found it possible to interpret these data very successfully using the "orthodox" theory of Averin and Likharev [1] and a computer program created by Karatkov and Likharev. In the course of doing this, we have developed a new,

considerably simplified way [2] to use analytic predictions of this theory for $T \approx 0$ in the limiting case in which one of the two tunnel junctions connecting the isolated tiny bit of metal to the electrodes has much higher resistance than the other. This analysis enables us to make a rather direct interpretation of the I-V curve by first identifying which of 4 possible “cases” its shape belongs to, and then reading off the positions of corners and slopes of steps which allow determination of the parameters C_1 , C_2 , R_1 , R_2 , and Q_0 . Of these, the most controversial and poorly understood is the fractional residual charge Q_0 , which is required to explain asymmetries in the I-V curves, and which also controls the “transistor action” by modulating the small signal conductance of the device from zero to a finite value (see Fig. I.5). Our data show that Q_0 can be changed systematically by moving the point nearer or farther from the other electrode. This suggests that a more fundamental parameter may be a contact potential between the electrodes, which leads to a variation of Q_0 by several times e when we vary the capacitance by changing the point separation.

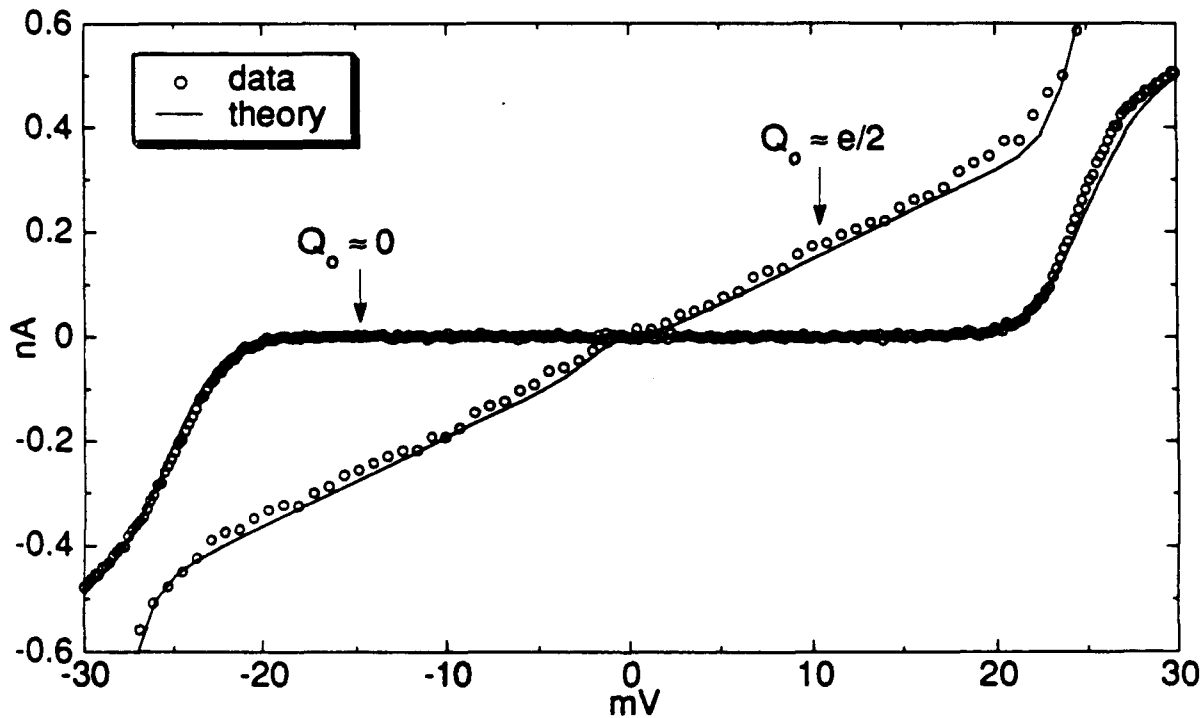


Figure I.5. Illustration of change of low-voltage conductance of device when the fractional residual charge is changed by half an electronic charge by changing the point separation in the STM.

References:

1. D. V. Averin and K. K. Likharev, in *Mesoscopic Phenomena in Solids*, Eds. B. L. Altshuler, P. A. Lee, and R. A. Webb, Elsevier, Amsterdam, 1991, p. 169.
2. A. E. Hanna and M. Tinkham, *Phys. Rev. B* (submitted).

ANNUAL REPORT OF
PUBLICATIONS/PATENTS/PRESENTATIONS/HONORS

a. **Papers Submitted to Refereed Journals (and not yet published)**

L. L. Sohn, M. S. Rzchowski, J. V. Free, S. P. Benz, and M. Tinkham, "Absence of Fractional Giant Shapiro Steps in Diagonal Josephson Junction Arrays," *Phys. Rev. B*, to appear.

M. B. Cohn, M. S. Rzchowski, S. P. Benz, and C. J. Lobb, "Vortex-defect Interactions in Josephson Junction Arrays," *Phys. Rev. B*, to appear.

T. S. Tighe, A. T. Johnson, and M. Tinkham, "Vortex Motion in Two-dimensional Arrays of Small, Underdamped Josephson Junctions," *Phys. Rev. B*, (submitted).

A. E. Hanna and M. Tinkham, "Variation of the Coulomb Staircase in a Two Junction System by Fractional Electron Charge" *Phys. Rev. B* (submitted).

b. **Papers Published in Refereed Journals**

M. S. Rzchowski, S. P. Benz, M. Tinkham, and C. J. Lobb, "Vortex Pinning in Josephson-junction Arrays," *Phys. Rev. B* **42**, 2041-2050 (1990).

S. P. Benz, M. S. Rzchowski, M. Tinkham, and C. J. Lobb, "Critical Currents in Frustrated Two-dimensional Josephson Arrays," *Phys. Rev. B* **42**, 6165-6171 (1990).

S. P. Benz, M. S. Rzchowski, M. Tinkham, and C. J. Lobb, "Fractional Giant Shapiro Steps in 2D Josephson Arrays," *Physica B* **165&166**, 1645-1646 (1990).

S. P. Benz, J. U. Free, M. S. Rzchowski, M. Tinkham, and C. J. Lobb, "Dynamical Simulations of Fractional Giant Shapiro Steps," *Physica B* **165&166**, 1647-1648 (1990).

A. T. Johnson, C. J. Lobb, and M. Tinkham, "Effect of Leads and Energy Gap upon the Retrapping Current of Josephson Junctions," *Phys. Rev. Lett.* **65**, 1263-1266 (1990).

L. Ji, M. S. Rzchowski, and M. Tinkham, "Microwave Surface Resistance and Vortices in High- T_c Superconductors: Observation of Flux Pinning and Flux Creep," *Phys. Rev. B* **42**, 4838-4841 (1990).

M. S. Rzchowski, L. L. Sohn, and M. Tinkham, "Frequency Dependence of Shapiro Steps in Josephson-junction Arrays," *Phys. Rev. B* **43**, 8682-8685 (1991).

c. **Books (and sections thereof) Submitted for Publication**

M. Tinkham, "Josephson Effects in Weak Links," article in *Concise Encyclopedia of Magnetic and Superconducting Materials*, edited by J. Evetts, Pergamon Press, to appear.

M. Tinkham, "Josephson Effect in Low-capacitance Tunnel Junctions," series of invited lectures at NATO ASI on *Single Charge Tunneling*, Les Houches, March 1991, to appear as chapter in book of same name by Plenum Press.

g. **Invited Presentations at Topical or Scientific/Technical Society Conferences**

M. Tinkham, "Flux Motion and Resistance in High-temperature Superconductors: An Overview," invited paper LT19 Conference, *Physica B169*, 66-71 (1991).

M. Tinkham, "Flux Motion and Dissipation in High Temperature Superconductors," invited paper Applied Superconducting Conference, Snowmass, CO; *IEEE Trans. Magn. MAG-27*, 828-832 (1991).

h. **Contributed Presentations at Topical or Scientific/Technical Society Conferences**

L. L. Sohn, M. S. Rzchowski, J. U. Free, S. P. Benz, and M. Tinkham, "Absence of Fractional Giant Shapiro Steps in Diagonal Josephson Junction Arrays," March 1991 Meeting of the American Physical Society.

M. S. Rzchowski, L. L. Sohn, and M. Tinkham, "Frequency Dependence of Shapiro Steps in Josephson Junction Arrays," March 1991 Meeting of the American Physical Society.

L. Ji, M. S. Rzchowski, N. Anand, and M. Tinkham, "Intergranular Fluxons in Granular Superconductors," March 1991 Meeting of the American Physical Society.

j. **Graduate Students and Postdoctorals Supported Under the JSEP for the Year Ending July 31, 1991**

Dr. M. S. Rzchowski and Mr. N. Anand.

Note: Five other students share JSEP facilities, but have no JSEP salary.

I.6 Planar Networks for Vision Processing. F. R. Waugh and R. M. Westervelt, Grant N00014-89-J-1023; Research Unit 5.

We have completed a systematic analysis of clocked neural networks [1-5], with JSEP support. The architecture we consider is a feedback network composed of analog "neurons" which can be fully or partially interconnected; updates of the state of the network are performed in parallel as an iterated map. Clocking of the analog neural network has the same benefits as clocking digital computers: all neurons in the network are synchronized and variations in neuron delays and information path differences drop out. Clocked networks are fast and well suited to implementation in analog or digital hardware. However, it is well known that parallel update can produce oscillations and complex behavior; serial update has been used in the past to avoid these problems, but it is much slower. By constructing a Lyapunov function for clocked neural networks, we have proven a global stability criterion which can be used to design stable networks with parallel update [2]. We have applied these stability criteria to the design of clocked analog associative memories [4,5] similar in function to the type considered by Hopfield and others.

In the past year, we have studied clocked planar neural networks in which the neurons are arranged in a planar array and interconnected primarily, but not exclusively, to nearby neurons. This architecture shows promise for feature recognition, and is well suited to implementation, for example using CCD technology as demonstrated recently for the M.I.T. vision chip project. Cellular automata with similar architectures have been studied for many years for vision and pattern recognition problems, and more recently for two-dimensional lattice-gas fluid dynamics. The approach usually taken is to examine a variety of interconnection kernels, and to classify the resulting behavior in numerical experiments. A wide variety of rich and complex patterns can be produced in this way, but with little control. Because planar clocked networks obey the same stability criteria as more fully interconnected nets, we can use our stability

analysis of associative memories to design stable feature-recognizing planar networks.

The simplest feature-recognizing planar network consists of an array of blocks of interconnected neurons with no inter-block connections. Each block is a small associative memory which can be programmed to recognize simple features, for example a cross or a blank background. Upon iteration, an image initially loaded into the network blocks evolves into one of the stored patterns, and the network performs feature recognition. For the simplest examples this network reduces to current practice. However, the ability to program more complex patterns with guaranteed stability is new and should prove useful. We have designed and numerically investigated the behavior of these types of networks over the past year.

Planar networks with a mix of local and longer-range connections between neurons offer the possibility of better performance, but raise new questions. We have examined a type of network in which the feature-recognizing blocks overlay each other, to reduce the spacing between recognized features, and have developed a method to program these networks using an extension of the pseudo-inverse rule. We have also investigated domain formation in networks for which each neuron has the same interconnection pattern. In these networks the tendency to settle into the locally preferred pattern is offset by information propagating inward from neurons farther away; the result is the formation of domains of each pattern with slowly-moving domain walls.

References:

1. K. L. Babcock and R. M. Westervelt, *Phys. Rev. A* **40**, 2022 (1989).
2. K. L. Babcock and R. M. Westervelt, *Phys. Rev. Lett.* **63**, 175 (1989).
3. K. L. Babcock, R. Seshadri, and R. M. Westervelt, *Phys. Rev. A* **41**, 1952 (1990).
4. K. L. Babcock and R. M. Westervelt, *Phys. Rev. Lett.* **64**, 2168 (1990).
5. K. L. Babcock and R. M. Westervelt, in *Nonlinear Structures in Physical Systems*, edited by L. Lam and H. C. Morris (Springer, New York, 1990) p. 214.

I.7 Spurious Fixed-point Attractors in Analog Neural Networks. F. R. Waugh, C. M. Marcus, and R. M. Westervelt, Grant N00014-89-J-1023; Research Unit 5.

Spurious minima can form in the energy landscape for an analog associative memory, and prevent the network from reaching a stored memory. In a continuation of our work on clocked neural networks, we have studied the dependence of the number of spurious minima (fixed-point attractors) on the neuron gain β and on the number of stored memories α using a thorough mathematical analysis supported by numerical data [1]. An initial account of this work was published last year as a *Physical Review Letter* [2,3]. These results show that the number of spurious minima increases exponentially fast with α and β , and demonstrate that reduced neuron gain plays the role of temperature in decreasing the number of spurious minima.

References:

1. C. M. Marcus and R. M. Westervelt, *Phys. Rev. A* **39**, 347 (1989).
2. C. M. Marcus and R. M. Westervelt, *Phys. Rev. A* **40**, 501 (1989).
3. C. M. Marcus and R. M. Westervelt, in *Advances in Neural Information Processing Systems*, edited by D. S. Touretzky (Morgan Kaufman, San Mateo, California, 1989) p. 568.

I.8 Dynamics of Magnetic Bubble Arrays. R. Seshadri and R. M. Westervelt, Grant N00014-89-J-1023; Research Unit 5.

In the past we have conducted an investigation into the collective dynamics of cellular magnetic domain patterns in magnetic garnet films [1-7], with partial JSEP support. These patterns show a variety of interesting dynamical processes including melting of polycrystalline hexagonal bubble arrays, and avalanches of cell destruction in disordered cellular patterns. This work has resulted in two *Physical Review Letters* and a number of invited talks.

In the past year we have used magnetic bubble arrays in magnetic garnet films to study the statistical mechanics and collective transport of two-dimensional liquids and solids. The properties of magnetic bubble domains have been extensively studied in the past for technological applications. Magnetic bubbles are cylindrical domains of magnetization which move about freely inside the garnet film; they form a two-dimensional fluid of interacting magnetic dipoles. The statistical mechanics of two-dimensional fluids and melting has been a topic of considerable interest and controversy over the past decade. Nelson and Halperin [8] have predicted that this melting occurs in two stages via the production, and dissociation of topological defects: 5- and 7-fold disclinations. The first stage produces a "hexatic" phase which has orientational order but lacks translational order, and the second a liquid with neither orientational nor translational order. Relatively few experiments (for a notable exception, see [9]) provide sufficient access to actually identify topological defects and distinguish between competing theories.

We have approached this problem from the point of view of nonlinear dynamics. Using computer video techniques, we are able to measure the position and velocity of every magnetic bubble in an array, and to compute statistical quantities from microscopic knowledge of the dynamics. With this system we can visualize two-dimensional melting as it appears in the corresponding gas of topological defects which are produced. This work has recently appeared as a *Physical Review Letter* [10]. A related topic of great current interest is the mechanics of flux line motion in high- T_c superconductors, which places severe limits on the critical current at higher temperatures. We plan to use our system to test theories of collective flux line motion. This project is being shifted to support from our ONR grant (partial support above), because its current subject matter seems more appropriate for this source.

References:

1. F. R. Waugh, C. M. Marcus, and R. M. Westervelt, *Phys. Rev.* **A43**, 3131 (1991).
2. F. R. Waugh, C. M. Marcus, and R. M. Westervelt, in *Proc. Int. Joint Conf. on Neural Networks*, Washington DC, 1990, edited by M. Caudill (Erlbaum Assoc., Hillsdale NJ, 1990) vol. 1, p. 321.
3. F. R. Waugh, C. M. Marcus, and R. M. Westervelt, *Phys. Rev. Lett.* **64**, 1986 (1990).
4. C. M. Marcus and R. M. Westervelt, *Phys. Rev.* **A42**, 2410 (1990).
5. C. M. Marcus, F. R. Waugh, and R. M. Westervelt, *Phys. Rev.* **A41**, 3355 (1990).
6. R. M. Westervelt and K. L. Babcock, in *Chaos/Xaoc: Soviet-American Perspectives on Nonlinear Science* (American Institute of Physics, New York, 1990), p. 205.
7. R. M. Westervelt, K. L. Babcock, M. Vu, and R. Seshadri, in *Proc. 35th Conf. on Magnetism and Magnetic Materials*, San Diego, 1990, *J. Appl. Phys.* **69**, 5436 (1991).
8. D. R. Nelson and B. I. Halperin, *Phys. Rev.* **B19**, 2547 (1979).
9. C. A. Murray and D. H. van Winkle, *Phys. Rev. Lett.* **58**, 1200 (1987).
10. R. Seshadri and R. M. Westervelt, *Phys. Rev. Lett.* **66**, 2774 (1991).

ANNUAL REPORT OF
PUBLICATIONS/PATENTS/PRESENTATIONS/HONORS

a. **Papers Submitted to Refereed Journals (and not yet published)**

C. M. Marcus, F. R. Waugh, and R. M. Westervelt, "Nonlinear Dynamics and Stability of Analog Neural Networks," in *Proc. of the Conf. on Nonlinear Science: The Next Decade*, Los Alamos, May 1990, *Physica D* (in press). (Partially supported by N00014-89-J-1592)

C. M. Marcus, F. R. Waugh, and R. M. Westervelt, "Connection Topology and Dynamics in Lateral Inhibition Networks," in *Advances in Neural Information Processing Systems* (Morgan Kaufman, San Mateo, 1991) (in press). (Partially supported by N00014-89-J-1592 and AFOSR-89-0506)

b. **Papers Published in Refereed Journals**

F. R. Waugh, C. M. Marcus, and R. M. Westervelt, "Nonlinear Dynamics of Analog Associative Memory Neural Networks," in *Proc. Int. Joint Conf. on Neural Networks*, Washington DC, 1990, edited by M. Caudill (Lawrence Erlbaum Assoc., Hillsdale NJ, 1990) vol. 1, pp. 321-323. (Partially supported by N00014-89-J-1592)

R. M. Westervelt and K. L. Babcock, "Dynamics of Cellular Magnetic Domain Patterns," in *Chaos/Xaoc: Soviet-American Perspectives in Nonlinear Science*, (American Institute of Physics, New York, 1990), pp. 205-221. (Partially supported by N00014-89-J-1592)

R. M. Westervelt and K. L. Babcock, "Dynamics of Cellular Magnetic Domain Patterns," in *Nonlinear Structures in Physical Systems*, edited by L. Lam and H. C. Morris (Springer, New York, 1990) pp. 214-221. (Partially supported by N00014-89-J-1592)

C. M. Marcus and R. M. Westervelt, "Stability and Convergence of Analog Neural Networks with Multiple-time-step Parallel Dynamics," *Phys. Rev. A* **42**, 2410 (1990). (Partially supported by N00014-89-J-1592 and AFOSR-89-0506)

R. M. Westervelt, K. L. Babcock, M. Vu, and R. Seshadri, "Avalanches and Self-Organization in the Dynamics of Cellular Magnetic Domains," *J. Appl. Phys.* **69**, 5436 (1991). (Partially supported by N00014-89-J-1592)

F. R. Waugh, C. M. Marcus, and R. M. Westervelt, "Reducing Neuron Gain to Eliminate Fixed-point Attractors in an Analog Associative Memory," *Phys. Rev. A* **43**, 3131 (1991). (Partially supported by N00014-89-J-1592 and AFOSR-89-0506)

R. M. Westervelt and K. L. Babcock, "Avalanches and Self-organization in Cellular Magnetic Domain Patterns," *Mat. Res. Soc. Extended Abstract* **25**, 85-88 (1990). (Partially supported by N00014-89-J-1592)

R. Seshadri and R. M. Westervelt, "Hexatic-to-liquid Melting Transition in Two-dimensional Magnetic-bubble Lattices," *Phys. Rev. Lett.* **66**, 2774 (1991). (Partially supported by N00014-89-J-1592)

g. Invited Presentations at Topical or Scientific/Technical Society Conferences

R. M. Westervelt, "Avalanches and Self-organization in Magnetic Cellular Domain Patterns," 35th Annual Conference on Magnetism and Magnetic Materials, October 29 - November 1, 1990, San Diego, CA.

R. M. Westervelt, "Avalanches and Self-organization in Magnetic Cellular Domain Patterns," Materials Research Society, Fall Meeting, October 26-30, 1990, Boston, MA.

R. M. Westervelt, "Dynamics of Two-dimensional Electronic Neural Networks," Neural Networks for Computing, April 2-5, 1991, Snowbird, Utah.

R. M. Westervelt, "Avalanches in Magnetic Cellular Domain Patterns," Washington Meeting of the American Physical Society, April 22-26, 1991, Washington, D.C.

h. Contributed Presentations at Topical, or Scientific/Technical Society Conferences

R. Seshadri, Meeting of the American Physical Society, March 18-22, 1991, Cincinnati, Ohio.

F. Waugh, Neural Information Processing Systems, Denver, December 1990.

i. Honors/Awards/Prizes

R. M. Westervelt, Board of Editors, *Physica D*

C. M. Marcus, IBM Postdoctoral Fellow

F. Waugh, JSEP Fellowship

j. Graduate Students and Postdoctorals Supported under the JSEP for the Year Ending July 31, 1991

Dr. Charles Marcus, Mr. Fred Waugh and Ms. Raj Seshadri

I.9 Structural and Electronic Studies of Semiconductor Interfaces and Surfaces. J. A. Golovchenko, Grant N00014-89-J-1023; Research Unit 6.

We report here on several advances and new directions in our program that have been made possible by JSEP support.

A significant part of the support has gone into pursuing surface studies centered around the tunneling microscope facility at Harvard. A major effort has been put into the study of metal overlayers on semiconductors because of the inherently interesting and diverse material science systems they represent and because of the unique insight one can gain into these systems with the analytical tools, like the tunneling microscopes, available at Harvard and because of their technological applications. A system we have chosen for scrutiny is lead on silicon. This choice was made in part because other investigators had found that different Schottky barrier heights for this system could be obtained by varying the substrate conditions during lead deposition and in part because of the compatibility of our *in situ* preparation capabilities with these materials.

The structural part of our studies proved to be quite fruitful because the system turns out to have many possible phases and the tunneling microscope is the ideal tool to articulate and isolate the interesting structures that occur in this generally nonhomogeneous system. The obvious possibility for controlling the interface structure and hence structure-dependent Schottky barrier height is clearly tempered by our tunneling observation of mixed surface phases which, should they persist at a metal semiconductor interface, would certainly complicate any attempt at a simple model interpretation of barrier heights measured on macroscopic samples. We have attempted to use the tunneling microscope to probe the electronic structure of the various surface phases of lead on silicon, however, as yet it has been difficult to isolate tip from surface effects as well as get consistent data sets open to clear interpretation from sample to sample.

The extension of these studies from silicon to germanium substrates has proven extremely fruitful. Our initial studies of lead on the Ge(111) surface showed that there are many mobile atoms on this surface at temperatures accessible to simple operation of the microscope. As a result, we have been able to study the complex diffusional motions of individual surface atoms. Systematic thermal cycling and studies of sequential tunneling images has resulted in a collection of 10,000 atom surface displacement events. Examples are shown in Fig. I.6. In what we believe to be the first study of its kind with a tunneling microscope, the activation energy and diffusion constant for the lead surface atoms has been determined. Figure I.7 shows a plot of hopping frequencies vs. $1/T$ from which these constants are determined. In addition, the anisotropy in the diffusion coefficient is clearly isolated from these atomic scale measurements. The geometry of available sites for motion is contained in Fig. I.8. We believe that the ability to obtain data of this type will stimulate parallel theoretical studies which will both test our fundamental understanding of the details of diffusion kinetics at finite temperature as well as enhance the fundamental theoretical understanding of these systems. A manuscript entitled "Direct Observation of Atomic Diffusion by Hot Tunneling Microscopy" is being submitted to a Letters journal.

In our last report we indicated that we were beginning a research program aimed at understanding the VLS crystal growth mechanism and developing it in the context of recent technology connected with molecular beam epitaxy. JSEP funds have also been used to support our continuing effort in this area and we are greatly pleased to report significant progress. In this mechanism, semiconductor atoms are delivered to a semiconductor coated with a thin liquid metal. They diffuse through the liquid layer and are incorporated in the bulk crystal lattice below, and as a result macroscopic crystal growth can occur normal to the sample surface. Our efforts have concentrated on the low temperature growth of germanium through liquid gold layers as thin as ten angstroms, at temperatures as low as 400 degrees. A liquid metal layer at this

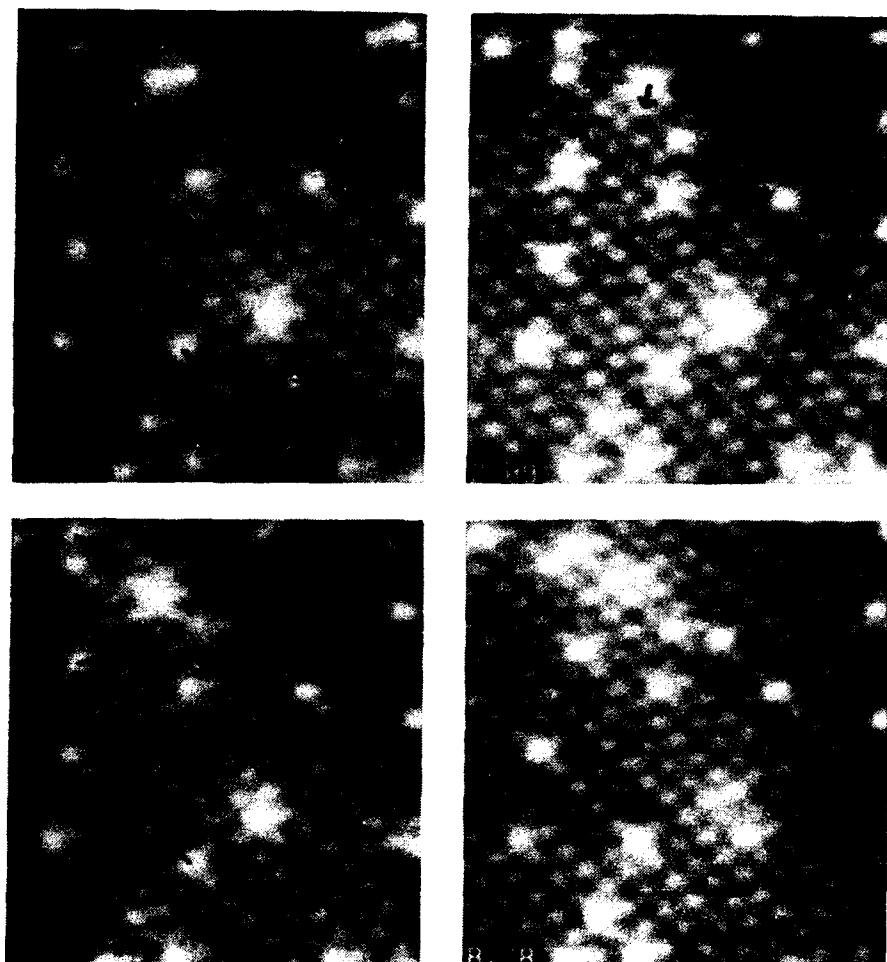


Figure 1.6. Four successive $90 \times 100 \text{ \AA}$ STM images of Pb adatoms in substitutional sites in a Ge(111)- $c(2 \times 8)$ reconstructed surface. Relative times in [minutes:seconds] are indicated at the bottom of each image. The black arrows indicate the direction and length of eight single jumps. Four long jumps are also observed.

$$y = 3.28 \text{ E}5 * 10^{(-2.756x)}$$
$$r^2 = 0.98$$

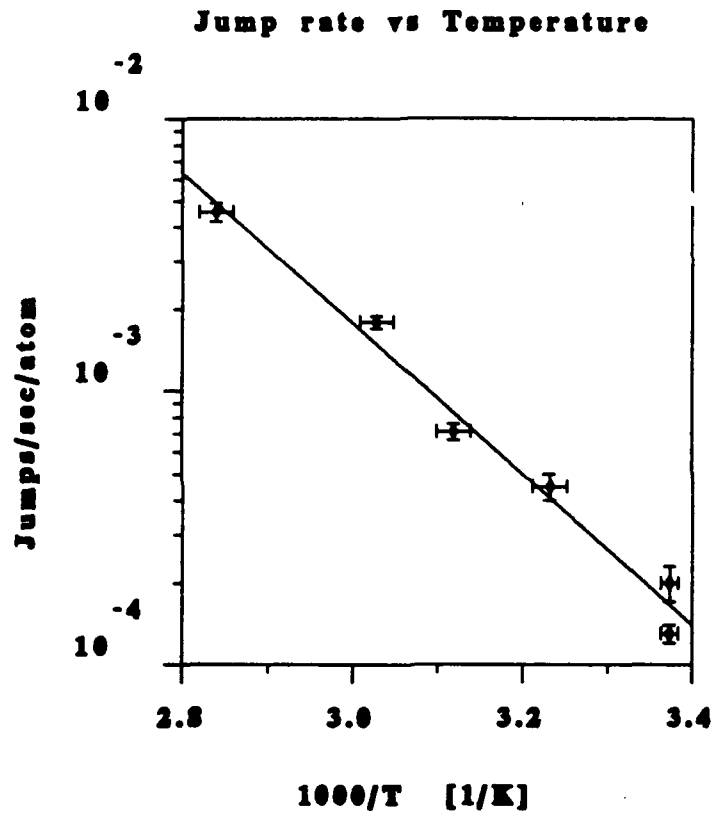


Figure 1.7. Arrhenius plot of the observed jump rate for Pb adatoms at temperatures from 24°C to 79°C.

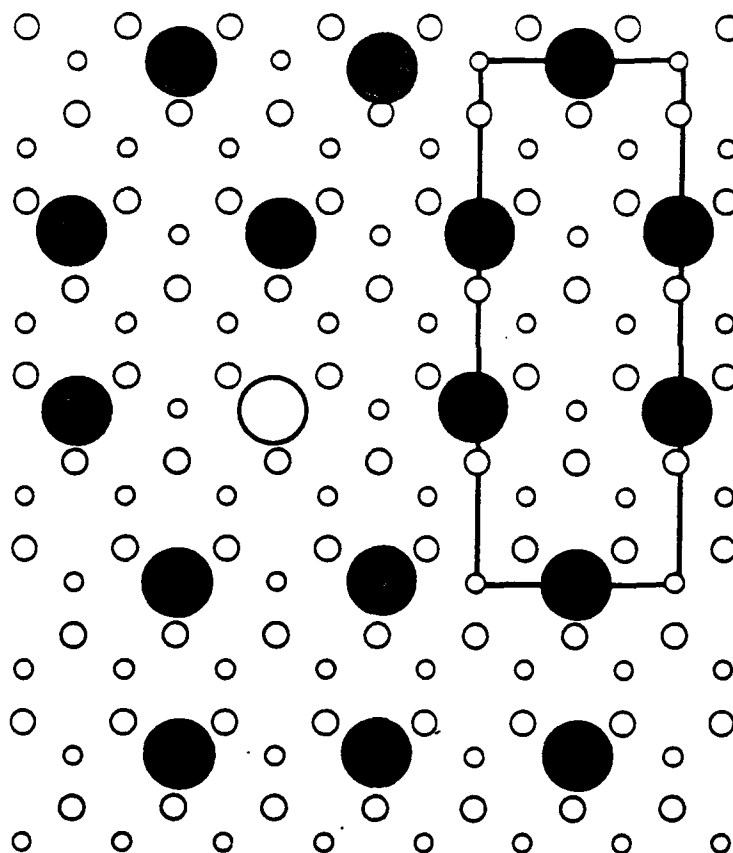


Figure 1.8. Schematic diagram of the Ge(111)-c(2x8) surface. Small circles represent top layer bulk Ge atoms, large circles are Ge adatoms (open) and Pb adatoms (filled). Seven near neighbors are identified.

temperature is possible because of the low eutectic point for this system. We have observed excellent crystal quality for grown layers as thick as 1500 angstroms. Most importantly, we have been able to obtain completely planar growth without the standard problems of classical VLS where one invariably observes inhomogeneous whisker growth. This is essential if this approach is ultimately to have serious technological application for the production of integrated circuits. A survey of our preliminary results have been published this past year and an article entitled "Liquid Metal Mediated Homoepitaxial Growth of Germanium at Low Temperature" has been submitted for publication to a Letters journal.

Finally we have used JSEP funds to initiate a collaboration with Herb Mook of ORNL to study the anomalous thermal vibration amplitudes of copper atoms at the critical temperature in high temperature superconductors. A strong neutron absorption resonance exists for Cu 63 at approximately 250 electron volts. Its natural width is much smaller than the Doppler width associated with the thermal and zero point motion of the copper atoms in their lattice sites. One can therefore measure the momentum spread of the copper atom wavefunctions directly with this probe. Preliminary experiments stimulated by earlier channeling measurements show a very large softening of the lattice around the copper atoms in the BSCCO 2212 material below the critical temperature. We have used JSEP funds to cover travel to the Oak Ridge neutron facility to participate in and test these ideas. We hope to expand this into a major program involving positron annihilation and channeling radiation as well as neutron absorption spectroscopy. A proposal towards this end has been submitted to the NSF.

**ANNUAL REPORT OF
PUBLICATIONS/PATENTS/PRESENTATIONS/HONORS**

a. Papers Submitted to Refereed Journals (and not yet published)

E. Ganz, S. Leonard, I.-S. Hwang, and J. A. Golovchenko, "Direct Observation of Anisotropic Atomic Diffusion by Hot Tunneling Microscopy," *Physical Review Letters* (1991) (submitted).

F. Xiong, E. Ganz, A. G. Loeser, J. A. Golovchenko, and F. Spaepen, "Liquid-metal-mediated Homoepitaxial Film Growth of Ge at Low Temperature," *Applied Physics Letters* (1991) (submitted).

E. Ganz, I.-S. Hwang, F. Xiong, S. Leonard, and J. A. Golovchenko, "Growth and Morphology of Pb on Si(111)," *Surface Science* (1991) (in press).

b. Papers Published in Refereed Journals

E. Ganz, F. Xiong, I.-S. Hwang, and J. A. Golovchenko, "Submonolayer Phases of Pb on Si(111)," *Phys. Rev. B* **43**, 7316 (1991).

F. Xiong, E. Ganz, J. A. Golovchenko, and F. Spaepen, "In Situ RBS and Channeling Study of Molecular Beam Epitaxial Growth of Metals and Semiconductors on Semiconductors," *Nuclear Instruments and Methods in Physics Research B* **56/57**, 780-784 (1991).

h. Contributed Presentations at Topical, or Scientific/Technical Society Conferences

E. Ganz, F. Xiong, I.-S. Hwang, and J. A. Golovchenko, "Growth and Morphology of Pb on Si(111) 7×7 ," abstract for the 18th Annual Conf. on the *Physics and Chemistry of Semiconductor Interfaces*, Long Beach, California (1991).

j. Graduate Students and Postdoctorals Supported under the JSEP for the Year Ending July 31, 1991

Dr. Eric Ganz, Miss Silva Leonard and Miss Nancy Hecker

II. QUANTUM ELECTRONICS

Personnel

Prof. N. Bloembergen
Prof. E. Mazur
Dr. C.-Z. Lü
Mr. K. H. Chen
Mr. D. S. Chung
Mr. S. Deliwala

Mr. J. Goldman
Ms. K. Y. Lee
Mr. P. Saeta
Mr. Y. Siegal
Mr. J. K. Wang

II.1 Ultrashort Laser Interactions with Semiconductor Surfaces. N. Bloembergen, E. Mazur, P. Saeta, Y. Siegal, and J. K. Wang, Grants N00014-89-J-1023 and NSF DMR-8858075; Research Unit 7.

In this research unit the electronic and material properties of semiconductors and metals are studied using ultrashort laser pulses. Because of the small penetration depth of the laser light in such materials and because thermal diffusion is negligible for times shorter than ten picoseconds, subpicosecond laser irradiation concentrates the laser pulse energy in a very thin layer at the surface of the material. At high pulse energies the melting threshold can thus easily be reached, and the material at the surface can transform into short-lived phases that can sometimes not be obtained by any other method. At pulse energies below the melting threshold, measurements on a femtosecond timescale probe the carrier and lattice dynamics of the material — a topic of high current interest because of the technological applications of high-speed electronics.

We recently completed an ultrafast laser-induced disordering experiment on GaAs. The technique involves using a 150-fs laser pulse which is split into a pump and a probe. Sending one of the beams through a variable delay line allows us to set the relative time delay between the pump and the probe. In this manner we are able to

trace out the time evolution of the response of the material to the pump. By measuring the linear reflectivity of the sample, we obtained information about the change in the dielectric constant as a function of time. In addition, we are able to directly monitor the symmetry of the sample by detecting the reflected second harmonic radiation produced in the material. Upon disordering, the second harmonic signal disappears because the second-order susceptibility vanishes in centrosymmetric media.

The results of our experiment show that GaAs disorders on a time scale of about 100 fs. This time scale should be compared with the time for energy transfer from the electronic system to the lattice, which is on the order of several picoseconds. The discrepancy in these times suggests that the disordering cannot be due to thermal heating of the lattice, as is the case for picosecond and nanosecond pulse excitation of semiconductors. Rather, the lattice is directly driven to disorder by the effective bond breaking that occurs when electrons are excited from bonding valence states to antibonding conduction states. These results suggest the exciting possibility of disordering a cold lattice.

In order to clarify the nature of this electronically induced disordering, we plan to perform a series of ultrafast disordering experiments using both electronic and phonon probes. Our ability to carry out this work will be vastly improved when we complete the implementation of an important improvement in our laser facility. By taking advantage of self-phase modulation and spatial mode selection in an optical fiber, we have successfully created a high-energy, tunable source for 40-fs pulses of nearly perfect Gaussian spatial profile that are synchronized with the main beam. By inserting this fiber optic setup into the main amplifier and splitting the fiber output into two amplifier arms, we will have a very powerful system capable of producing two synchronized, independently tunable beams of 40 fs pulses with uniform spatial profiles. The improvement in spatial profile will increase the signal-to-noise ratio in pump-probe style experiments while the decreased pulse width will give us greater time

resolution. Furthermore, having two independently tunable frequencies will allow us to examine how the GaAs results change if we vary either the pump or the probe frequencies, and to study the temporal evolution of optical phonon frequencies using coherent anti-Stokes Raman spectroscopy in reflection.

II.2 Laser Light Scattering from Surfaces and Monolayers. E. Mazur and K. Y. Lee, Grants N00014-89-J-1023 and NSF DMR-8858075; Research Unit 7.

There has been a growing interest in recent years in the properties of Langmuir-Blodgett films, monolayers and surfactants because of the many technological applications of such systems such as multilayer structures, and because such mono-molecular layers can serve as models for the study of two-dimensional systems. In spite of this interest, viscoelastic properties of monolayers remain poorly understood. This is partly due to the lack of experimental results accurate enough to put the existing theories to a vigorous test.

Like their three-dimensional counterparts, two-dimensional systems undergo phase transitions, and conventionally such transitions have been identified by measuring surface pressure-area (Π -A) isotherms for these systems. These isotherms are analogous to pressure-volume isotherms in three-dimensions. The surface pressure, which is the difference in surface tension between a pure subphase and one with an adsorbed monolayer, is typically measured by the Wilhelmy-plate method. It is well-known, however, that isotherms obtained by such measurements are not very reproducible.

We have developed a novel method for accurately measuring the spatial damping of waves on liquid surfaces covered by a monolayer using laser light scattering. Our project on surfactant monolayers has two goals. The first is to extract viscoelastic information of surface films from the damping of surface waves. The second is to study the phase-behavior of these films in greater detail; our initial damping results show,

namely, that the damping coefficient is a very reliable indicator of phase transitions in monolayers.

The spatial damping coefficient is measured directly using an apparatus that employs a novel Fourier transform heterodyning spectroscopy (FTHS) technique developed in our laboratory. The apparatus probes the surface in two spots and employs a 'phase-matched geometry' for the main laser beam and the local oscillator. Such a two-beam probing geometry eliminates calibration problems, and the spatial damping coefficients are obtained directly without any deconvolution.

During this past year, the experimental setup has been improved in a number of ways: 1) A better surface area control device was added to the Langmuir-Blodgett trough, to make it possible to obtain a more accurate value for the area A occupied by each surfactant molecule; 2) temperature stabilization of the apparatus allows us now to carry out experiments over a range of temperatures and, in particular, near critical points; and 3) new software was developed to automate and speed up data analysis. We are currently extending our work on the damping of capillary waves in the presence of a monolayer of pentadecanoic acid (PDA). Experiments will be carried out at a number of different temperatures in order to investigate how damping is affected in different regions of the Π - A phase diagram. We also plan to extend our study to fatty acids with longer carbon chains.

**ANNUAL REPORT OF
PUBLICATIONS/PATENTS/PRESENTATIONS/HONORS**

a. Papers Submitted to Refereed Journals (and not yet published)

P. Saeta, J.-K. Wang, Y. Siegal, N. Bloembergen, and E. Mazur, "Ultrafast Electronic Disordering During Femtosecond Laser Melting of GaAs," *Phys. Rev. Lett.* (submitted).

P. Saeta, J.-K. Wang, Y. Siegal, N. Bloembergen, and E. Mazur, "Femtosecond Carrier-induced Disordering of GaAs," *Phys. Rev. B* (submitted).

J.-K. Wang, Y. Siegal, C.-Z. Lü, and E. Mazur, "A Tunable, Dual-frequency, Synchronized Source for Femtosecond Laser Pulses with a Nearly Perfect Gaussian Profile," *Opt. Comm.* (submitted).

b. Papers Published in Refereed Journals

D. S. Chung, K. Y. Lee, and E. Mazur, "Spectral Asymmetry in the Light Scattered from a Nonequilibrium Liquid Interface," *Phys. Lett. A* **145**, 348 (1990).

d. Books (and sections thereof) Published

J.-K. Wang, P. Saeta, Y. Siegal, E. Mazur, and N. Bloembergen, "Second-harmonic Efficiency and Reflectivity of GaAs during Femtosecond Melting," in *Ultrafast Phenomena VII*, eds. C. B. Harris, E. Ippen and A. H. Zewail (Springer Verlag, 1990) p. 321.

g. Invited Presentations at Topical or Scientific/Technical Society Conferences

N. Bloembergen, Invited Lecture: "Nonlinear Optics; a Historical Perspective," Int. Conf. to Commemorate the 300th Anniversary of the Publication of the Book by Christiaan Huyghens *Traité de la Lumière*, November 1990.

N. Bloembergen, Invited Lecture: "Research with Dye Lasers at Harvard University," IBM Symposium to Celebrate the 25th Anniversary of Dye Lasers, Yorktown Heights, NY, May 1991.

h. Contributed Presentations at Topical or Scientific/Technical Society Conferences

E. Mazur, "Reflectivity and Second Harmonic Efficiency of GaAs During Femtosecond Melting," *Ultrafast Phenomena Conference*, Monterey, California, June 1990.

E. Mazur, "Femtosecond Melting of GaAs Probed by Reflectivity and Second-harmonic Generation," *1990 Annual Meeting of the Optical Society of America*, Boston, November 1990.

i. Honors

N. Bloembergen served as President of the American Physical Society in 1991.

j. Graduate Students and Postdoctorals Supported

Dr. C.-Z. Lü

II.3 Multiphoton Vibrational Excitation of Molecules. E. Mazur, C.-Z. Lü, S. Deliwala, and J. Goldman, Grant N00014-89-J-1023 and Contract ARO DAAL03-88-K-0114; Research Unit 8.

In this research unit we continued the study of infrared multiphoton excited molecules in a free supersonic jet expansion using time-resolved broadband coherent Raman spectroscopy (CARS). The following changes were made to the experimental setup: 1) the time resolution of the measurements was improved using Hamamatus streak camera, and 2) the signal-to-noise was improved by overlaying spectra from multiple laser shots onto a single streak image. With this improved apparatus we studied the infrared multiphoton excitation in SO_2 and SF_6 .

In SO_2 we were able to unambiguously identify the multiphoton excitation pathway. We found that pumping at a variety of CO_2 laser lines leads to the excitation of the ν_1 -mode at 1151.3 cm^{-1} despite a bandhead detuning as large as 75 cm^{-1} . In addition our measurements lead to accurate values of the anharmonic constants x_{11} and x_{12} .

Detailed measurements of the infrared multiphoton excitation in SF_6 , which we performed recently, allow us to directly observe the evolution of the population distribution in low-lying states during and after multiphoton excitation and to better evaluate the role collisions play in the relaxation dynamics. Quantitative analysis of the data yield approximate vibrational state populations of the excited molecular ensemble as a function of time. Interestingly, we find a non-thermal distribution of energy in a laser pumped mode which persists for up to 400 ns after excitation—a time much longer than any intramolecular relaxation time scale.

With the recent renovation of the laboratory we have decided to terminate the current CO_2 laser experiment and develop a new apparatus that will allow us to study intramolecular processes on the femtosecond time scale (an improvement of six orders of magnitude). To this end we designed and started construction of a Ti:Sapphire

laser oscillator and amplifier system. This laser will produce tunable, high intensity femtosecond pulses that will enable us to interrogate isolated and surface-adsorbed molecules at ultrafast timescales. This will allow us to investigate energy pathways for the relaxation of excited electronic and vibrational states in molecular systems. We plan initially to study the dynamics of simple systems such as hydrogen-terminated Si(111) surfaces. Recently, we have also done preliminary experiments using femtosecond interferometry demonstrating in principle that one can probe dynamics over time scales shorter than the probe pulse by obtaining phase information.

ANNUAL REPORT OF
PUBLICATIONS/PATENTS/PRESENTATIONS/HONORS

a. **Papers Submitted to Refereed Journals (and not yet published)**

C.-Z. Lü, J. Goldman, S. Deliwala, K.-H. Chen and E. Mazur, "Direct Evidence for ν_1 -mode Excitation in the Infrared Multiphoton Excitation of SO_2 ," *Chem. Phys. Lett.* (submitted).

K.-H. Chen, C.-Z. Lü, N. Bloembergen, and E. Mazur, "Multiplex Pure Rotational Coherent Anti-Stokes Raman Spectroscopy in a Molecular Beam," *J. Raman Spectroscopy* (submitted).

K.-H. Chen, C.-Z. Lü and E. Mazur, "Time-resolved Coherent Anti-Stokes Raman Spectroscopy of SF_6 in a Supersonic Jet," *J. Chem. Phys.* (submitted).

b. **Papers Published in Refereed Journals**

C.-Z. Lü, J. Goldman, S. Deliwala, K.-H. Chen and E. Mazur, "Direct Evidence for ν_1 -mode Excitation in the Infrared Multiphoton Excitation of SO_2 ," *Chem. Phys. Lett.* **176**, 335 (1991).

N. Bloembergen, K.-H. Chen, C.-Z. Lü, and E. Mazur, "Multiplex Pure Rotational Coherent Anti-Stokes Raman Spectroscopy in a Molecular Beam," *J. Raman Spectroscopy* **21**, 819 (1990).

d. **Books (and sections thereof) Published**

E. Mazur and C.-Z. Lü, "Nonlinear Spectroscopy of Infrared Multiphoton Excited Molecules," in *Resonances, a Volume in Honor of the 70th Birthday of Nicolaas Bloembergen*, eds. M. Levenson, E. Mazur, P. S. Pershan and Y. R. Shen (World Scientific, Singapore, 1990) p. 165-174.

E. Mazur, C.-Z. Lü, S. Deliwala, J. Goldman, "Coherent Anti-Stokes Raman Spectroscopy of Highly Vibrationally Excited Molecules in a Jet," *XII Int. Conf. Raman Spectr.*, eds. J. R. Durig and J. F. Sullivan (Wiley, New York, 1990) pp. 232-233.

E. Mazur, C.-Z. Lü, S. Deliwala and J. Goldman, "Collisional and Intramolecular Dynamics of Low-lying Vibrational States of Infrared Multiphoton Excited Molecules," *Tech. Digest. XVII Int. Conf. on Quantum Electronics* **8**, 214 (1990). (Partially supported by ARO DAAL03-88-K-0114)

g. Invited Presentations at Topical or Scientific/Technical Society Conferences

E. Mazur, "Coherent Anti-Stokes Raman Spectroscopy of Highly Vibrationally Excited Molecules in a Jet, *International Conference on Raman Spectroscopy*, Columbia, S. Carolina, August 1990.

h. Contributed Presentations at Topical or Scientific/Technical Society Conferences

E. Mazur, "Collisional and Intramolecular Dynamics of Low Lying Vibrational States of Infrared Multiphoton Excited Molecules," *International Quantum Electronics Conference*, Anaheim, California, June 1990. (Partially supported by ARO DAAL03-88-K-0114)

j. Graduate Students and Postdoctorals Supported

Mr. J. Goldman and Mr. S. Deliwala

III. INFORMATION ELECTRONICS: CIRCUITS AND SYSTEMS

Personnel

**Prof. R. Brockett
Assoc. Prof. J. J. Clark
Prof. Y. C. Ho
Dr. R. Sreenivas
Dr. Z. B. Tang**

**Mr. K. Budka
Mr. L. Y. Dai
Mr. D. J. Friedman
Mr. N. Saxena**

**III.1 CMOS Current Mode Realizations of Neural Network Structures.
J. J. Clark, Contracts N00014-89-J-1023, NSF-IRI-90-03306 and NSF-
CDR-85-00108; Research Unit 9.**

In this research program we are concerned with the development of analog CMOS circuits and systems based on "neural" principles. In particular, we have been developing electronic structures, based on the current mode CMOS circuitry designed in earlier years of this research program, that allow the construction of artificial dynamical systems which map sensory data into temporal patterns.

This past year we have designed and fabricated a CMOS analog VLSI circuit which integrates photo-sensitive devices, simple feature extraction circuitry, and temporal pattern selection logic. The temporal pattern generation is currently done with off-chip circuitry but can be easily integrated onto a single chip along with the other circuitry.

In addition, we have carried out a careful study of the design of phototransistors in standard CMOS fabrication processes. This study provides information, not currently available in the literature, on the dependence of phototransistor sensitivity on various parameters under the control of the integrated circuit designer. This information is crucial to the design of high quality, repeatable, integrated photosensors using standard CMOS fabrication processes.

1. VLSI Sensor-Motor Systems

We have been working on a novel application of our current mode neural network based sensory information processing circuits (described in earlier JSEP reports). This device, unlike standard sensors which output a steady stream of sensory data (like the video signal of a CCD camera), outputs motor patterns (i.e., temporal sequences of motor oriented signals). When perfected this chip might find application in various autonomous systems, whose behavior (motor activity) depends on the data that it senses. These devices contain arrays of sensors (which are typically less dense than a video camera sensor array) and circuitry which processes and examines the raw sense data and outputs a low bandwidth stream of motor signals.

A CMOS circuit has been developed which integrates sensors and processing circuitry aimed at implementing a sensor data-to-temporal pattern generation unit. The circuit has been fabricated at the Massachusetts Microelectronics Center (M2C) as well as through the MOSIS facility (as the M2C foundry is still in the stages of working the bugs out of its fabrication process). The fabricated parts have been received and tested and shown to be fully functional.

The sensory capability of the chip consists of a 5 by 5 array of photodetectors. The photodetectors are implemented by using the parasitic bipolar junction transistors (BJT) available in most CMOS processes. In use as phototransistors the base region is left floating. In the n -well process used by the Massachusetts Microelectronics Center the emitter of the phototransistor is a p -diffusion region, the collector is the p -type substrate, and the base is a (floating) n -well. Two diode-connected pFETs connected in series to the BJT emitter serve to generate a logarithmic (if the FETs are operating in subthreshold) or square root (if the FETs are operating in saturation) voltage response at the output node to photocurrent produced by the phototransistor.

The sensor-plane processing circuitry analyzes the array data to extract a basic set of sensory primitives, to be used in generating a temporal pattern or sequence. The in sensor-plane processing is done by modules which calculate spatial convolutions of the sensor array data. The output of each phototransistor is fed into a transconductance amplifier configured as a unity gain buffer amplifier (follower). The output of each of the 25 followers is sent to two subunits. The first subunit is common to all 25 followers and calculates the root-mean-square average of the 25 photovoltages. This average is used to provide an adaptive offset signal, which is used to extend the dynamic range of the system. The other subunits are high gain differential amplifiers and are local to the phototransistor and follower. The follower output is connected to one of the inputs of the differential amplifiers while the other amplifier input is connected to the output of the averaging circuit. As the average light level varies, the operating point of the high gain amplifiers also varies under the control of the averaging circuit, so that the amplifier does not saturate and lose sensitivity. Further processing is performed on the amplified signals in a parallel manner. The amplified signals fan out as inputs to three processing units, one of which calculates a discrete approximation to the spatial first derivative in the x -direction, one of which calculates a discrete approximation to the spatial first derivative in the y -direction, and one of which calculates a discrete approximation to the Laplacian operator.

Convolution kernels which were implemented were chosen based on the basis of their usefulness in solving low-level vision problems. Specific kernels on the current chip include discrete approximations to the x -direction first derivative operator, the y -direction first derivative operator, and the Laplacian operator. The current mode analog signal processing techniques that have been developed in previous years by this JSEP research unit are used to provide for input signal weighting, signal inversion, and generation of the output voltage of each processing unit. The

amplified and offset adjusted outputs from the photoreceptor units are connected to convolution cell input cells. Changes in sign of a receptor signal, required for negative weighting, are performed by interposing a bidirectional current mirror inverter stage between the receptor output and the convolution input. Different weights are assigned to the input signals by designing the input transistors in the convolution cell with different $\frac{W}{L}$ ratios. The convolution kernels can thus be fixed in the design by choosing both these ratios as well as the connection pattern of receptor outputs to convolution cell inputs. The convolution cell output is available directly on a current summing node. The currents are summed and converted to a voltage using a high compliance transresistance amplifier. This amplifier is designed to have a low transresistance to allow for wide current swings on the current summing node without saturation.

The results of tests done on the sensori-motor chip, although demonstrating the desired functionality, point to a number of conditions which warrant modification of its circuitry. First of all, the photoreceptor outputs varied significantly across the chip. The maximum measured variation of two different receptors receiving the same input was 200 mV. This value is comparable to the variation of the output of a single receptor as a high contrast illumination edge passes over it. We are currently investigating methods for offset compensation using floating gate MOSFET devices coupled with adaptive compensation circuitry. The adaptation circuitry cause a charge to be stored on the floating gate of a MOSFET which will create an imbalance in a differential amplifier. The magnitude of this charge, and hence of the imbalance, will be such as to cancel out the photosensor offsets. Another significant error was the relatively large 545 mV variation in the output of the vertical edge detector to a horizontal edge. The response of the same detector to a vertical edge of equal contrast was 3200 mV.

In the testing process the sensory stimuli were adjusted to mimic the illumination levels and patterns expected in the planned application of these devices. No absolute photometric measurements were made, although relative illumination levels were recorded for the purposes of demonstrating the logarithmic voltage vs. illumination curve of the photosensors.

2. Design and Characterization of Phototransistors in CMOS Processes

The foundation of the sensori-motor system is the photosensor array. In fabricating the sensori-motor chip it became apparent that the phototransistors were not as sensitive as we had expected. The β (and hence the sensitivity) of the phototransistor depends on a number of fabrication process variables, such as doping levels and depths of diffused regions, as well as on geometric parameters such as the shapes and sizes of the emitter and bases regions. As circuit designers using a standard fabrication process, we only have control over some of the geometric variables, and have no control over the fabrication process. The literature on analog image processing hardware, of the sort that we are building, does not describe phototransistor design and performance in any detail. Nor is there any literature describing the optimal design and layout of phototransistors *in standard CMOS fabrication processes*. There is a large body of literature devoted to mathematical models of phototransistor action. The previously existing equations that model phototransistor operation are only of limited use in the design of phototransistors as they involve parameters that are poorly controlled or whose values integrated circuit designers have no access to. The mathematical models are useful, however, in providing general principles which can guide the construction of test circuits for the purposes of determining optimal phototransistor designs.

The basic models of phototransistor action involve the photogeneration of carriers in the base region only. These photocarriers contribute to the base current

which controls the collector current through the regular bipolar junction transistor action. In order to be as accurate as possible in characterizing phototransistor performance it is necessary to consider other sources of carriers in the base region aside from carriers generated either thermally or photoelectrically in the base. If light falls on the emitter and collector regions, carriers will be generated there and these carriers will contribute to the overall current. Detailed mathematical models indicate that the emitter photocurrent serves to reduce the sensitivity of the phototransistor, while the collector photocurrent enhances the sensitivity.

3. Design of Phototransistors Fabricated in a Standard CMOS Process

In a phototransistor designed using a standard digital CMOS process several constraints must be borne in mind. First of all, the phototransistor will have a lateral as well as a vertical structure. The typical CMOS process phototransistor is essentially the parasitic, latchup-inducing bipolar transistor that CMOS designers strive to avoid. Specifically, for a *pnp* transistor, the emitter consists of a region of *p*-diffusion, the base consists of a surrounding *n*-well region, and the collector is formed from the *p*-type substrate. This design has the advantage of automatically taking on the p^+np form, thus producing a high emitter efficiency.

A potential problem with the CMOS process-based phototransistor is that the phototransistor base width is a difficult parameter to control and analyze. Because the *n*-well (which forms the base region) surrounds the emitter, while the base is surrounded by the substrate (the collector) there will be a lateral as well as a vertical base width. The lateral base width is under the control of the designer, but the vertical base width is not under his/her control, and is often not even known to the designer. The emitter diffusion in the MOSIS 2 micron CMOS process has a vertical extent of approximately $0.5 \mu\text{m}$ and the well depth has a vertical extent of approximately $4.0 \mu\text{m}$. In the vertical direction, then, the base width

is approximately $3.5 \mu\text{m}$. Design rules require the n -well to extend at least $5 \mu\text{m}$ beyond the p -diffusion edge, however, implying that the lateral base width must be at least $5 \mu\text{m}$ as well. Note that violation of the well width design rule is possible; violating this design rule could yield higher β phototransistors.

A complication which arises in analyzing the MOSIS phototransistor is that much of the collector-base junction is perpendicular to the incoming light, as opposed to parallel to it. The junction is approximately $4 \mu\text{m}$ deep into the substrate in the vertical direction. Because different frequencies of light penetrate to different depths in the device, it is clear that the relative importance of the lateral junction (located at the sidewalls of the n -well) as compared to the vertical junction (located at the bottom of the n -well) will vary with frequency.

In order to design effective phototransistors we need to determine the effect of the following design variables on the sensitivity of the phototransistors.

- Emitter Size
- Size of Emitter-Base Junction
- Base Size
- Size of Collector-Base Junction
- Collector Size
- Shielding of Base and Collector Regions
- Location of Ohmic Contacts

Choosing a small emitter area has a number of advantages. In a vertical phototransistor, the emitter lies on top of the base and thus can absorb photons before they can reach the high-gain absorption region in the base. Hence, keeping the emitter size to a minimum reduces the amount of photons absorbed by the emitter. In the same vein, keeping the emitter area small keeps the parasitic emitter currents small, improving β . Using a small emitter has its drawbacks as well, however. If the lateral base area expands to occupy the area once covered by the emitter, then the lateral base width will increase, possibly adversely affecting

phototransistor gain. If the base area is made smaller to preserve the lateral base width, however, the portion of the base region which can absorb incoming light is greatly reduced. One way in which to retain a large emitter, without generating an excessively large emitter photocurrent is to shield the emitter by covering it with a metal layer.

The wider the lateral portion of the base, the more photocarriers can be generated in that base, thus increasing the base current. On the other hand, however, increasing the lateral base width will reduce the gain of the phototransistor. Furthermore, increasing the base width increases the chip area occupied by the phototransistor.

One question which arises in collector layout is whether including substrate contacts in close proximity to phototransistor base regions improves device performance. In the case of a *pn*p phototransistor, the substrate contacts would pin the collector low. The collector, which is the substrate in the MOSIS digital CMOS process, is normally pinned at various locations on the chip to the negative supply voltage, in order to prevent latchup in the CMOS circuitry. Because the collector is the substrate, its distributed resistance may be quite high. Including a local substrate contact makes the reverse bias voltage seen by the base-collector junction consistent and predictable. Furthermore, if there are other circuit elements near the phototransistors in a circuit design, including substrate contacts will make the collector voltage more independent of signals generated by these adjacent circuit elements. On the other hand, adding substrate contacts covers some of the substrate and hence prevents light from reaching part of the collector. If the photogenerated collector current is a significant portion of the overall device current, however, the increase in reverse bias voltage and collector voltage predictability may be too slight to make up for the lost collector-generated signal.

4. Results from Fabricated Photodiodes

In order to bypass the difficulties involved in obtaining information about optimal phototransistor design from mathematical models, we fabricated a test chip containing a number of different phototransistor designs. These phototransistors were laid out so as to determine the effect of varying the design parameters listed above, save the emitter size. The role of the emitter size in device performance was not investigated in this chip.

Insufficient information was available in the original test set to calculate specific device parameters like β . This was due to the fact that we had no way of measuring the base current (which consisted entirely of photocurrent).

Two shapes of the phototransistor were constructed, a square shape and a cross shape, in order to test the hypothesis that the response should depend primarily on base area and not on overall area. Thus, the cross and the square should have similar responses. The sizes were also varied, but only in the case of the squares. The three sizes of the emitter plus base area which were implemented are 484 square microns, 900 square microns, and 1600 square microns. The base areas were 340, 500, and 700 square microns, respectively. Again, as we expected response to be directly related to base area, the most sensitive photoreceptor should be the largest one.

Another element which was varied in the photoreceptors was whether or not substrate contacts were placed in the collector region immediately around the base area. The hypothesis was that the substrate contacts would anchor the collector voltage more securely, increasing the emitter-collector voltage in the bipolar transistor (bypassing any distributed substrate resistance-induced voltage change which might occur at the collector) and thus increasing collection efficiency. Both the cross and square type photoreceptor cells were laid out with and without substrate

contacts.

A significant observation was that the collector photocurrent contributes a great deal to the phototransistor sensitivity. This conclusion emerges from the fact that phototransistor response varied directly (though not linearly) with the amount of exposed substrate acting as the collector near a given phototransistor. A second conclusion, at least for this process, is that including substrate contacts does not help device performance. In fact, substrate contacts slightly degrade overall photosensitivity, almost certainly because the photogenerated collector current is reduced by the metal lines covering collector regions connecting the substrate contacts to supply voltages.

An interesting experimental result which admits at least two possible interpretations is that cross-shaped emitter and base regions having identical lateral base areas and base-collector junction areas as square-shaped emitter and base regions had significantly lower light sensitivity. The first possible explanation for this phenomena, which no doubt at least contributes to it, is that the cross shape effectively reduces collector-volume within a diffusion length of the base-collector junction. This fact implies that there will be a reduced number of carriers generated in the collector and hence a reduced photocurrent. A second possible explanation for the superior performance of square-shaped emitter regions over cross-shaped ones is that the square regions yield a greater vertical base volume. Thus, more carriers will be generated in the square regions than in the cross-shaped regions and the photocurrent for the square-based devices will be larger. Because penetration depth is highly frequency dependent, the degree to which the two explanations model the observed behavior should also be highly frequency dependent. We plan to measure the dependence of the phototransistor sensitivity on the illumination wavelength in the near future.

Because of design rules in the process requiring a 5 micron overhang of well beyond diffusion boundaries, the minimum width of the bipolar transistor base is 5 micron. This figure is quite large and hence the β for the phototransistor is expected to be extremely low, on the order of 5 to 10. Under standard, high β circumstances it is normal to expect that the carriers generated in the base will result in an emitter current which swamps the contribution of the collector. If, however, β is quite low, the contribution of the current generated in the collector to the overall device current and hence to the output voltage can be quite significant. Under these circumstances, the phototransistor behaves much like a photodiode.

The hypothesis that the phototransistor has a low β explains many if not all of the deviations from expected behavior in that circuit. We observed an anomalous yet persistent result that phototransistors which were at the end of transistor arrays (on the chip) and therefore adjacent to areas of bare substrate had stronger responses to light than do the devices in the rest of the arrays. If the collector current is making a significant contribution to the overall output, this observation would be quite reasonable; a larger bare substrate region near a device implies a larger collector area near the device and therefore a larger collector current and greater sensitivity to light. A related line of reasoning would explain why cross shaped emitters and bases yield less sensitive phototransistors than square shaped emitters and bases, and leads to the conclusion that, under low- β conditions, a square phototransistor should indeed be more light-sensitive than a cross-shaped phototransistor, even if the base areas of the two devices are identical.

The observation that adding substrate contacts tended to reduce device sensitivity is also explained by the low phototransistor β . Adding substrate contacts in the collector region covers area in the collector region of the substrate with a layer of metal. In addition, the contacts are connected to the supply rail with metal wires running over the substrate. If the collector contribution to the overall device

current is significant, the fact that a large part of the collector area is placed in shadow will necessarily reduce the sensitivity of the photoreceptor.

The following conclusions can be made from our test results. One is that phototransistors constructed using a standard CMOS fabrication process have very low β and do not have much more sensitivity than photodiodes. Carver Mead (personal communication) has observed this low β as well in his designs and proposes temporal integration of photo-current onto a reverse biased base-emitter junction capacitance. After a period of time the junction is forward biased and a large current pulse briefly flows. The advantages of this are two-fold. One is that the photo-current is larger due to the integration over time and the other is that the transistor β increases with base current. Thus the brief pulse of high base current results in an increased β . Such an approach, however, is incompatible with our system due to the synchronous nature of this technique. Square emitter and base regions should be used to maximize the vertical base volume. The collector contacts (substrate contacts) should be as far away from the transistor as possible while maintaining isolation from other circuitry (i.e., the collector contacts should be on the periphery of the phototransistor).

**ANNUAL REPORT OF
PUBLICATIONS/PATENTS/PRESENTATIONS/HONORS**

b. Papers Published in Refereed Journals

J. J. Clark, "Split Drain MOSFET Magnetic Sensor Arrays," *Sensors and Actuators A-24*(2), 107-116 (1990). (Partially supported by NSF CDR-85-00108)

g. Invited Presentations at Topical or Scientific/Technical Society Conferences

J. J. Clark and R. P. Hewes, "Active Sensing at a Microscopic Scale," *IEEE Symposium on Intelligent Control*, Philadelphia, September 1990. (Partially supported by NSF CDR-85-00108)

J. J. Clark, 10th Annual Phoenix Conference on Computers and Communications, Phoenix, March 1991

J. J. Clark, California Institute of Technology, April 1991

J. J. Clark and D.J. Friedman, "VLSI Sensori-Motor Systems," *IEEE Robotics and Automation Conference*, Sacramento, April 1991. (Partially supported by NSF CDR-85-00108)

i. Honors/Awards/Prizes

D. J. Friedman was awarded Second Prize in the 1991 Student VLSI Design Contest held by the Massachusetts Microelectronics Center. This award was for the sensorimotor chip described in this progress report.

J. J. Clark was appointed Guest Editor for a Special Issue on "VLSI for Computer Vision" of *The International Journal of Computer Vision*.

j. Graduate Students and Postdoctorals Supported Under JSEP for the Year Ending July 31, 1991

Mr. D.J. Friedman and Mr. N. Saxena.

III.2 Discrete Event Dynamic Systems Study. Y. C. Ho, Contracts ONR-N00014-86-K-0075, NSF-CDR-88-03012, and DAAL-03-86-K-0171; Research Unit 10.

In 1990-91, we continued our research in Discrete Event Dynamic Systems (DEDS) and Perturbation Analysis (PA). Considerable efforts were spent in consolidating the progress in this new field. To this end, the following three books on the subject were produced by members or former members of this research group:

1. *Gradient Estimation via Perturbation Analysis* by Paul Glasserman (Kluwer Academic Press, Dec. 1990),
2. *Perturbation Analysis of Discrete Event Dynamic Systems* by Y. C. Ho and X. R. Cao (Kluwer Academic Press, June 1991), and
3. *Introduction to Discrete Event Dynamic Systems*, Y. C. Ho (editor) (IEEE Press Reprint Book, Sept. 1991).

In addition, the first issue of the *International Journal on DEDS* under the editorship of Y. C. Ho was published in June 1991. An international workshop on DEDS sponsored by NSF and organized by members or former members of this research group took place on June 21-23, 1991 at Amherst, MA.

Furthermore, research results were obtained in the area of gradient surface optimization and in the analysis of communication networks including FDDI.

Gradient Surface Optimization using PA

We studied a gradient surface method (GSM) for the optimization of DEDS. GSM combines the advantages of Response Surface Methodology (RSM) and efficient derivative estimation techniques like Perturbation Analysis (PA) or Likelihood Ratio method (LR). In GSM, the gradient estimation is obtained by PA (or LR), and the performance gradient surface is obtained from observations at various points in a fashion similar to the RSM. The advantages of this approach are greatly increased efficiency of computation. Many experiments were conducted for comparison purposes including previously computationally-infeasible problems.

Analysis of the Performance of Communication Networks

We present and analyze several flow control schemes for packet networks. Using simple path comparisons, we establish stochastic monotonicity and concavity properties of the packet acceptance process with respect to control parameters of the various schemes. Our main results specify precisely how the choice of control parameters influences both the flow of packets into a packet network and the level of congestion within the network. We compare the performance of the various mechanisms and exploit their stochastic properties to develop efficient stochastic optimization algorithms that may be used to dynamically adjust the control parameters "on-line" to maintain optimal performance.

A study of the performance of a 100 Million bits/sec token ring protocol called the *Fiber Distributed Data Interface* (FDDI) was carried out using a fluid model. This work is currently under a review as a possible contribution to the *IEEE Transactions on Communications* as a correspondence item [1].

Reference:

1. R. S. Sreenivas, "Performance Analysis of FDDI Token Ring Networks using a Fluid Model," *IEEE Trans. on Commun.* (February, 1991) (submitted).

ANNUAL REPORT OF
PUBLICATIONS/PATENTS/PRESENTATIONS/HONORS

a. Papers Submitted to Refereed Journals (and not yet published)

M. C. Fu and J.-Q. Hu, "On Smoothed Perturbation Analysis for Second Derivative Estimation of the G1/B/1 Queue," *IEEE Trans. on Auto. Control* (1991) (to appear).

J.-Q. Hu, P. Glasserman, and S. Strickland, "Strongly Consistent Steady State Derivative Estimations," *Engineering and Information Sciences* (1991) (to appear).

J.-Q. Hu, "Consistency of Infinitesimal Perturbation Analysis for Queueing Systems with Load-Dependent Arrival and/or Service Rate," *Queueing Systems*, (1991) (to appear).

J.-Q. Hu and M. C. Fu, "Consistency of Infinitesimal Perturbation Analysis for the G1/G/m Queue," *European Journal of Operational Research* (1991) (to appear).

J.-Q. Hu, "Convexity of Sample Path Performances and Strong Consistency of Infinitesimal Perturbation Analysis Estimates," *IEEE Trans. on Auto. Control* (1991) (to appear).

B. Zhang and Y. C. Ho, "Performance Gradient Estimation for Very Large Markov Chains," *IEEE Trans. on Auto. Control* (1991) (to appear).

B. Zhang and Y. C. Ho, "Likelihood Ratio Methods Using A-segments," *Performance Evaluation* (1991) (to appear).

Y. C. Ho, L. Y. Shi, L. Y. Dai, and W. B. Gong, "Optimization Discrete Event Dynamic Systems via Gradient Surface Method," *Journal of Discrete Event Dynamic Systems* (submitted).

R. S. Sreenivas, "Performance Analysis of FDDI Token Ring Networks using a Fluid Model," *IEEE Trans. on Communications* (February, 1991) (submitted).

L. Shi, "Approximate Analysis for Queueing Networks with Blocking," *Queueing Systems: Application and Theory* (1991) (submitted).

Z. B. Tang and L. Shi, "Note on 'Distributed Scheduling Based on Due Dates and Buffer Priorities' by S. H. Lu and P. R. Kumar," *IEEE Trans. on Auto. Control* (1991) (submitted).

K. Budka and D. D. Yao, "First- and Second-Order Stochastic Properties of Rate Control Throttles," *IEEE Trans. on Communications* (submitted).

K. Budka and D. D. Yao, "First- and Second-Order Stochastic Properties of Rate-based Flow Control Mechanisms," *IEEE Trans. on Auto. Control* (submitted).

b. Papers Published in Refereed Journals

J.-Q. Hu, "Steady-State Sample Path Derivative Estimators," *Appl. Math. Lett.* 3(3), 57-60 (1990).

J.-Q. Hu and S. G. Strickland, "Strong Consistency of Sample Path Derivative Estimates," *Appl. Math. Lett.* 3(4), 55-58 (1990).

Y. Wardi and J.-Q. Hu, "Strong Consistency of Infinitesimal Perturbation Analysis for Tandem Queueing Networks," in *Discrete Event Dynamic Systems: Theory and Applications I* (Kluwer Academic Publishers, Boston 1991) pp. 37-59.

M. C. Fu and J.-Q. Hu, "Bias Properties of Infinitesimal Perturbation Analysis for Multi-server Queues," *Proceedings of the Winter Simulation Conference*, 377-381 (1990).

K. C. Budka and D. D. Yao, "Monotonicity and Convexity Properties of Rate Control Throttles," *Proceedings of the 29th IEEE Conference on Decision and Control*, 883-884 (December, 1990).

g. Invited Presentations at Topical or Scientific/Technical Society Conferences

Y. C. Ho, US/Japan Mfg. Research Exchange, July, 1990.

Y. C. Ho, IFAC World Congress Planetary Talk, August, 1990.

Y. C. Ho, U. of Vienna, CS and Statistics Conference, August, 1990.

Y. C. Ho, IBM Yorktown Research Center, September, 1990.

Y. C. Ho, Harvard-MIT-BU-UMass DEDS Seminar, September, 1990.

Y. C. Ho, IEEE Conf. on Decision and Control, December, 1990.

Y. C. Ho, MIT Operation Research Center, March, 1991.

Y. C. Ho, Academia Sinica, PRC, June, 1991.

Y. C. Ho, ACC DEDS Workshop, June, 1991.

j. Graduate Students and Postdoctorals Supported Under JSEP for the Year Ending July 31, 1991

Drs. R. Sreenivas and Z. Bo Tang, and Mr. K. Budka, Mr. L. Y. Shi, and Mr. L. Y. Dai

IV. ELECTROMAGNETIC PHENOMENA

Personnel

Prof. T. T. Wu
Prof. R. W. P. King
Dr. J. M. Myers
Dr. S. S. Sandler
Dr. H.-M. Shen

Mr. G. Fikioris
Mr. D. K. Freeman
Mr. V. Houdzoumis
Ms. M. Owens
Ms. B. H. Sandler

Research in the area of electromagnetic radiation is directed toward the solution of practical problems through the complete understanding of the underlying physical phenomena. This involves the coordinated application of modern analytical, numerical, and experimental techniques and the use of high-speed computers and precision instrumentation. Application is also made of modeling techniques and the principle of similitude. Most practically significant problems in the area are sufficiently complicated that extensive computation and measurement are often required to justify approximations that are usually necessary. Where possible, general formulas are obtained and verified experimentally so that the phenomenon under study can be understood physically in analytical form and not just as a set of numbers.

The researches are concerned primarily with the properties of antennas and arrays and of the electromagnetic fields they generate in various practically important environments that lead to difficult problems with complicated boundary conditions. Examples include dipoles, insulated antennas, traveling-wave antennas and arrays, crossed dipoles, and loops near the boundary between two media such as air and the earth or sea, or the oceanic crust and sea water; microstrip patch antennas and Beverage-type antennas for over-the-horizon radar; the properties of lateral electromagnetic waves; remote sensing with lateral waves from the surface of the earth or

sea, the arctic ice or the sea floor; lateral waves and reflected waves in horizontally-layered media; the generation, propagation, and reception of lateral electromagnetic pulses; arrays of antennas along curved lines; and solitary electromagnetic pulses with slow rates of decay.

IV.1 On the Radiation Efficiency of a Vertical Electric Dipole in Air Above a Dielectric Half-Space. R. W. P. King, B. H. Sandler, and M. Owens, Grant N00014-89-J-1023 and MITRE Corp. Project No. 91260; Research Unit 11.

A study of the fraction of power that remains in the air (upper half-space) and the fraction that is transferred into the earth (lower half-space) when the radiating source is a vertical dipole at a height d in the air has been completed [1]. The power P radiated by the dipole was separated into two parts by Hansen [2]: a part P_a that remains in the air, and a part P_g that is transferred into the earth. Hansen introduced this division of power in order to define the *radiation efficiency* as $\eta = P_a / (P_a + P_g)$. This is the fraction of the power radiated by the dipole that remains in the upper half-space. Since it appears superficially obvious that radio transmission between antennas in the air depends on the power that remains in the upper half-space, it seems reasonable to assume that the most desirable antenna is one that has the highest radiation efficiency. Actually, this ignores the important fact that power ultimately transferred to the earth at large radial distances is available in the air at all shorter distances.

The determination of the power in each region as a function of the height d of the dipole involves not only direct, reflected, and refracted or transmitted waves, but also a surface wave that travels along the boundary in the air. The recently derived formulas [3] for the electromagnetic field in air of a vertical electric dipole at the height d in air show that, when $d \sim 0$, the entire field along the surface of the earth is given by a surface wave that propagates along the boundary in the air and

transfers power into the earth as it travels. The surface wave is shown to contribute a major part of the low-angle field needed for over-the-horizon radar. Since all the power associated with the surface wave is transferred into the earth, an antenna that generates a large surface wave—like the vertical dipole on the earth—must have a low radiation efficiency.

The design of an antenna that maximizes the surface wave and the entire low-angle field in the range $80^\circ \leq \Theta \leq 90^\circ$ is a problem of considerable interest. Such an antenna will have a low radiation efficiency and most of the power radiated will not remain in the upper half-space (air) but will be transferred to the lower half-space (earth). It may be concluded that the concept of radiation efficiency as defined by Hansen is not a useful figure-of-merit.

References:

1. R. W. P. King, "On the Radiation Efficiency and the Electromagnetic Field of a Vertical Electric Dipole in the Air Above a Dielectric or Conducting Half-Space," Chapter 1 in *Progress in Electromagnetics Research*, Vol. 4, edited by J. A. Kong, Elsevier Science Publ. Co., Inc., New York, 1990, pp. 1-43.
2. P. Hansen, "The Radiation Efficiency of a Dipole Antenna Located Above an Imperfectly Conducting Ground," *IEEE Trans. Antennas Propagat.* AP-20, 766-769 (1972).
3. R. W. P. King, "Electromagnetic Field of a Vertical Dipole Over an Imperfectly Conducting Half-Space," *Radio Science* 25, 149-160 (1990).

IV.2 The Circuit Properties and Complete Fields of Wave Antennas and Arrays. R. W. P. King, Grant N00014-89-J-1023; Research Unit 11.

The wave antenna is important for communication between points on or near the surface of the earth and especially as a versatile backscatter radar capable of detecting targets in the whole range from distant and high-flying to quite close and low-flying. For distant targets the curvature of the earth makes the use of reflection from the ionosphere a necessary complication. Transmission to the 300 to 500 km

distant ionosphere requires quantitative knowledge of the field at all upward angles. When the target is not an ICBM thousands of kilometers away but a cruise-missile launched by a submarine or a low-flying drug-carrying aircraft within 1000 km of the radar transmitter-receiver, reflections from the ionosphere are best supplemented by the surface wave. This is unaffected by geomagnetic storms and independent of skip distances.

The wave antenna consists of a long horizontal wire in air electrically very close to the surface of the earth or sea and so terminated that a pure traveling wave propagates along it in both the transmitting and receiving modes. This can be accomplished with suitable ground connections in series with a resistor as in the familiar Beverage antenna. Alternatively, each termination may be a resistor in series with a horizontal, quarter-wave monopole to form a horizontal-wire antenna. With either form, the generator-receiver is located adjacent to the resistor at one end. The wave antenna was analyzed previously [1] subject to the condition $\rho^2 \gg z'^2$ where ρ is the radial distance from the source and $z' = -z$ is the height of the point of observation above the surface of the earth.

In a new investigation [2], the complete electromagnetic field generated by a wave antenna—including both the space wave and the surface wave at all points in the air and on the surface of the earth or sea—has been derived. A knowledge of this complete field is essential for an over-the-horizon radar that makes use of both ionospheric reflection for detecting distant high-flying targets and the surface wave for detecting near and low-flying targets.

Although the electromagnetic field of a unit electric dipole is smaller by the factor $|k_2/k_1|$ when it is horizontal at a small height d than when it is vertical, a long traveling-wave antenna with a very substantial directive gain that can approximate or exceed the ratio $|k_1/k_2|$ can be constructed of horizontal elements. Indeed, an array of broadside and collinear wave antennas can provide an electromagnetic

field of much greater intensity and at much lower constructional cost than can be achieved with vertical monopoles alone. This is not obvious from the earlier analysis [1] since it determined only the surface-wave field of a single Beverage or horizontal-wire antenna.

It is also possible to combine the directive wave antenna with a vertical monopole to obtain a useful omnidirectional antenna that generates a powerful surface wave combined with a significant space wave. In [2] the design of such an array is presented. It consists of a vertical monopole and $N = 10$ horizontal wave antennas at a small height $d = 45$ cm over the earth. No ground connections are required. It is shown that the use of an array of horizontal wave antennas with a vertical monopole in place of the usual grounding network not only increases the space wave but uses the power ultimately dissipated in the earth to generate a large and useful surface wave.

In some applications in radar and in point-to-point communication, a directive array is preferred over an omnidirectional one. In such cases, an antenna that radiates a large field within a specified angle and a small field in all other directions is advantageous. Such an array is readily obtained by a simple modification of the omnidirectional array discussed above. Other combinations of vertical monopoles and horizontal wave antennas have interesting and useful characteristics. An example is a highly directive broadside array in which each element is a single vertical antiresonant monopole in series with a single horizontal wave antenna. A base-insulated resonant dipole is used as a parasitic reflector for each vertical element.

References:

1. R. W. P. King, "The Wave Antenna for Transmission or Reception," *IEEE Trans. Antennas Propagat.* AP-31, 956-965 (1983).
2. R. W. P. King, "The Circuit Properties and Complete Fields of Wave Antennas and Arrays," *Space Communications*, submitted for publication.

IV.3 Generalized Theory for a Three-Layered Region; Application to Microstrip and Patch Antennas on Microstrip. R. W. P. King, B. H. Sandler, M. Owens, and T. T. Wu, Grant N00014-89-J-1023; Research Unit 11.

The analysis of the electromagnetic field generated by a horizontal electric dipole on the surface of the dielectric-coated conductor used in microstrip can be carried out subject to the inequalities $k_0^2 \ll |k_1^2| \ll |k_2^2|$, with k_2 relatively large rather than infinite. This generalization greatly increases the mathematical formalism and the complexity of the integrals that define the surface wave. Since it is unnecessary for microstrip, the simplification $k_2 \rightarrow \infty$ can be made. However, it is of theoretical interest to determine precisely what is neglected when k_2 is set equal to infinity and, simultaneously, to learn what happens when propagation can take place in three regions.

General expressions have been derived [1] in simple integrated form for the complete electromagnetic field generated by a horizontal electric dipole in the air above a two-layered region consisting of an electrically thin sheet of dielectric on a conducting or dielectric half-space. This includes the field at all points in all three regions. No conditions are imposed other than the basic inequalities $k_0^2 < k_1^2 \ll |k_2|^2$ and $k_1 l < 1$. The complete analysis of the field in the air over a dielectric-coated region with a large wave number reveals the following interesting properties:

1) The lateral wave generated in the air along the air-dielectric boundary and the trapped surface wave in the thin dielectric layer on a perfectly conducting plane ($k_2 \rightarrow \infty$) combine into a single surface wave when $k_1 l$ is electrically small. This propagates in the air and in the thin dielectric with the wave number k_0 . Its amplitude is multiplied by the small quantities $k_0 l$ or $k_0^2 l^2$ so that it vanishes when $l = 0$.

2) When $k_1 l$ is small and $|k_2|$ is large but finite, a second lateral wave—

associated with conduction and polarization currents in Region 2—is generated along the air-dielectric boundary. It has the same properties as when $l = 0$, but involves the factor $(k_0/k_2)(1 - ik_1^2 l/k_2)^{-1} = k_0(k_2 - ik_1^2 l)^{-1}$ instead of k_0/k_2 .

3) The complete surface wave when $|k_2|$ is large but finite and $k_1 l$ is electrically small is a superposition of the surface waves associated with the dielectric layer and the imperfectly conducting half-space. It involves the combined factor $k_0(k_2^{-1} - il)(1 - ik_1^2 l/k_2)^{-1}$. When $k_2 \rightarrow \infty$, this reduces to 1); when $l = 0$, it reduces to 2).

The detailed application of the formulas to problems in the theory of microstrip—including especially microstrip patch antennas—is presented in a new paper [2]. The formulas for the complete electromagnetic field of a unit horizontal electric dipole on the surface of a dielectric-coated conductor (microstrip) as derived in [1] are used to derive expressions for the far field. This includes the space wave and the surface wave. The radiated power and radiation resistance are derived. The corresponding formulas for the far field of an antiresonant rectangular patch antenna with an assumed sinusoidal current distribution are derived.

Another application of the generalized theory is to surface-wave propagation over the ice-coated sea of the Arctic and possible communication with submarines. The detection of submarines under the ice is also of interest. This is discussed under Topic IV.4.

References:

1. R. W. P. King, "The Electromagnetic Field of a Horizontal Electric Dipole in the Presence of a Three-Layered Region," *J. Appl. Phys.* **69**, 7987-7995 (1991).
2. R. W. P. King, "Electromagnetic Field of Dipoles and Patch Antennas on Microstrip," *Radio. Sci.*, submitted for publication.

IV.4 Generalized Theory for a Three-Layered Region; Application to Remote Sensing from the Arctic Ice. R. W. P. King, Grant N00014-89-J-1023 and Raytheon Co. (participant in Project ICEx-91 under DTRC Contract N61533-90-C-0080 managed by ONT); Research Unit 11.

In a recent paper [1], a detailed quantitative analysis is made of the problem of locating a submerged submarine by means of transmitting and receiving antennas located just below the air surface of the ocean. The problem at hand is to treat the closely related problem of locating a submarine in the ocean under the Arctic ice. This is a more complicated problem for two principal reasons. The first of these is the presence of a layer of salt-water ice with a thickness l of the order of 2.5 m. The second is the need to locate both the transmitting and receiving elements on the surface of the ice instead of at a small depth in the sea.

The generalized theory for a three-layered region [2]—described under Topic IV.3—can be applied to a three-layered region of air, ice and sea with the source and the receiver in the air and the scattering object in the sea. It is found that the layer of ice is electrically sufficiently thin at the frequencies of interest so that it can be ignored, and the data supplied in the earlier paper [1]—in which the antenna is at a depth d in the ocean instead of on an electrically thin layer of ice—can be used with only minor changes. These include setting $d = 0$ and making use of vertical bare terminations lowered into the sea through holes in the ice.

References:

1. R. W. P. King, "Lateral Electromagnetic Waves from a Horizontal Antenna for Remote Sensing in the Ocean," *IEEE Trans. Antennas Propagat.* 37, 1250-1255 (1989).
2. R. W. P. King, "The Electromagnetic Field of a Horizontal Electric Dipole in the Presence of a Three-Layered Region," *J. Appl. Phys.* 69, 7987-7995 (1991).

IV.5 The Propagation of a Gaussian Pulse in Sea Water; Application to the Detection of Submarines. R. W. P. King, Grant N00014-89-J-1023 and Raytheon Co. (participant in Project ICEX-91 under DTRC Contract N61533-90-C-0080 managed by ONT); Research Unit 11.

The propagation of electromagnetic waves in sea water is much more complicated than in lake water because the attenuation and phase constants are practically equal and both depend strongly on the frequency in a nonlinear manner. The interesting question arises: How does a single pulse progress in sea water? Is such a pulse a useful vehicle for detecting submarines at a considerable depth in the ocean? These questions can be investigated conveniently with a Gaussian pulse of current applied to a horizontal electric dipole on the surface of the sea. The Gaussian pulse is essentially a low-frequency pulse in the sense that the amplitudes of the constituent frequencies decrease very rapidly with increasing frequency. It is clearly well-suited to propagation in sea water where the exponential attenuation decreases with the frequency. When a Gaussian pulse is applied to a horizontal electric dipole on the surface of the sea, an electromagnetic pulse is generated that propagates upward into the air, downward into the sea, and horizontally along the boundary in a surface wave. Of interest here is the pulse propagating vertically downward and impinging on a submarine. Can this be detected by observing the backscattered pulse?

Detailed quantitative information has been obtained for the properties of a Gaussian pulse propagating in sea water. Of particular significance are the following points: 1) The amplitude of the propagating pulse decreases very rapidly with distance. 2) The shape of the pulse changes continuously with distance from the initial Gaussian shape to that of the time-derivative of the Gaussian. 3) The velocity of propagation of electromagnetic waves in sea water is frequency-dependent, decreasing with frequency. As the pulse propagates, the higher frequencies in its spectrum are more rapidly attenuated than the lower frequencies so that the higher

frequency content of the pulse decreases rapidly and with it the velocity of propagation of the pulse. 4) The apparent velocity of propagation of the maximum magnitude of the Gaussian pulse is anomalous. Because of the change in shape from the Gaussian to that of the derivative, the maximum of the pulse moves backwards for a short time. Actually all components move forward, only the maximum of their sum moves backwards.

To study the possible use of such a pulse in the detection of submarines, a direct transmission-reflection method has been used. This makes use of a horizontal electric dipole in the form of an insulated conductor with the length $2h$ terminated in bare ends. The dipole is electrically short for all frequencies involved in the Gaussian current pulse that is generated in it. The electromagnetic-field pulse travels vertically down into the sea. It induces a current in a submarine with length 100 m and cross-sectional diameter 12.5 m located at a depth $z = 100$ m. The current in the submarine radiates an electromagnetic field in all directions in the sea including upward. The signal reaching a receiver adjacent to the transmitting dipole is the means for detecting the submarine.

The shape and amplitude of the pulse reflected by the submarine depends on the spectrum of frequencies involved and, therefore, on the width of the incident pulse. The current induced in the submarine by each component of frequency is given in [1]. In the general case, the field scattered by each component of frequency has to be determined as in [1] and then summed over all frequencies. In a preliminary study this step can be avoided if the range of relevant frequencies is restricted to those for which the length of the submarine is electrically short in sea water. Gaussian pulses with widths $2t_1 \geq 0.1$ sec satisfy this condition. For them the current induced in the submarine has the same frequency dependence as the incident field so that the scattered field will also have this dependence. This means that an incident Gaussian field pulse should be scattered as a Gaussian field pulse.

If significant higher frequencies are present, the induced current becomes frequency-dependent and the scattered field is modified. Actually the induced current distribution differs little from the parabolic shape for electrically much longer scattering elements. The principal difference is an increase in the amplitude of the induced current as the scatterer approaches the resonant length near $\beta_1 h = \pi/2$. It follows that the range of pulse widths can be decreased to $2t_1 = 0.01$ sec with the understanding that a scattered pulse will preserve the shape of the incident-field pulse quite accurately, but that the actual scattered-field amplitude should be somewhat greater than that calculated using the approximate current.

It has been found that a submarine at a depth of 100 m is detectable with a Gaussian pulse of width $2t_1 = 0.01$ sec, but with a Gaussian pulse of width $2t_1 = 1$ sec only if the large direct signal can be cancelled. A complete investigation of a range of relevant depths and pulse widths can be made. However, for pulses shorter than $2t_1 = 0.01$ sec, the general formula for the current induced in the submarine must be used and, since this is frequency-dependent, the response to an incident pulse requires numerical evaluation.

Reference:

1. R. W. P. King, "Lateral Electromagnetic Waves from a Horizontal Antenna for Remote Sensing in the Ocean," *IEEE Trans. Antennas Propagat.* 37, 1250-1255 (1989).

IV.6 The Propagation of a Low-Frequency Burst in Sea Water. R. W. P. King, Grant N00014-89-J-1023 and Raytheon Co. (participant in Project ICEX-91 under DTRC Contract N61533-90-C-0080 managed by ONT); Research Unit 11.

The study of the propagation of single Gaussian pulses in sea water—discussed under Topic IV.5—has been extended to include the propagation in sea water of a short burst of oscillations when its amplitude is limited by a Gaussian envelope. In

particular, a complete analysis has been made of the propagation in sea water of a burst of 25 cycles at $f \sim 25$ Hz with amplitudes limited by a Gaussian envelope with the half-width $t_1 = 0.5$ sec. The properties of the burst in transmission are governed in part by the Gaussian envelope, in part by the burst of oscillations. The most important characteristic is the very rapid decrease in the overall amplitude due to the electrically short distances involved and the initial $1/z^3$ dependence on distance. Owing to the very low frequencies involved in the burst and the spectrum of the envelope, the exponential attenuation is not great.

Just as for the isolated Gaussian pulse, the apparent continuity of Gaussian shape is misleading. Actually, the initial burst begins with a Gaussian envelope but the entire configuration changes rapidly to its time-derivative. In the process the maximum of the burst shifts to the initial maximum of the time-derivative. The initial backward movement of the maximum can be observed but this is much more difficult owing to the oscillations; also it is much more restricted to very short distances. A careful study of the numerical evaluation of the amplitudes of the individual oscillations shows that the apparent velocity of propagation $v_a = z/t$ of the maximum of the envelope decreases from large values near $z' = (\mu_0\sigma_1/2t_1)^{1/2}z = 0.1$ to an approximately constant value of the order of magnitude of the phase velocity for a steady-state traveling wave in sea water at $f \sim 25$ Hz. This behavior differs from that of the single Gaussian pulse which continuously loses higher frequencies from its spectrum as it travels in sea water and, hence, advances more and more slowly. The burst has primarily the properties of the 25 Hz oscillations at all distances.

Primary interest is in the electric field observed at a receiver on the air-sea surface near the transmitting dipole. As for the single Gaussian pulse, it is assumed that the back-scattered field is approximately the field incident on the scatterer but reversed in direction. The scattered burst is smaller than the direct burst observed at the receiver on the surface by a factor of the order 10^{-4} . It arrives at

the receiver while the direct burst is still rising to its maximum. If the direct burst can be balanced out in its entirety at the receiver, the scattered burst is sufficiently large to be detectable.

IV.7 The Detection of Dielectric Spheres Submerged in Water. R. W. P. King and S. S. Sandler, Grant N00014-89-J-1023 and the SBIR Program of the Small Business Administration; Research Unit 11.

The use of lateral electromagnetic waves to locate buried or submerged metal objects in the earth or sea with the horizontal electric dipole as the source has been described [1]-[3]. A related problem is the corresponding search for *dielectric* objects embedded in a general dissipative medium. Examples are plastic mines in the ocean and fragments of exploded plastic land mines embedded in human flesh. The important difference between the remote sensing for metal and plastic targets is the inverse nature of the relative magnitudes of the wave numbers characteristic of electromagnetic wave propagation in the ambient medium and in the embedded target. For simplicity the target can be taken to be a sphere consisting of air bubbles or plastic embedded in lake water, sea water or human flesh. The purpose of the study is to investigate the possibility of locating dielectric spheres in water or flesh by means of observations made on the boundary surface in the air.

The source is a horizontal electric dipole in the air on its boundary with the ambient medium that contains the target. It generates an electromagnetic field that propagates in the air along the boundary as a surface wave of a type known as a lateral wave. The amplitude fronts of the field in the earth or water propagate vertically downward; the phase fronts travel at an angle. It is this field that is incident on a target located at a depth z . In practice the field is not maintained by an infinitesimal unit dipole, but by a center-driven antenna located parallel to and at a small height in the air above the plane boundary. The source is, in effect, a center-driven eccentrically insulated dipole. If the dipole antenna is adjusted in

length to be resonant and the height is carefully chosen, the driving-point impedance will be resistive and, hence, readily matched to a feeding transmission line.

The basic theory has been developed [4] for the use of horizontal electric dipoles on the surface of a dissipative region to detect small dielectric spheres embedded at some depth in that region. Since interest is in the detection of quite small targets and the scattering by dielectrics is much weaker than by metals, it is necessary to make use of quite high frequencies in order to have adequate resolving power. It has been shown that detectable reflected signals can be generated with acceptable power so that it should be possible to locate small dielectric objects with suitably designed apparatus. Work on the design and operation of such apparatus is in progress.

References:

1. R. W. P. King, "Scattering of Lateral Waves by Buried or Submerged Objects. I. The Incident Lateral-Wave Field," *J. Appl. Phys.* 57, 1453-1459 (1985).
2. R. W. P. King, "Scattering of Lateral Waves by Buried or Submerged Objects. II. The Electric Field on the Surface Above a Buried Insulated Wire," *J. Appl. Phys.* 57, 1460-1472 (1985).
3. R. W. P. King, "Lateral Electromagnetic Waves from a Horizontal Antenna for Remote Sensing in the Ocean," *IEEE Trans. Antennas Propagat.* 37, 1250-1255 (1989).
4. R. W. P. King and S. S. Sandler, "The Detection of Dielectric Spheres Submerged in Water," in preparation.

IV.8 Lateral Electromagnetic Waves (Manuscript for Book). R. W. P. King, T. T. Wu, M. Owens, and B. H. Sandler, Grant N00014-89-J-1023; Research Unit 11.

It has become a tradition in the publication of researches in the area of electromagnetic phenomena to periodically summarize and coordinate major segments in book form. Accordingly, a book is in preparation which contains the results of current and past researches on lateral electromagnetic waves that have been sup-

ported in large part by the Joint Services Electronics Program. The book is entitled "Lateral Electromagnetic Waves: Theory and Applications to Communication, Geophysical Exploration, and Remote Sensing." It has been accepted for publication by Springer/Verlag and the final camera-ready form is very near completion. The chapter headings are: 1. Historical and Technical Overview of Electromagnetic Surface Waves; Introduction to Lateral Waves, 2. Electromagnetic Preliminaries, 3. The Electromagnetic Field of a Unit Vertical Electric Dipole in the Presence of a Plane Boundary, 4. Applications of the Theory of the Vertical Dipole Near The Boundary Between Two Half-Spaces, 5. The Electromagnetic Field of a Horizontal Electric Dipole in the Presence of a Plane Boundary, 6. Interference Patterns; Comparison of Approximate Formulas with General Integrals and Measurements, 7. Applications of the Theory of the Horizontal Dipole Near the Boundary Between Air and Earth or Sea, 8. The Measurement of the Conductivity of the Oceanic Lithosphere with a Horizontal Antenna as the Source, 9. Lateral Waves in a One-Dimensionally Anisotropic Half-Space, 10. The Propagation of Lateral Electromagnetic Waves in Air over Vertical Discontinuities, 11. The Horizontally Layered Half-Space, 12. The Three-Layer Problem for Sediment on the Oceanic Crust, 13. Lateral Electromagnetic Pulses Generated by Vertical Dipoles, 14. Approximate Formulas for Lateral Electromagnetic Pulses Generated by Vertical and Horizontal Electric Dipoles, 15. The Propagation of Signals Along a Three-Layered Region: Open Microstrip, 16. Antennas in Material Media Near Boundaries: The Bare Metal Dipole, 17. Antennas in Material Media Near Boundaries: The Terminated Insulated Antenna, 18. The Wave Antenna.

IV.9 Theoretical Study of Electromagnetic Pulses with a Slow Rate of Decay. T. T. Wu, J. M. Myers, H. M. Shen, R. W. P. King, and V. Houdzoumis, Grant N00014-89-J-1023 and Army LABCOM Contract DAAL02-89-K-0097; Research Unit 11.

The interesting possibility of generating electromagnetic pulses of finite total radiated energy that decreases with distance much more slowly than the usual r^{-2} is being investigated both theoretically (this topic) and experimentally (see Topic IV.10). Such pulses are conveniently referred to as electromagnetic (EM) missiles [1].

Work during the past year has been concerned with the scattering of EM missiles from round objects, where "round" is taken to mean convex with a piecewise continuous, bounded, nowhere-zero surface curvature. The analysis treats the incident missile locally as a plane-wave transient impinging on the point of specular reflection, and applies geometrical optics to compute the reflection. This "geometric approximation" has been validated [2] by comparing its consequences with a detailed analysis of the two-dimensional problem of the scattering of an EM missile by a perfectly conducting circular cylinder, based on an expansion of the field in terms of Bessel functions. The two methods are found to agree exactly, justifying both the local approximation by a plane wave and the use of geometrical optics. The geometrical method has also been applied in [2] to the scattering of an EM missile by a sphere or by any perfectly conducting round object. The result for the sphere is that the backscattering preserves linear polarization, reverses circular polarization, and in both cases returns an energy flux proportional to $r^{-(2+\epsilon)}$, where the incident missile delivers a flux $r^{-\epsilon}$. The backscattered energy varies as the square of the radius of the sphere.

The $r^{-2-\epsilon}$ behavior of the energy of EM missiles scattered from spheres differs drastically from the $r^{-\epsilon}$ dependence of the backscattered energy on range from a flat plate. A study of other shapes that may exhibit behavior intermediate to these

two extremes is in progress.

References:

1. T. T. Wu, "Electromagnetic Missiles," *J. Appl. Phys.* 57, 2370-2373 (1985).
2. M. F. Brown and J. M. Myers, "Scattering of Electromagnetic Missiles by Perfectly Conducting 'Round' Objects," *J. Appl. Phys.*, submitted for publication.

IV.10 Experimental Study of Electromagnetic Pulses with a Slow Rate of Decay. H.-M. Shen, R. W. P. King, and T. T. Wu, Grant N00014-89-J-1023 and Army LABC0M Contract DAAL02-89-K-0097; Research Unit 11.

During this reporting period, an electromagnetic (EM) missile launched from a hyperboloidal lens has been investigated experimentally [1]. The lens system consists of two parts: a feeder which emits a spherical wave, i.e., serves as a point source; and a lens which refracts the spherical wave into a plane wave. The feeder is a V-conical antenna (VCA). Because it has a wide frequency band, the waveform of the EM field emitted from the VCA is very close to that fed from the pulse generator. The lens chosen in the experiment is a hyperboloidal lens, made from Paraffin Wax; its thickness is 0.49 ft.

An exact analysis of the lens system was not feasible; however, an approximate theory was developed using geometrical optics [1]. The first set of measured waveforms of the EM pulses did not agree with theoretical predictions. It was discovered that the EM field from the VCA-lens system is not due solely to a pure plane-wave aperture field. There exists, in addition, a spherical wave emitted by the VCA outside the lens. The combination of these two radiations causes a reduction of the second negative pulse. In order to eliminate the spherical wave outside the lens, absorbers were placed around the outside of the lens. The waveform of the EM pulse from the VCA-lens system after the absorber was added is a pair of mutually opposite pulses, as predicted by the theory. Thus the lens system performs like an

aperture field similar to that from a parabolic reflector. The waveform variation with distance is nearly the same as that from the parabolic reflector. In fact, the only difference between the two launchers is that the EM pulses from the reflector have a sign change because of the reflection from the metal paraboloid.

A new experimental program to generate subpicosecond EM pulses using lasers has been initiated at Harvard this year. Several entirely new techniques have been developed in recent years by other researchers for the generation of EM pulses based on the conversion of a subpicosecond light pulse into a subpicosecond electromagnetic pulse. A technique of *laser-triggered electrical discharge* (LTED) demonstrated at Columbia University by Zhang et al. [2] has the advantage of producing a current pulse synchronized over an aperture in a way that is ideal for generating an EM missile. From the measurements made so far, the LTED shows great promise for the generation of picosecond and subpicosecond electromagnetic pulses free of any optical carrier, with bandwidths on the order of 10^{12} Hz, and peak power densities of several MW/cm². This corresponds to an energy flux per pulse at the launcher on the order of 10^{-6} J/cm². For a train of 10^6 pulses, one therefore launches a flux on the order of 1 J/cm² per pulse train.

Equipment needed to generate subpicosecond optical pulses has been procured, installed and tested. This equipment consists of a Coherent, Inc., Model 702, dual-jet dye laser, which in a test after installation produced light pulses of 0.75 ps duration at a peak power of 3.9 kW. The 702 laser is pumped by a Coherent, Inc., Antares YAG laser. This is an infrared mode-locked laser that produces 80-ps pulses at a repetition rate of 38 MHz with 20 Watts of average power; these pulses are put through a frequency doubler to produce slightly shorter pulses at 532 nm that pump the 702 dye laser. The 702 laser produces pulses adequate for an initial investigation into the possibilities of light-triggered EM missiles, and is less expensive than the faster Satori pulse laser. A 5 ft × 16 ft Newport optical table, air-mounted, has

been procured and installed as the platform for experiments in the generation and measurement of light pulses and of other EM pulses made by rectifying them.

Current efforts are concerned with supplementing this equipment with suitable semiconductor surfaces, a power supply to provide electrical pulses to bias the semiconductors, and photo-conductive receiving antennas adequate to measure and confirm the production of an EM missile produced by a laser-triggered electrical discharge. Other interesting areas for future work include the development of microminiature antennas, especially photoconductively switched antennas, and associated instrumentation to more accurately measure the electromagnetic pulses obtained by laser triggering. The L-antenna, shown to be an effective receiver and probe for 50-ps pulses, may be adaptable to the newer shorter EM pulses.

References:

1. H.-M. Shen, T. T. Wu, and J. M. Myers, "Experimental Study of Electromagnetic Missiles from a Hyperboloidal Lens," SPIE Proceedings, Vol. 1407, Intense Microwave and Particle Beams II, 286-294 (1991).
2. J. T. Darrow, B. B. Hu, X.-C. Zhang, and D. H. Auston, "Subpicosecond Electromagnetic Pulses from Large-Aperture Photoconducting Antennas," *Optics Letters* 15, 323-325 (1990).

IV.11 Idiosyncrasy in Optimal Quantum Measurements. J. M. Myers, Grant N00014-89-J-1023 and Army LABCOM Contract DAAL02-89-K-0097; Research Unit 11.

An unexpected new finding on measurements for decisions has resulted from a study of quantum measurements that decide between alternative hypotheses. As a preparation to working with lasers, a review was made of the quantum theory of light detection (as in laser communication), where a measurement is made to decide between two possible signals. Even without noise, quantum theory implies a nonzero minimum probability of a wrong decision. The study has found that measurements that achieve this minimum probability of error have some unexpected features, of

value in many situations where decisions are based on measurements.

A measurement takes place in some region of space and time. A region can be split up into loci—smaller spaces and shorter times. A measurement can be composed of local measurements, each confined to a single locus. From quantum theory one knows that the results of the same local measurement in the same situation can vary from one occurrence of the measurement to another. The new finding is that the local measurement for a given locus must be selected from alternative possibilities, based on the communication of results of outcomes from earlier loci, if the minimum probability of error is to be achieved. That means the measurement procedure—not just the outcome—varies. When one considers many occurrences of the same measurement, there is not just one possible local measurement for a given locus, but many alternative possibilities, with one of these selected during any particular occurrence, not prior to the whole measurement, but during the measurement, on the basis of outcomes from earlier loci. This is *outcome-guided* selection of local measurements.

If one thinks of the measurement as made by many local agents organized in a network of communication, an agent cannot be asked to perform a fixed local measurement for a given locus; variation of local measurements for a given locus is necessary to achieving minimum error:

- 1) Minimizing the probability of a wrong decision requires that agents—local measurers—make use of their neighbor's earlier outcomes, in selecting next operations. In the detection of binary coherent light signals, this outcome-guided selection reduces by half the probability of error compared with the best scheme of local measurements fixed in advance.
- 2) Because outcomes are random variables, outcome-guided selection of local measurements implies that identical measurers in the same situation select dif-

fering local measurements. This is called *idiosyncrasy in local measurements*.

Two symmetrically located agents choose different local measurements.

- 3) Constraints on idiosyncrasy increase the probability of error: differences between agents in choosing local measurements are essential to minimizing error.

Outcome-guided selection, with idiosyncratic variation, will be found in local measurements that compose any optimal measurement for which: i) the outcome of a local measurement for a given situation can vary from one occurrence to another; and ii) the least probability of error is obtained by employing local measurements selected according to earlier outcomes. A wide variety of decision situations meet these criteria.

Reference:

1. F. H. Madjid and J. M. Myers, "Axiom Inflow and Idiosyncrasy in Optimal Quantum Measurements," in preparation.

IV.12 Theoretical Studies of Large Circular Arrays of Dipoles. T. T. Wu, R. W. P. King, G. Fikioris, D. K. Freeman, B. H. Sandler, and H.-M. Shen, Grant N00014-89-J-1023, RADC Contracts F19628-88-K-0024 and F19628-91-K-0020, and Army LABCOM Contract DAAL02-89-K-0097; Research Unit 11.

The purpose of this research project has been to explore the properties and possible applications of a remarkable new resonator that combines the characteristics of an antenna array with those of a cavity resonator. It consists of a large number of parallel coplanar dipoles, equally spaced along a closed loop that may be circular, elliptical or serpentine. The single driven element excites electromagnetic waves that travel in both directions around the loop. These excite electric currents in the elements. The loop can be tuned to one of many possible resonant modes by correctly choosing the length and radius of each element, the distance between them, and their total number. When the loop is resonant, extremely large currents

oscillate in all of the elements with phase relations characteristic of the particular mode. These generate a far field pattern determined by the phase relations of the currents and the particular shape of the closed loop. The driving-point impedance is a very low resistance with negligible reactance.

Unlike wire and waveguide resonators in which the currents travel the entire length of the circuit with correspondingly large losses, the open resonator involves only transverse currents in very short, widely spaced conductors. Possible applications as a resonant circuit include oscillators and frequency control where its unusual shape and extremely low losses make it useful. Since the conditions of resonance are largely independent of the shape of the closed loop so long as there is no radius of curvature smaller than two wavelengths, an enormous range of possible shapes and associated field patterns is available. An important discovery recently is that field patterns are very sensitive to changes in the shape. Thus, the variety of possibilities may include particular phase relations, shapes and sizes that lead to extremely high directivity. Such an array would have important practical applications in point-to-point communication and radar; another application is as a microwave beacon.

The general methodology involves a highly precise analytical formulation, its accurate evaluation by computer—where the use of quadruple precision is needed for certain quantities—and, finally, a meticulous verification using an experimental model constructed to close dimensional tolerances. The results obtained to date have been highly encouraging. They show conclusively that this novel open resonator can be designed and built and that it is a device with very unusual properties that can have applications of major importance.

A summary of recently completed work on the theory for circular arrays is given below. More recent refinements in the theory of the resonant circular array with one element driven are described under Topic IV.13. Current efforts to analyze

closed-loop arrays of arbitrary shape are discussed under Topic IV.14. Related theoretical research on arrays of pseudodipoles is described under Topic IV.15. Finally, experimental studies of large circular arrays are the subject of Topic IV.16.

It was initially thought that elements near an antiresonant length were appropriate and a systematic study of the three-term theory was undertaken as a tool for analyzing circular arrays with elements up to a wavelength long. In the first part of this investigation the properties of the vector potentials of coupled antennas were examined and used to show that great simplification is achieved when the distance between adjacent elements is equal to or greater than the half-length of the elements [1]. The complete analysis of circular arrays in which the three-term theory is applied to determine the currents in the elements is contained in a companion paper [2]. An important conclusion is that the simpler two-term theory is entirely adequate when the elements are electrically short.

The application of the two-term theory to 60- and 90-element circular arrays of electrically long and thin elements yielded no sharply resonant arrays. On the other hand, the two-term theory applied to 60- and 90-element circular arrays of electrically short and quite thick tubular elements led to the discovery of a variety of sharply resonant modes with large currents in all elements and radiation patterns consisting of many sharp spikes. These modes and the underlying theory are described in detail in [3]. The properties of the different resonant modes are related to the resonances of particular phase sequences in the method of symmetrical components used in the analysis. They depend critically on the radius and length of each element and the distance between adjacent elements.

References:

1. R. W. P. King, "Electric Fields and Vector Potentials of Thin Cylindrical Antennas," *IEEE Trans. Antennas Propagat.* AP-38, 1456-1461 (1990).

2. R. W. P. King, "The Large Circular Array with One Element Driven," *IEEE Trans. Antennas Propagat.* AP-38, 1462-1472 (1990).
3. G. Fikioris, R. W. P. King, and T. T. Wu, "The Resonant Circular Array of Electrically Short Elements," *J. Appl. Phys.* 68, 431-439 (1990).

IV.13 Improved Analysis of the Resonant Circular Array. G. Fikioris, D. K. Freeman, R. W. P. King, H.-M. Shen, and T. T. Wu, Grant N00014-89-J-1023, RADC Contracts F19628-88-K-0024 and F19628-91-K-0020, and Army LABC0M Contract DAAL02-89-K-0097; Research Unit 11.

Recent investigations have shown that, while the real part is adequate, the imaginary part $K_I^{(m)}(z)$ of the kernel of the m^{th} phase-sequence integral equation used in [1] does not take into account the coupling effects with enough accuracy to predict the extremely narrow resonances of circular arrays. The need for a theory that is more accurate and from which it is easier to obtain information analytically has led to the development of a modified kernel, $K_I^{(m)}(z)$ (modified), which is simply $K_I^{(m)}(z)$ (old) with the electrical radius $ka = 2\pi(a/\lambda)$ set equal to zero in the self-coupling term [2]-[4].

The new formulation of the m^{th} phase-sequence integral equation treats self- and mutual coupling symmetrically, by averaging the mutual contribution to the vector potential over the surface of the dipole; thus the kernel takes the form of a double integral. The imaginary part of this kernel— $K_I^{(m)}(z)$ (double integral)—is, under suitable conditions, exponentially small in N (the number of elements), suggesting the existence of resonances that are exponentially narrow. Furthermore, this exponential smallness is independent of ka ; i.e., when $K_I^{(m)}(z)$ (double integral) is expanded in powers of ka , each term is exponentially small. The leading term in this expansion is simply $K_I^{(m)}(z)$ (modified).

The leading term in the asymptotic expansion of $K_I^{(m)}(z)$ (modified) for large N is sufficiently simple to permit an analytical study of the two-term theory formulas. The conclusions of this study (supplemented where necessary by numerical

information) are summarized in [5], [6]. A sequence of twelve basic properties relating to the kernel, the conductances, the susceptances, and the horizontal and vertical field patterns are formulated. They include:

- 1) The m^{th} phase-sequence resonance occurs when the real part of a two-term theory denominator is exactly zero. At resonance, the input conductance $G_{1,1}$ attains its maximum. The input susceptance $B_{1,1}$ has a zero very close to resonance.
- 2) At or near the m^{th} phase-sequence resonance, the self- and mutual admittances around the array vary as $\cos[2\pi(l-1)m/N]$, and the far-field pattern consists of $2m$ pencil-like beams.
- 3) It is possible to obtain narrower resonances and a vertically more directive field pattern by making N larger (fixed m/N resonance) or by making the dipoles longer or thicker (fixed m resonance), at least in the range below individual element resonance.
- 4) Any perturbation of the shape of the resonant circular array that results in only a slight change in the current distribution around the array will significantly change the field pattern. This is discussed in more detail under Topic IV.14.

References:

1. G. Fikioris, R. W. P. King, and T. T. Wu, "The Resonant Circular Array of Electrically Short Elements," *J. Appl. Phys.* 68, 431-439 (1990).
2. G. Fikioris, D. K. Freeman, R. W. P. King, H.-M. Shen, and T. T. Wu, "Analytical Studies of Large Closed-Loop Arrays," SPIE Proceedings, Vol. 1407, Intense Microwave and Particle Beams II, 295-305 (1991).
3. D. K. Freeman and T. T. Wu, "An Improved Kernel for Arrays of Cylindrical Dipoles," presented at the 1991 IEEE/AP-S Symposium, London, Ontario, June 24-28, 1991.
4. D. K. Freeman and T. T. Wu, "An Improved Kernel for Arrays of Cylindrical

Dipoles," in preparation.

5. G. Fikioris, R. W. P. King, H.-M. Shen, and T. T. Wu, "Novel Resonant Circular Arrays," presented at the Progress in Electromagnetics Research Symposium (PIERS), Cambridge, MA, July 1-5, 1991.
6. G. Fikioris, "Improved Analysis of the Resonant Circular Array of Electrically Short Elements," in preparation.

IV.14 Closed Loops of Parallel Coplanar Dipoles—Arrays of Arbitrary Shape. T. T. Wu, R. W. P. King, G. Fikioris, and H.-M. Shen, Grant N00014-89-J-1023, RADC Contracts F19628-88-K-0024 and F19628-91-K-0020, and Army LABC0M Contract DAAL02-89-K-0097; Research Unit 11.

One of the properties characteristic of resonant circular arrays [1], [2]—as discussed under Topic IV.13—is that, at or near a narrow resonance, the sine part of the current on the driven element contributes negligibly to the field pattern, so that it is possible to define and study an *array factor*. It has been shown that the array factor for a resonant circular array of electrically short elements is exponentially small. The array factor's smallness has an interesting consequence. For resonant noncircular arrays, an array factor $A(\theta, \phi)$ may be defined exactly as for the circular array. This array factor will depend on the geometry of the array and on the relative current distribution around the array. It will be a sum of N terms of order 1, each term depending on the location of element l and its relative current (admittance). If the noncircular array is thought of as a perturbation of some corresponding circular array, then it is logical to assume that the current distribution around the array will not be significantly affected. Hence, each term in the sum for $A(\theta, \phi)$ will be close to each term in the sum for the circular array. However, any very small quantity that can be written as the sum of terms of order 1 is extremely sensitive to perturbations of these terms. Therefore, the array factor (field pattern) for the noncircular array will not be close to that of the circular array. The conclusion is that any perturbation of the shape of the resonant circular array resulting in only a slight change in the current distribution around the array will significantly change

the field pattern. This means that a wide variety of field patterns may be obtained by resonant noncircular arrays, perhaps even a superdirective pattern. However, one must be very careful in dealing with noncircular arrays. The N linear algebraic equations for the currents, to which the N coupled integral equations reduce by the two-term theory approximations, must be solved with high accuracy. The currents must be known precisely in order to obtain any reasonable estimate of the far-field pattern.

References:

1. G. Fikioris, R. W. P. King, H.-M. Shen, and T. T. Wu, "Novel Resonant Circular Arrays," presented at the Progress in Electromagnetics Research Symposium (PIERS), Cambridge, MA, July 1-5, 1991.
2. G. Fikioris, "Improved Analysis of the Resonant Circular Array of Electrically Short Elements," in preparation.

IV.15 Properties of Closed Loops of Pseudodipoles. T. T. Wu and D. K. Freeman, Grant N00014-89-J-1023 and DOE Grant DE-FG02-84ER40158; Research Unit 11.

As part of the general study of the resonant and directive properties of closed-loop arrays, various mathematical models for the interaction between array elements are being studied. These include, for the Schrödinger equation, the pseudopotential in three and five dimensions and the separable kernel potential; and for the Maxwell equations, the pseudodipole and various models for the cylindrical dipole. A number of properties of closed-loop arrays are common to all these models.

The simplest possible context for studying the natural resonances in arrays is the Fermi pseudopotential in three dimensions. It was previously known [1] that the infinite linear array admits real (zero-width) resonances and that the circular array admits resonances whose widths are exponentially small as the number N of pseudopotentials becomes large. Numerical investigations have been carried out which show that there is a one-to-one correspondence between these resonances and the

frequencies at which the directivity of the field pattern is maximum. Subsequently, the integral operator with separable kernel was studied as a generalization of the Fermi pseudopotential to an interaction of nonzero range [2]. It was concluded that the narrow resonances of the circular array in [1] are a property of the closed loop, and not contingent on the zero range of the Fermi-pseudopotential.

The pseudodipole is being studied as the simplest possible scatterer in the context of the Maxwell equations. The pseudodipole is a point interaction, i.e., the induced current density depends only on the value of the electric field at a point. It is therefore intuitively clear that if the pseudodipole is to approximate a physical dipole, the physical dipole should be, in some sense, small. Moreover, in order for such a small object to produce a significant scattered field, one expects that it must be resonant. This suggests the idea of taking a center-loaded cylindrical dipole, and letting its size tend to zero while simultaneously adjusting the load reactance in order to keep the magnitude of the scattered field constant. A paper on this subject has been accepted for publication [3] in which it is shown that, for an incident plane-wave, this procedure results in a scattered field which is precisely the scattered field of a pseudodipole. Although the calculation has been carried out for plane-wave scattering, the relationship between the pseudodipole and the resonant cylindrical dipole is in fact more general. For example, the two-term theory can also be applied to a circular array of parallel, nonstaggered, resonant cylindrical dipoles, in which one element is driven and the rest are parasitic. In this case, the same relationship is obtained. That this must be so becomes apparent in the light of recent investigations [4] which have shown that the vector potential impressed on one element of the array by another (for sufficiently large element separations) is essentially that of a plane wave, even when more sophisticated current approximations are used.

The circular array of pseudodipoles has been analyzed asymptotically for arbitrary dipole orientation. Although the resonance width is exponentially small for

all orientations, in some cases the resonances lie in the wrong half plane. It has been found that this stability problem already exists for the two pseudodipole interaction. It is believed that this problem can be corrected by redefining the pseudodipole parameter a to depend on the wave number k . A paper on the stability problem is being written [5]; further study of the frequency dependence of the pseudodipole parameter is in progress.

A preliminary numerical study of the elliptical array of pseudopotentials has also been carried out. All software written for the circular array has been modified to handle the elliptical array, in order to determine the dependence of the results (resonance width, directivity, etc.) on the ellipticity. The eigenfields (corresponding to the symmetric component fields in the circular case) were calculated numerically, along with the driven fields. As expected, the resonance width increases with ellipticity, but not in a sensitive way. However, the eigenfields for the higher-order resonances (along with their directivity) are sensitive to small changes in the ellipticity. Consequently, the directivity achieves a maximum as a function of the ellipticity. For the case with $N = 20$ and arc-length spacing equal to 0.2λ , it was found that the maximum directivity achievable from the circular array could be exceeded by a factor of approximately 2.3. It is believed that the resonance width for the elliptical array is also exponentially small in N . Current efforts are aimed at calculating this width explicitly.

References:

1. A. Grossmann and T. T. Wu, "A Class of Potentials with Extremely Narrow Resonances," *Chinese Jour. Phys.* 25, 129-139 (1987).
2. D. K. Freeman, "A Generalization of the Pseudopotential to an Interaction with Nonzero Range," in preparation.
3. D. K. Freeman, "The Pseudodipole as the Limit of a Resonant Cylindrical Dipole," *J. Math. Phys.* (accepted).

4. R. W. P. King, "Electric Fields and Vector Potentials of Thin Cylindrical Antennas," *IEEE Trans. Antennas Propagat.* AP-38, 1456-1461 (1990).
5. D. K. Freeman, "Resonances and Stability in Arrays of Pseudodipoles," in preparation.

IV.16 Experimental Studies of the Resonance of a Circular Array. H.-M. Shen and G. Fikioris, Grant N00014-89-J-1023 and Army LABCOM Contract DAAL02-89-K-0097; Research Unit 11.

In order to verify the existence of the theoretically predicted, extremely sharp resonances that occur in a circular array with many identical elements but only one driven, two experimental investigations of such an array are being carried out. In the first experiment, the circular array consists of 90 monopole elements equally spaced around a 6-meter circumference. The monopole elements are tubular cylinders. Only one element is driven by a swept generator through a coaxial line. The properties of the array are observed through three windows: the input admittance of the array, the relative currents on the parasitic elements, and the radiation patterns.

The major considerations in the design of this experiment were the choice of the parameters of the array and their mechanical and electrical implementation. The parameters are the number of elements N , the height h and radius a of each tubular cylinder, and the space d between adjacent elements. According to the preliminary calculation, if the parameters are chosen to be $N = 90$, $h \doteq 0.18\lambda$, $a \doteq 0.028\lambda$ and $d \doteq 0.4375\lambda$, where λ is the wavelength, the resonance will be very sharp. In this experiment, the resonant frequency was chosen to be 2 GHz (or $\lambda = 15$ cm). Thus, the parameters are $h = 27$ mm, $a = 4.2$ mm and $d = 65.615$ mm; the diameter of the array is about 2 meters (188 cm). The elements were placed on a small, rotatable metal plate set on a large 50 ft by 12 ft ground plane which serves as an image plane.

In order to assure that the cylinders make good contact with and are stable

on the ground plate, the base of each cylinder is enlarged into a thin disk (1 mm thick and 14 mm in diameter). To measure the input admittance of the single driven element, the coaxial feeder is a slotted line; this offers the way to measure the standing-wave ratio. To measure the current in a parasitic element, a tiny loop is located at the base of the cylinder.

The usual way of measuring the input impedance or input admittance of an antenna system is through the measurement of the standing-wave ratio (SWR). This method is convenient for measurements at a single frequency but, to determine the frequency dependence of the impedance, hundreds of measurements at different frequencies are required. Using the Hewlett-Packard HP8753C Network Analyzer, an alternative method of measuring the frequency response has been developed. The main point of this method is that the locations of the measurement are fixed for all frequencies; only one measurement at two locations is needed. This fixed-point method is much more efficient and accurate than the SWR method.

Other considerations in the design are how to keep the individual elements identical and the spacing between adjacent elements equal, while at the same time allowing the overall shape of the array to vary. The tubular cylinders with a thin disk as the base were made on a computer-controlled lathe, which improves the tolerance to as high as 0.01%. To keep the distance between the adjacent elements equal, a special kind of connecting chain was designed which, like a bicycle chain, can keep the spacing equal while varying the shape. With the help of the connecting chain, the accuracy in the spacing can be as high as 0.05 mm. To maintain the elements on a circumference with a precise radius, a special bar with variable center and radius was used; this resulted in an accuracy as high as 0.1 mm or 0.01%. To reduce the contact resistance between the brass disks and the aluminum plate, a low resistance conductive cement was used to glue the disks onto the plate.

The series of adjustments to the array and the measured results are described

in detail in [1]. It is found that resonance—at which the conductance becomes very large and the susceptance very small—does occur. The experiment shows that the quality of the resonance, $Q (= f/\Delta f)$, depends strongly on the equality of the spacing between the elements and good conductive contact between the monopoles and the ground plate. A comparison of the measurements (after adjustments) and the end-corrected theory shows very close agreement.

A second experiment [2] with a 90-element circular array has been designed during this reporting period in order to improve the electrical contact between the tubular elements and the ground plane, and to remove any ambiguity in the element length caused by the presence in the first experiment of the thin-disk base. In the new setup, the elements of the array are thin-walled brass cylinders that are meant to realize tubular monopoles. They are securely fastened (screwed) onto the ground plane, which improves the electrical contact with the ground plane but does not allow the shape of the array to be varied. The new experiment has also been designed to obtain larger currents around the array since its choice of parameters is based on the results of the two-term theory with the modified kernel. To date, the whole setup has been assembled and measurements of the driving-point impedance as a function of frequency have been made by measuring the voltage amplitudes at 3 fixed points on the feeding measuring line. While some problems associated with the method of measurement and the feeding measuring line remain to be solved and minor adjustments to the array are needed, preliminary measurements have been taken which appear to determine accurately the locations of the resonances (resonant frequencies). The measured results show very close agreement with the resonant frequencies predicted by the end-corrected theory [3]. Also, many features of the measured frequency-response curve agree qualitatively with theoretical predictions.

References:

1. H.-M. Shen, "Experimental Study of the Resonance of a Circular Array," SPIE Proceedings, Vol. 1407, Intense Microwave and Particle Beams II, 306-315 (1991).
2. G. Fikioris, R. W. P. King, H.-M. Shen, and T. T. Wu, "Novel Resonant Circular Arrays," presented at the Progress in Electromagnetics Research Symposium (PIERS), Cambridge, MA, July 1-5, 1991.
3. G. Fikioris, D. K. Freeman, R. W. P. King, H.-M. Shen, and T. T. Wu, "Analytical Studies of Large Closed-Loop Arrays," SPIE Proceedings, Vol. 1407, Intense Microwave and Particle Beams II, 295-305 (1991).

IV.17 Plasma Waveguide: A Concept to Transfer EM Energy in Space. H.-M. Shen, Grant N00014-89-J-1023 and Army LABCOM Contract DAAL02-89-K-0097; Research Unit 11.

It has been shown that electromagnetic (EM) energy originating at a source in upper space can be transferred efficiently through a plasma waveguide [1]. Such a waveguide consists of a cylindrical vacuum core surrounded by a plasma cladding medium, which can be generated in upper space by a hollow laser beam [2]. An experiment demonstrating an actual 95-meter long laser-generated plasma channel was carried out six years ago by Livermore National Laboratory [3]. The analysis and survey show that the plasma waveguide at high frequencies ($\omega \gg \omega_p$) has many excellent performance characteristics for transporting a microwave pulse. The EM pulses that travel in such a waveguide are dispersion-free and have a speed close to that of light. In other words, the EM pulses can follow the laser-generated plasma channel and, like current pulses in a wire, "move" at the speed of light.

In the first model of the plasma waveguide [1], the plasma cladding was assumed to extend transversely to infinity. Therefore, the guided modes are loss-free. If the cladding is finite, there will be an energy loss from the outside surface of the cladding. To study this effect, an analysis of the plasma waveguide with finite thickness has been completed [4] and the coefficient of the energy decay calculated.

For the previous case of infinite thickness, it was found that the guided modes

$HE_{n,m}$ at high frequencies are split into two frequency-independent modes, a high- n mode and a low- n mode. In the analysis for the case of finite thickness, this property remains. The characteristic equation at high frequencies is also split into two equations. Most of the other properties for the case of infinite thickness are retained as well: the eigenvalue x (although now a complex number) is constant and much smaller than ka ; the EM pulse propagates with constant profile and shape and at the speed of light; and the loss due to the conductivity of the plasma and the anisotropic effect due to the earth's magnetic field are small.

The main concern of the new analysis is the loss from the outside surface of the plasma tube. It is natural to suspect the loss to be significant since the field does not decrease fast enough transversely. For instance, the field on the surface at $r = 2a$ is still 7% of the maximum field. However, the results of this analysis turn out to be quite different. For the case of finite thickness, the eigenvalue x of the characteristic equation becomes a complex number. The imaginary part x_I is much smaller than the real part x_R . It decreases exponentially with the thickness of the cladding. Especially for high-frequency operation—since the EM wave itself has better “directivity”—the plasma tube has the ability to hold most of the energy within the tube, i.e., the loss is surprisingly small.

References:

1. H.-M. Shen, “Plasma Waveguide: A Concept to Transfer EM Energy in Space,” *J. Appl. Phys.* 69, 6827–6835 (1991).
2. APS Study Group, “APS Study: Science and Technology of Directed Energy Weapons,” *Rev. Mod. Phys.* 59, No. 3, Part II, Sec. 4.2, S71–S79 (1987).
3. D. S. Prono, “Recent Progress of the Advanced Test Accelerator,” *IEEE Trans. Nucl. Sci.* NS-32, 3144–3148 (1985).
4. H.-M. Shen and H.-Y. Pao, “The Plasma Waveguide with a Finite Thickness of Cladding,” *J. Appl. Phys.*, submitted for publication.

ANNUAL REPORT OF
PUBLICATIONS/PATENTS/PRESENTATIONS/HONORS

a. Papers Submitted to Refereed Journals (and not yet published)

D. K. Freeman, "The Pseudodipole as the Limit of a Resonant Cylindrical Dipole," *J. Math. Phys.* (accepted). (Partial support from DOE Grant DE-FG02-84ER40158.)

R. W. P. King, "Electromagnetic Field of Dipoles and Patch Antennas on Microstrip," *Radio. Sci.*

R. W. P. King, "The Circuit Properties and Complete Fields of Wave Antennas and Arrays," *Space Communications.*

M. F. Brown and J. M. Myers, "Scattering of Electromagnetic Missiles by Perfectly Conducting 'Round' Objects," *J. Appl. Phys.* (Partial support from Army LABC0M Contract DAAL02-89-K-0097.)

H.-M. Shen and H.-Y. Pao, "The Plasma Waveguide with a Finite Thickness of Cladding," *J. Appl. Phys.* (Partial support from Army LABC0M Contract DAAL02-89-K-0097.)

b. Papers Published in Refereed Journals

G. Fikioris, R. W. P. King, and T. T. Wu, "The Resonant Circular Array of Electrically Short Elements," *J. Appl. Phys.* 68, 431-439 (1990). (Partial support from RADC Contract F19628-88-K-0024 and Army LABC0M Contract DAAL02-89-K-0097.)

R. W. P. King, "Electric Fields and Vector Potentials of Thin Cylindrical Antennas," *IEEE Trans. Antennas Propagat.* AP-38, 1456-1461 (1990). (Partial support from RADC Contract F19628-88-K-0024 and Army LABC0M Contract DAAL02-89-K-0097.)

R. W. P. King, "The Large Circular Array with One Element Driven," *IEEE Trans. Antennas Propagat.* AP-38, 1462-1472 (1990). (Partial support from RADC Contract F19628-88-K-0024 and Army LABC0M Contract DAAL02-89-K-0097.)

R. W. P. King, "On the Radiation Efficiency and the Electromagnetic Field of a Vertical Electric Dipole in the Air Above a Dielectric or Conducting Half-Space," Chapter 1 in *Progress in Electromagnetics Research*, Vol. 4, edited by J. A. Kong, Elsevier Science Publ. Co., Inc., New York, 1990, pp. 1-43.

H.-M. Shen, "Plasma Waveguide: A Concept to Transfer EM Energy in Space," *J. Appl. Phys.* 69, 6827-6835 (1991). (Partial support from Army LABCOM Contract DAAL02-89-K-0097.)

R. W. P. King, "The Electromagnetic Field of a Horizontal Electric Dipole in the Presence of a Three-Layered Region," *J. Appl. Phys.*, 69, 7987-7995 (1991).

h. Contributed Presentations at Topical or Scientific/Technical Society Conferences

H.-M. Shen, T. T. Wu, and J. M. Myers, "Experimental Study of Electromagnetic Missiles from a Hyperboloidal Lens," SPIE Proceedings, Vol. 1407, Intense Microwave and Particle Beams II, 286-294 (1991). (Partial support from Army LABCOM Contract DAAL02-89-K-0097.)

G. Fikioris, D. K. Freeman, R. W. P. King, H.-M. Shen, and T. T. Wu, "Analytical Studies of Large Closed-Loop Arrays," SPIE Proceedings, Vol. 1407, Intense Microwave and Particle Beams II, 295-305 (1991). (Partial support from Army LABCOM Contract DAAL02-89-K-0097 and RADC Contract F19628-88-K-0024.)

H.-M. Shen, "Experimental Study of the Resonance of a Circular Array," SPIE Proceedings, Vol. 1407, Intense Microwave and Particle Beams II, 306-315 (1991). (Partial support from Army LABCOM Contract DAAL02-89-K-0097.)

G. Fikioris, R. W. P. King, H.-M. Shen, and T. T. Wu, "Novel Resonant Circular Arrays," presented at the Progress in Electromagnetics Research Symposium (PIERS), Cambridge, MA, July 1-5, 1991. (Partial support from RADC Contracts F19628-88-K-0024 and F19628-91-K-0020, and Army LABCOM Contract DAAL02-89-K-0097.)

D. K. Freeman and T. T. Wu, "An Improved Kernel for Arrays of Cylindrical Dipoles," presented at the 1991 IEEE/AP-S Symposium, London, Ontario, June 24-28, 1991. (Partial support from Army LABCOM Contract DAAL02-89-K-0097.)

j. Graduate Students and Post-Doctorals Supported under the JSEP for the Year Ending 30 June 1991

Mr. G. Fikioris and Mr. V. Houdzoumis.

V. SIGNIFICANT ACCOMPLISHMENTS REPORT

V.1 Study of the Band Gap in HgTe/CdTe Superlattices through the Pressure Dependence of the Photoluminescence. H. M. Cheong, J. H. Burnett, and W. Paul; Research Unit 1, SOLID STATE ELECTRONICS.

Infrared detectors operating in the 10 micron range of wavelengths are important in both civilian and military applications. The best detectors are currently made from an alloy of HgTe and CdTe. These alloys suffer from a variety of defects, some of them stemming from compositional inhomogeneities. It has been suggested that superlattices consisting of repeated, alternating layers of the unalloyed compounds, HgTe and CdTe, would provide at least as good detectors as the HgCdTe alloy and perhaps be more stable. There has also been a number of experiments, mostly of optical absorption and of photoluminescence, which, however, have not been consistent in their conclusions. A satisfactory confrontation of theoretical prediction and experimental result has not yet been achieved.

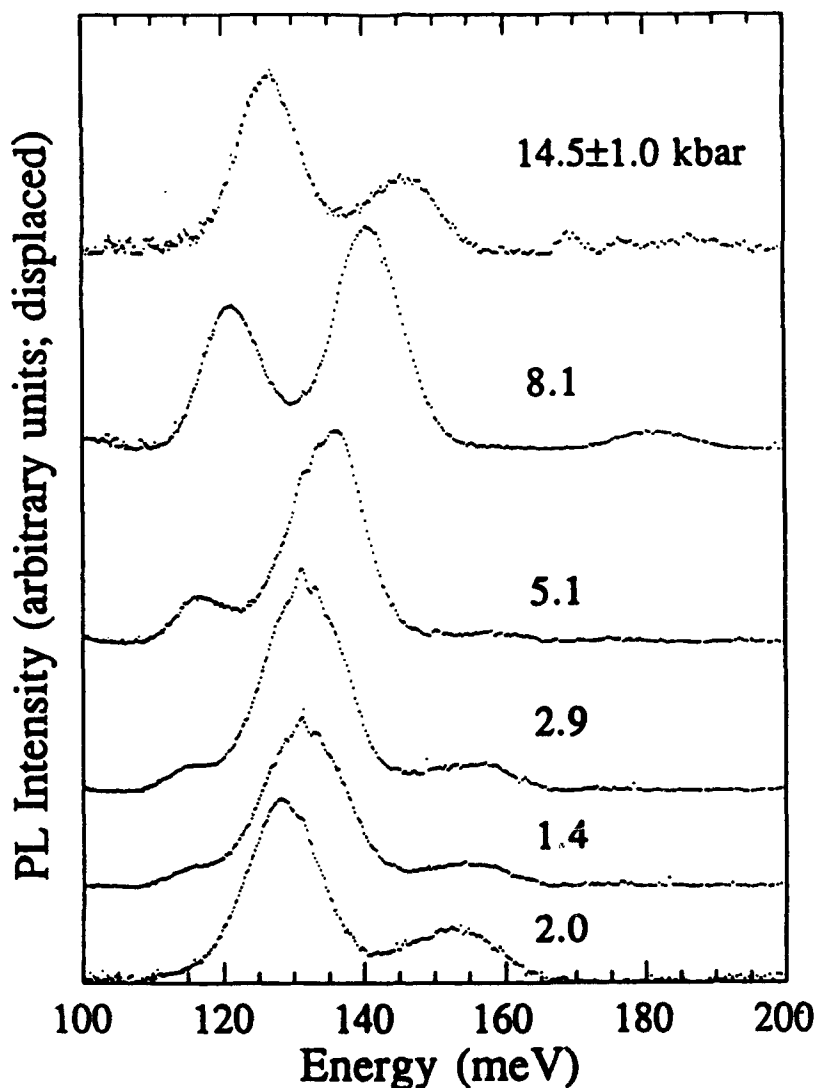
We have succeeded in carrying out an experiment in which the fundamental energy gap of a HgTe/CdTe superlattice has been estimated from the position in wavelength of a peak in the photoluminescence, and we have determined how it changes with hydrostatic pressure, produced in a diamond anvil cell. This is the first time, to our knowledge, that such an experiment has been carried out at low temperatures, in this wavelength range, and to the pressures available in diamond anvil cells.

The result is an increase in the energy of the photoluminescence peak seen at atmospheric pressure at a rate which is about five times smaller than is predicted by preliminary calculations based on current theory. Either the theory is not appropriate, or the identification of the (only) photoluminescence peak seen at atmospheric pressure as a measure of the optical energy gap is incorrect. Either way, this experiment is very likely to be useful in advancing understanding of this important system.

Pressure Dependence of the Photoluminescence of HgTe/CdTe Superlattices

H.M. Cheong, J.H. Burnett and W. Paul

Harvard University



The shift of the lowest energy (band gap) peak with pressure is five times smaller than current theory has predicted. Either the theory, or the present interpretation of the PL spectrum, must be changed.

V.2 Structure of the Si/SiO₂ Interface. T. Rabedeau, I. Tidswell, and P. S. Pershan; Research Unit 2, SOLID STATE ELECTRONICS.

Technological demands for increasingly faster solid-state electronic devices has resulted in attempts to make smaller and smaller structures in which the ultimate properties are increasingly sensitive to the structure and other properties of the surfaces and interfaces. In view of the fact that a large portion of our technology is based on silicon it is quite likely that future developments might well be limited by understanding of the surface, or the interface between silicon and its oxides. Although there is an increasingly powerful arsenal of techniques for studying the interface between one or another crystal and vacuum there are relatively few nondestructive ways to study buried interfaces, such as the one between two solids such as silicon and its oxide. Fortunately, the recent development of dedicated X-ray synchrotron facilities has stimulated the development of techniques that are suitable for just this problem.

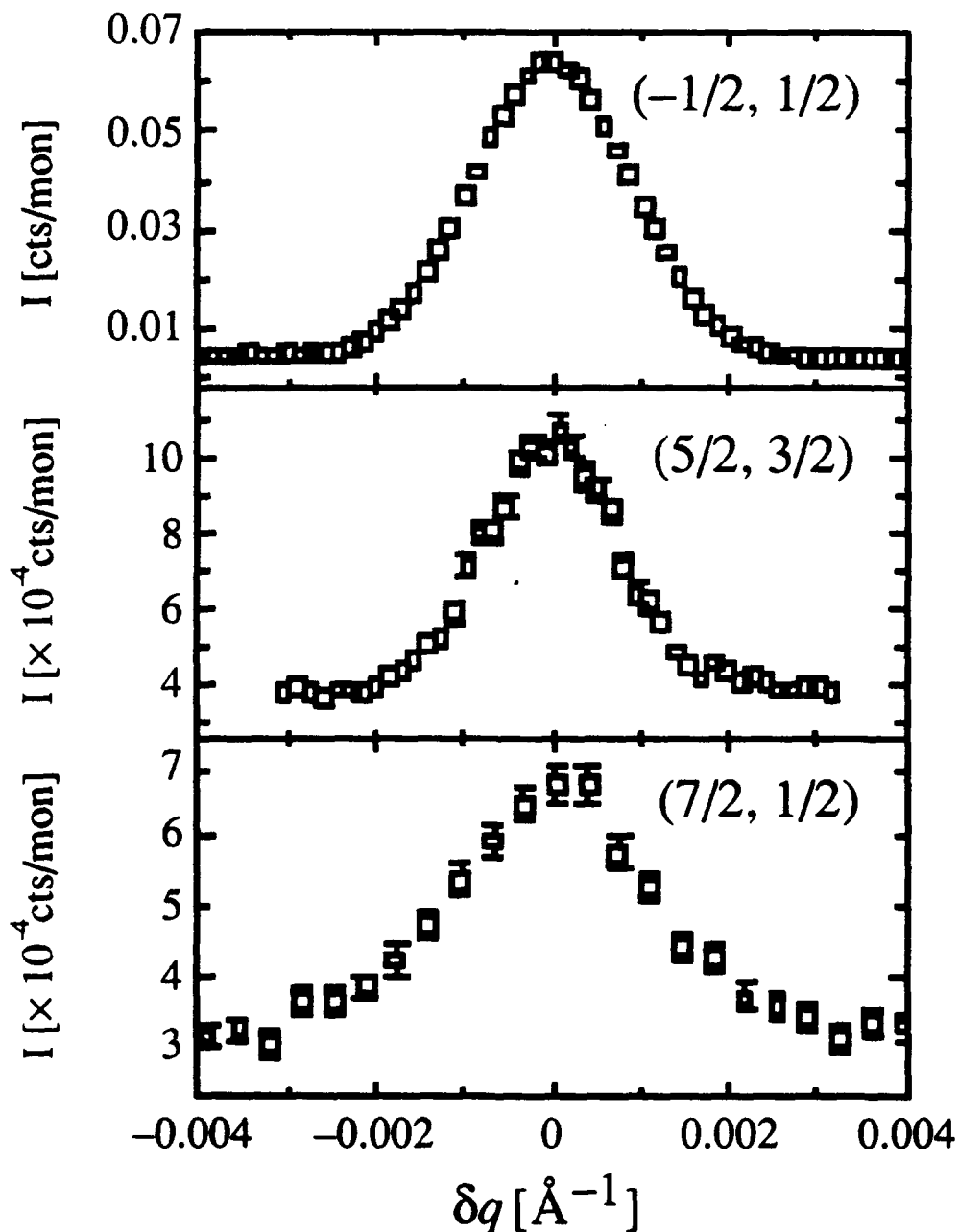
X-ray techniques can be surface specific because the energy of 8 to 10 keV X-rays are much larger than the binding energies of most of the electrons in any solid. The electrons respond to the electric field of the X-rays like a plasma that is driven by a frequency that is high compared to its plasma frequency; i.e., the dielectric constant is less than unity. Since the dielectric constant of air is unity X-rays incident at a glancing angle to the surface are refracted *towards the surface* and if the angle is sufficiently small, they are totally externally reflected analogously to the optical phenomena of total internal reflection. Since under total external reflection the only part of the material that sees the incident X-rays is the region near the surface the scattering cross section is completely dominated by the near surface region and even though that cross section is relatively small, by using the very high brilliance of synchrotron sources it is easily observed.

The data in the first viewgraph illustrates X-ray scattering measurements of surface diffraction from ordered SiO_2 regions at the interface between the $\text{Si}(001)$ lattice and a layer of amorphous SiO_2 . This peak is at an angle corresponding to a surface unit cell that is twice the size of the surface unit cell of an ideally terminated Si lattice. The second viewgraph illustrates the atomic positions for a Si dimer model that can quantitatively account for the intensity distribution of eight physically inequivalent peaks. This data absolutely rules out previously proposed cristobalite or tridymite related structures for this interface. Secondly, since quantitative intensity measurements indicate that this ordered interfacial structure accounts for no more than $\sim 10\%$ of the interface, and since the order decreases on exposure to either moist air or modest thermal annealing, the ordered structure that results from dry oxidation at room temperature is only metastable.

Structure of the Si/SiO₂ Interface

T. Rabedeau, I. Tidswell, and P. S. Pershan

Harvard University

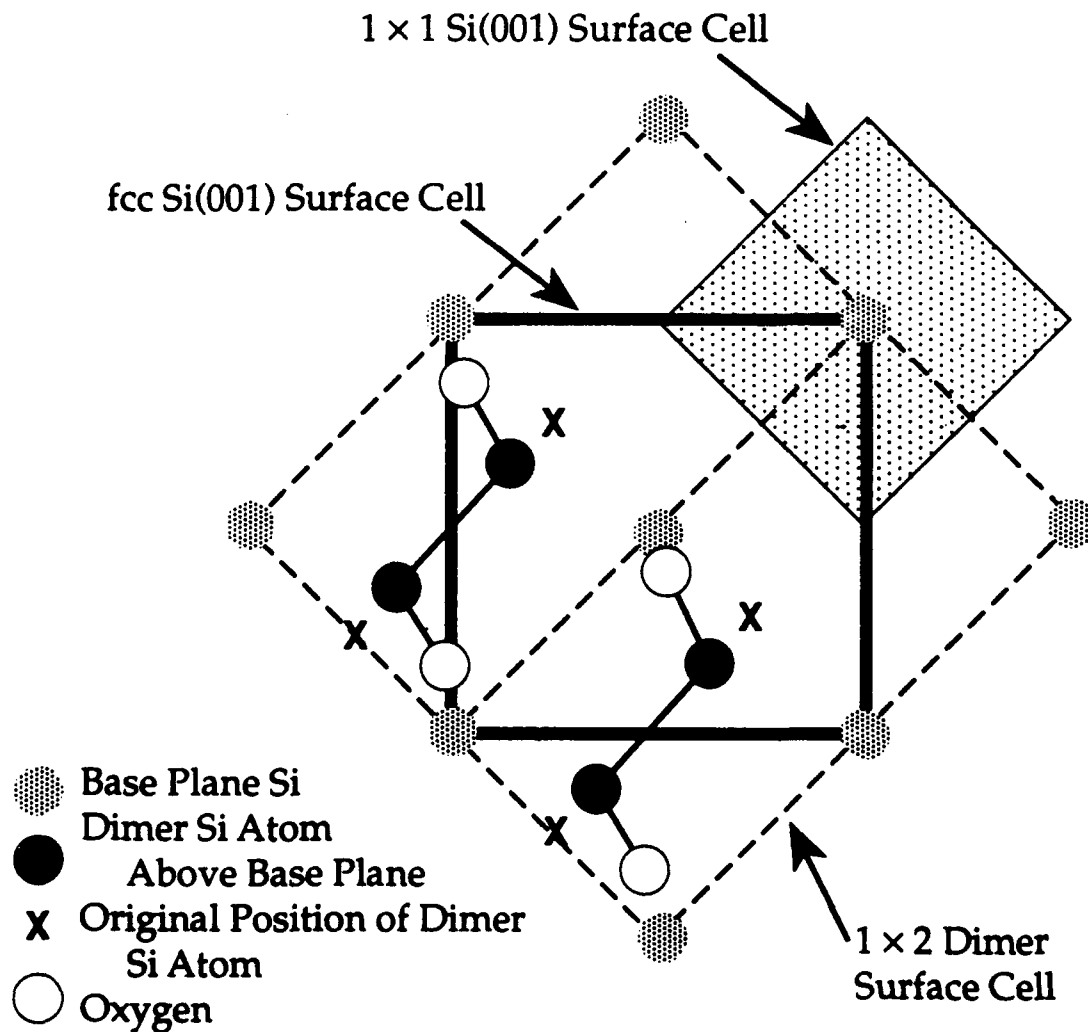


Transverse in-plane scans through fractional order diffraction peaks associated with ordered portions of the interface between the Si(001) lattice and an amorphous SiO₂ layer.

Structure of the Si/SiO₂ Interface

T. Rabedeau, I. Tidswell, and P. S. Pershan

Harvard University



Schematic illustration of a model for the interfacial SiO₂ unit cell that accounts for the observed surface diffraction peaks.

V.3 Fluxon Motion in Superconducting Junction Arrays. M. Tinkham; Research Unit 4, SOLID STATE ELECTRONICS.

We have made rapid progress in understanding fluxon motion in large arrays of SNS Josephson junctions, a fabricated system which we use to model the behavior of granular superconductors, such as high temperature superconductors. For example, the temperature- and field-dependence of the array resistance for small flux densities can be accounted for on the basis of fluxons moving independently through *intrinsic pinning* sites, one in each cell of the array, with a pinning energy (found from thermal activation fits) of $\sim 0.2E_J$, as predicted several years ago in a paper from our group [1]. (This intrinsic pinning is analogous to the pinning due to the atomic planes in YBCO.)

Much interest has been generated by our recent work on "*fractional giant Shapiro steps*" which are observed when one of these 1000×1000 arrays is driven simultaneously by a.c. and d.c. currents in the presence of a commensurate magnetic field. If the number of flux quanta per unit cell $f = p/q$, where p and q are small integers so that the field is "strongly commensurate," Benz found that, in addition to the giant Shapiro steps at 1000 times the single junction voltage, *fractional giant steps* are observed at $1/q$ times that value, and multiples thereof. These observations can be explained in terms of coherent motion of a superlattice of vortices through the array. However, our subsequent work has revealed more subtlety, namely that the fractional giant steps are *absent* if the direction of the bias current relative to the array axes is rotated by 45° . We have confirmed this surprising result by computer simulations. By extending these measurements in still unpublished work [2] to other geometries, including arrays with triangular rather than square symmetry of the unit cell with two different current directions as well, we have gained a clearer picture of the role of symmetry in controlling the observability of the fractional Shapiro steps. This relationship is illustrated in the

following viewgraph.

After completing his JSEP-supported thesis work on these arrays, Benz, now at NIST, Boulder, has used their facilities to fabricate a 10×10 array of SIS (as opposed to our SNS) junctions, and shown that they can be used as a voltage-tunable *microwave source* whose power output ($\sim 1 \mu\text{W}$) is near the theoretical limit for an array of that size [3]. This suggests that by scaling up the size of the array, considerably larger amounts of power may be obtainable. To the best of our knowledge, this work is the first to show that a 2-D array of junctions can be used as a voltage-tunable microwave source. Because it has N^2 instead of N junctions, and hence greater power capability than a 1-D array, this is an important advance. It is directly derivative from the basic Harvard thesis work, following within less than a year, and has obvious potential for technological applications.

References:

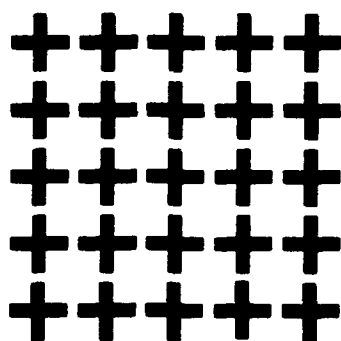
1. M. S. Rzchowski, S. P. Benz, M. Tinkham, and C. J. Lobb, "Vortex Pinning in Josephson Junction Arrays," *Phys. Rev. B* **42**, 2041 (1990).
2. L. L. Sohn, M. S. Rzchowski, J. V. Free, S. P. Benz, and M. Tinkham, "Absence of Fractional Giant Shapiro Steps in Diagonal Josephson Junction Arrays," to appear in *Phys. Rev. B*.
3. S. P. Benz and C. J. Burroughs, "Coherent Emission from Two-dimensional Josephson Junction Arrays," *Appl. Phys. Lett.* **58**, 2162 (1991).

Dependence of Strength of Fractional Giant Shapiro Steps on Current Direction and Array Geometry

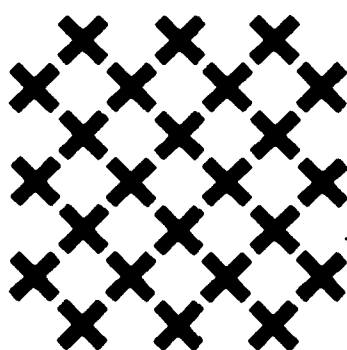
L. L. Sohn, *et al.*,
Harvard University

Step Strength:

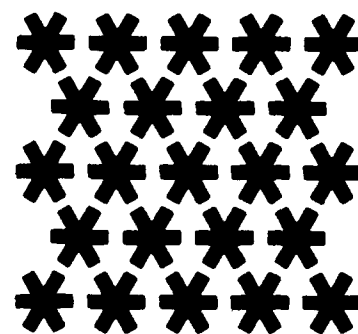
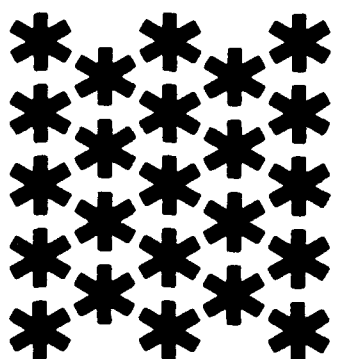
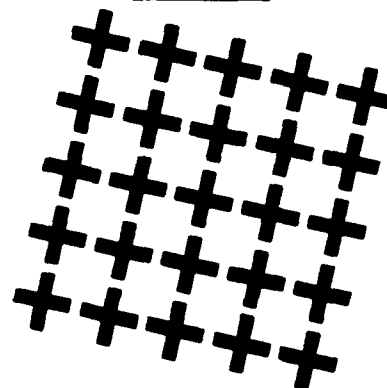
Strong



Weak



Absent



Fractional giant steps are strong when the array contains junctions perpendicular to the macroscopic current direction; these carry vortex circulating current but not transport current. Simulations confirm our experimental results. Such 2-D arrays show technological promise as voltage-tunable microwave sources.

V.4 A Comprehensive Study of Electromagnetic Methods for the Detection of Submerged Submarines. R. W. P. King and T. T. Wu; Research Unit 11, ELECTROMAGNETIC PHENOMENA.

An accurate theory has been developed and applied in a detailed quantitative manner for the following methods of remote sensing from near the surface of the sea. 1) A crossed, insulated and terminated dipole source located just below the surface of the sea generates an omnidirectional lateral-wave field at 10–100 Hz. This travels radially outward in the air just above the surface and continuously transmits a downward-directed field into the sea. A submarine backscatters this field upward to be detected by a receiver near the surface. 2) The theory for 1) has been generalized to take account of a layer of ice on the sea. The source and receiver can be located on the ice or just below it. The latter is fixed at a distance from the source to detect a moving submarine or is moved along the surface to detect a stationary submarine. This method has been tested by the U.S. Navy on the arctic ice. 3) An electric dipole near the surface in the sea transmits a sequence of single pulses vertically down into the sea to be backscattered upward by a submarine and detected by a nearby receiver. With a pulse width of 1 sec, the small scattered pulse from the submarine and the large direct-field pulse from the source arrive simultaneously at the receiver, so that the latter would have to be balanced out. With a pulse width of 0.01 sec, the direct pulse has died out when the scattered pulse arrives and this is large enough to be readily detectable. 4) The dipole source is excited with a burst of 25 cycles at $f \sim 25$ Hz with its amplitude limited by a Gaussian envelope with a 1 sec width. A small burst backscattered by a submarine arrives at the receiver simultaneously with the large direct burst from the source. When this latter is automatically cancelled, the small scattered burst is large enough to be detected.

Significant Accomplishments for FY1991

Research Unit 11 on ELECTROMAGNETIC PHENOMENA

Harvard University—JSEP Grant N00014-89-J-1023

Principal Investigator: Professor Tai Tsun Wu

A Comprehensive Study of Electromagnetic Methods for the Detection of Submerged Submarines

Accurate theoretical formulas have been developed and applied to remote sensing in the ocean for the following methods:

- **Bistatic radar using steady-state lateral waves:**

A dipole source on the surface of the sea or above or below a layer of ice generates waves that diffuse into the ocean, are scattered by a submarine, and detected by a receiver on the surface.

- **Bistatic radar using a direct, pulsed field:**

A dipole near the surface in the sea transmits a single EM pulse or a burst into the sea. This is scattered by a submarine and detected by a receiver near the source.